



QEX

\$5

July/August 2011

www.arrl.org

A Forum for Communications Experimenters

Issue No. 267



AA0ZZ uses a Silicon Labs Si570 DSPLL phase-locked loop synthesizer IC and custom software to build a local oscillator that produces a stable 10 to 157 MHz output signal with no DDS spurs.

SkyCommand II

Allows Global Communication Through Remote Operation on HF Frequencies



TS-2000

The ultimate in remote control.

TH-D72A
required for remote use

KENWOOD
Listen to the Future

KENWOOD U.S.A. CORPORATION
Communications Sector Headquarters
3970 Johns Creek Court, Suite 100, Suwanee, GA 30024
Customer Support/Distribution
P.O. Box 22745, 2201 East Dominguez St., Long Beach, CA 90801-5745
Customer Support: (310) 639-4200 Fax: (310) 537-8235


www.kenwoodusa.com


JQA-1206 091-A
Communications Equipment Division
Registered Corporation
ISO9001 certification

ADS#22311



QEX (ISSN: 0886-8093) is published bimonthly in January, March, May, July, September, and November by the American Radio Relay League, 225 Main Street, Newington, CT 06111-1494. Periodicals postage paid at Hartford, CT and at additional mailing offices.

POSTMASTER: Send address changes to: QEX, 225 Main St, Newington, CT 06111-1494 Issue No 267

Harold Kramer, WJ1B
Publisher

Larry Wolfgang, WR1B
Editor

Lori Weinberg, KB1EIB
Assistant Editor

Zack Lau, W1VT
Ray Mack, W5IFS
Contributing Editors

Production Department

Steve Ford, WB8IMY
Publications Manager

Michelle Bloom, WB1ENT
Production Supervisor

Sue Fagan, KB1OKW
Graphic Design Supervisor

David Pingree, N1NAS
Senior Technical Illustrator

Carol Michaud, KB1QAW
Technical Illustrator

Advertising Information Contact:

Janet L. Rocco, W1JLR
Business Services
860-594-0203 – Direct
800-243-7768 – ARRL
860-594-4285 – Fax

Circulation Department

Cathy Stepina, QEX Circulation

Offices

225 Main St, Newington, CT 06111-1494 USA
Telephone: 860-594-0200
Fax: 860-594-0259 (24 hour direct line)
e-mail: qex@arrl.org

Subscription rate for 6 issues:

In the US: ARRL Member \$24,
nonmember \$36;

US by First Class Mail:
ARRL member \$37, nonmember \$49;

International and Canada by Airmail: ARRL member \$31, nonmember \$43;

Members are asked to include their membership control number or a label from their QST when applying.

In order to ensure prompt delivery, we ask that you periodically check the address information on your mailing label. If you find any inaccuracies, please contact the Circulation Department immediately. Thank you for your assistance.



Copyright © 2011 by the American Radio Relay League Inc. For permission to quote or reprint material from QEX or any ARRL publication, send a written request including the issue date (or book title), article, page numbers and a description of where you intend to use the reprinted material. Send the request to the office of the Publications Manager (permission@arrl.org).

About the Cover

Craig Johnson, AA0ZZ, uses a Silicon Labs Si570 DSPPLL programmable phase-locked loop synthesizer IC and custom software to build a local oscillator that produces a stable 10 to 157 MHz output signal. The oscillator can provide the local oscillator signals for quadrature sampling detector receivers and quadrature sampling encoder transmitters on the 80 through 10 meter amateur bands.



In This Issue

Features

3 Programmable PLL (Si570) Local Oscillator for HF Receivers, Transmitters and Transceivers

Craig Johnson, AA0ZZ

17 A 10 MHz to 6 GHz Power Meter

By James Hontoria, W1JGH

22 Filter Synthesis Using Equal Ripple Optimization

By Gary Appel, WA0TFB

31 Transmission and Reception of Longitudinally-Polarized Momentum Waves

By Robert K. Zimmerman, NP4B, VE3RKZ

36 Extended Bandwidth Crystal Ladder Filters With Almost Symmetrical Responses

By David Gordon-Smith, G3UUR

45 Upcoming Conferences

46 Next Issue in QEX

Index of Advertisers

American Radio Relay League:.....	47, 48,	Kenwood Communications:.....	Cover II
	Cover III, Cover IV	National RF, Inc:	35
Array Solutions:	30	Nemal Electronics International, Inc:.....	44
Coherent:	44	RF Parts:.....	43, 45
Down East Microwave Inc:.....	46	Tucson Amateur Packet Radio:	46

The American Radio Relay League



The American Radio Relay League, Inc. is a noncommercial association of radio amateurs, organized for the promotion of interest in Amateur Radio communication and experimentation, for the establishment of networks to provide communications in the event of disasters or other emergencies, for the advancement of the radio art and of the public welfare, for the representation of the radio amateur in legislative matters, and for the maintenance of fraternalism and a high standard of conduct.

ARRL is an incorporated association without capital stock chartered under the laws of the state of Connecticut, and is an exempt organization under Section 501(c)(3) of the Internal Revenue Code of 1986. Its affairs are governed by a Board of Directors, whose voting members are elected every three years by the general membership. The officers are elected or appointed by the Directors. The League is noncommercial, and no one who could gain financially from the shaping of its affairs is eligible for membership on its Board.

"Of, by, and for the radio amateur," ARRL numbers within its ranks the vast majority of active amateurs in the nation and has a proud history of achievement as the standard-bearer in amateur affairs.

A *bona fide* interest in Amateur Radio is the only essential qualification of membership; an Amateur Radio license is not a prerequisite, although full voting membership is granted only to licensed amateurs in the US.

Membership inquiries and general correspondence should be addressed to the administrative headquarters:

ARRL
225 Main Street
Newington, CT 06111 USA
Telephone: 860-594-0200
FAX: 860-594-0259 (24-hour direct line)

Officers

President: KAY C. CRAIGIE, N3KN
570 Brush Mountain Rd, Blacksburg, VA 24060

Chief Executive Officer: DAVID SUMNER, K1ZZ

The purpose of QEX is to:

- 1) provide a medium for the exchange of ideas and information among Amateur Radio experimenters,
- 2) document advanced technical work in the Amateur Radio field, and
- 3) support efforts to advance the state of the Amateur Radio art.

All correspondence concerning *QEX* should be addressed to the American Radio Relay League, 225 Main Street, Newington, CT 06111 USA. Envelopes containing manuscripts and letters for publication in *QEX* should be marked Editor, *QEX*.

Both theoretical and practical technical articles are welcomed. Manuscripts should be submitted in word-processor format, if possible. We can redraw any figures as long as their content is clear. Photos should be glossy, color or black-and-white prints of at least the size they are to appear in *QEX* or high-resolution digital images (300 dots per inch or higher at the printed size). Further information for authors can be found on the Web at www.arrl.org/qex/ or by e-mail to qex@arrl.org.

Any opinions expressed in *QEX* are those of the authors, not necessarily those of the Editor or the League. While we strive to ensure all material is technically correct, authors are expected to defend their own assertions. Products mentioned are included for your information only; no endorsement is implied. Readers are cautioned to verify the availability of products before sending money to vendors.

Larry Wolfgang, WR1B

Empirical Outlook

Web Update

In the last issue I wrote about older missing files on our *QEX* files website. Since then I have spent some time recreating the tables with file links, descriptions, author's names and call signs.

As I write this, I have added the files back through 2003 to our new website at www.arrl.org/qexfiles. I will continue restoring older files, as time permits. It won't happen immediately, but I will recreate as much of that broken web as I can. Like the spider whose web I keep knocking down at my back door, I've had some frustrations in building the new web. Just when things seemed to be going smoothly, I discovered that the newest update to Mozilla Firefox (the only web browser that the ARRL website's content management system will work with) no longer works with that system. Luckily, so far, only my computer at home updated to the new version. As long as I can prevent my office computer from updating, I should still be able to keep working on it.

If you are looking for an older file, please check the ARRL website to see if it has been restored. If you try to download a file and find that it is not the file you expected, or if you find other problems, please let me know. Since I haven't found an automated way to do this, I will be copying files and text, and creating hyperlinks as those files are put into the new web structure. Our new web may continue to have some holes in it, or some oddly spaced threads, but hopefully it will fulfill our needs.

Do You Have Some Technical Expertise to Share?

As I write this editorial, ARRL Field Day will be in a few weeks. By the time you receive this issue of *QEX*, it will likely be over. Do you operate Field Day? It has become one of my favorite operating events. Joining in with a local club adds variety and flavor to the experience, with a wide range of operator expertise and lots of good food and good friends to share it with.

What technical problems do you typically run into? How do you solve them? Do you have a piece of equipment that you use to make your Field Day more enjoyable and successful? Perhaps there is a good article there, to share with your fellow *QEX* readers. We are always looking for good technical articles for *QEX*, and would love to hear from you.

Preparing the Upcoming Conferences section of this issue reminded me that the coming months will have plenty of opportunities to share your knowledge at one of the technical conferences, and to learn from others who are attending. These are great opportunities to greet old friends and meet new ones. There are major technical conferences all across the country this year, from the Central States VHF Conference in Texas to the Eastern VHF/UHF Conference (and Microwave Update) in Connecticut, from the ARRL/TAPR Digital Communications Conference in Baltimore to the AMSAT Space Symposium in California. Of course there are also dozens of local hamfests and conventions around the country, and many of those have excellent technical presentations as well (or they could if you volunteered to present a program).

I'll be making plans to attend the ARRL/TAPR DCC again this year (Sep 16-18), and I hope to meet many readers (and perhaps recruit some new ones) in Baltimore at that time.



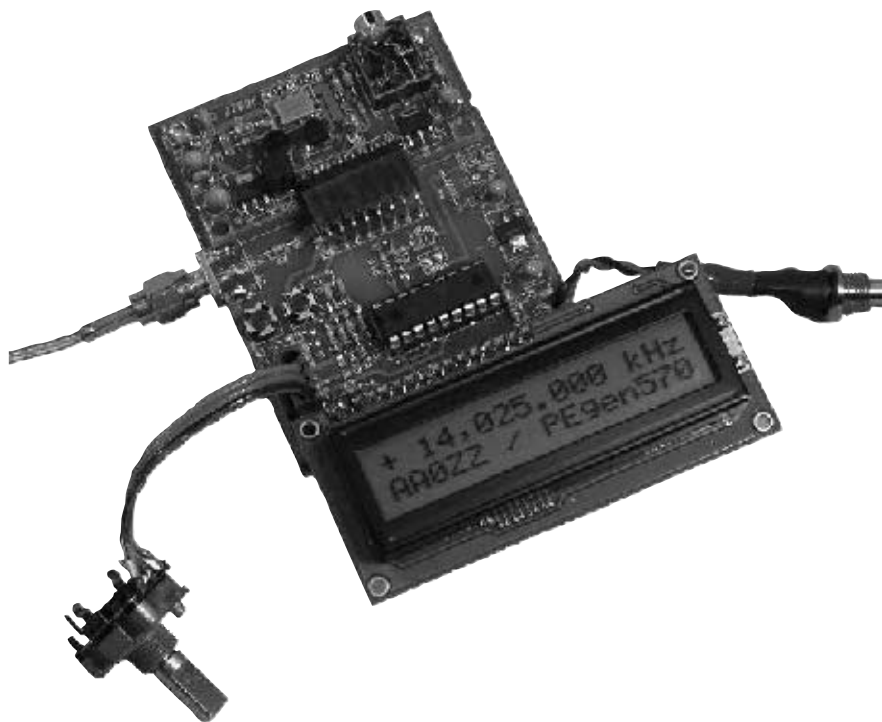
Programmable PLL (Si570) Local Oscillator for HF Receivers, Transmitters and Tranceivers

The Silicon Labs Si570 is a versatile programmable phase locked loop IC with many possible Amateur Radio applications. This PLL synthesizer is one good example.

A new product has recently been developed by Silicon Labs, the Si570 DSPLL[®] programmable frequency synthesizer, and it has great potential for use in many Amateur Radio applications. Here we will explore some possible uses. Phase locked loop technology has been in use for many years, but the ability to use variable software-supplied loop parameters in PLL technology to directly generate square waves with frequency resolutions of 1 Hz or better is now possible. The Si570 immediately puts the new technology into the sphere of uses that has recently been dominated by direct digital synthesis (DDS) products.

This AA0ZZ Si570 daughtercard uses the Silicon Labs Si570 (CMOS version) and, when controlled by a microcontroller, can generate RF signals in the continuous range of 10 to 157 MHz. (Other versions of the Si570 can go up to 1.4 GHz.) When the daughtercard is incorporated into a control board, the Si570 daughtercard can easily be used as the local oscillator of an Amateur Radio transceiver. Since many amateurs use divide-by-four mechanisms in quadrature sampling detectors (QSD) — also known as “Taylor” mixers — for their receivers and also in quadrature sampling exciters (QSE) for their transmitters, this Si570 daughtercard can provide the local oscillator signal for these receivers and transmitters on the 80 through 10 meter amateur bands.¹

¹Notes appear on page 16.



Si570 Operation

Figure 1 shows a block diagram of the Si570. The Si570 offers some significant advantages over the DDS parts that have been used by amateurs in applications in recent years. Two advantages are greatly reduced power consumption and the relatively clean output without DDS byproducts (spurs). The Si570 uses a combination of DSP processing and a PLL topology with frequency selection parameters set by the user via an PC serial communications link to

generate the desired output frequency.

Silicon Labs offers several versions of the Si570 with different output options and frequency limits. I used a CMOS version of the Si570 for this project. It has a 10.0 MHz default frequency and a 160 MHz maximum frequency. The internal crystal of the Si570 runs at a nominal 114.285 MHz. The crystal in any individual part will not oscillate at exactly this frequency, however. Since the crystal frequency is used in the frequency generation calculations for the Si570 input

parameter words, any deviation from nominal means that the Si570 generated frequency will not be accurate. Fortunately, Silicon Labs calibrates each individual part in the factory and saves the calibrated parameters in its nonvolatile memory to cause it to start up at the default frequency (in this case, 10.0 MHz). The software can retrieve these parameters from the nonvolatile memory and thus calculate the calibrated crystal frequency. This calibrated crystal frequency can then be used in subsequent calculations and the results will be much more accurate than they would be if the nominal crystal frequency was used for the calculations.

Si570 Functional Description

The spec sheet of the Si570 is a real challenge to interpret. The description given here will not substitute for a thorough reading of the spec sheet but it will get you started. (You can find the full details on the Silicon Labs website at www.silabs.com/SupportDocuments/TechnicalDocs/si570.pdf.)

Command data bytes are sent from the controller to the Si570 registers by way of the standard I²C serial communications protocol. (The I²C communications protocol is described later in the article.) The basic control registers are shown in Table 1.

Si570 Output Frequency Generation

The Si570 has a digitally-controlled oscillator (DCO), driven by a fixed-frequency crystal and PLL loop-control parameters. There are three frequency selection parameters that the software must set up for the Si570 to generate the desired output frequency. The basic frequency generation formula is:

$$F_{out} = (F_{xtal} \times RFREQ) / (HS_DIV \times N1)$$

where:

F_{xtal} is the fixed crystal frequency (114.285 MHz nominal) RFREQ is a 38 bit variable consisting of a 10 bit integer and a 28 bit fraction. HS_DIV can be 4, 5, 6, 7, 9 or 11. N1 can be 1 or any even integer between (and including) 2 and 128.

Additional parameter selection constraints are as follows. First, the DCO frequency specified in the numerator of this equation ($F_{xtal} \times RFREQ$) must always be in the range of 4.85 GHz to 5.67 GHz. Since the F_{xtal} value is 114.285 MHz, the RFREQ range is 42.44 to 49.613. This DCO

range can be stretched to some extent, as evidenced by the default setup parameters set up in a sample Si570 with factory settings for 10 MHz (see the SetupFxtal routine later in the article).

The second constraint is to optimize for minimal power consumption. Many different combinations of RFREQ, N1 and HS_DIV that will produce a given output frequency are possible to use. The lowest value of N1, along with the highest value of HS_DIV results in the lowest power consumption.

Si570 Freeze DCO

When specifying the parameters for

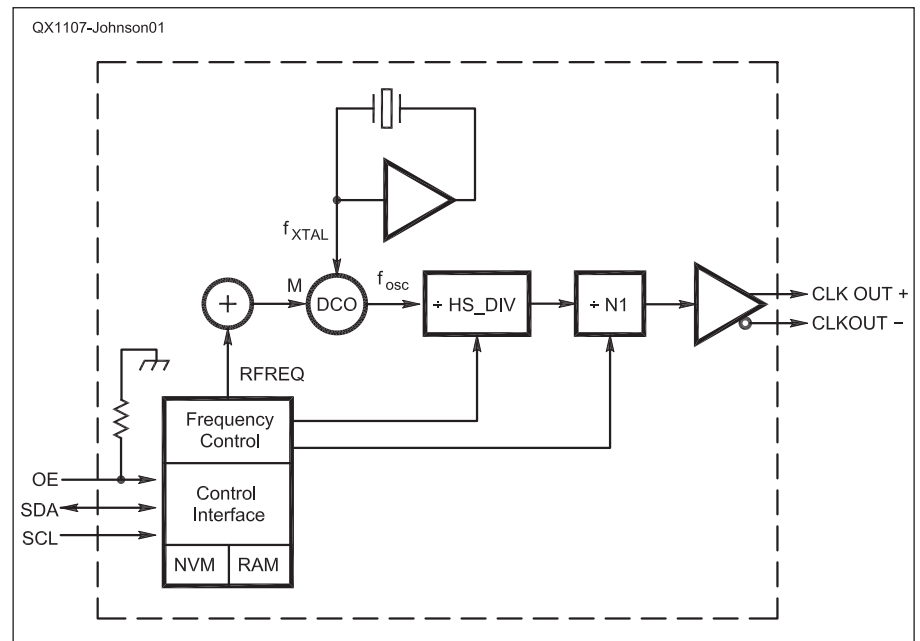


Figure 1 — Here is a simple block diagram illustrating the operation of the Silicon Labs Si570 programmable PLL IC.

Table 1

Si570 Control Registers

Register	Bit 7	Bit 6	Bit 5	Bit 4	Bit 3	Bit 2	Bit 1	Bit 0
Si Reg 7	HS_DIV_Index [2:0]			(N1 - 1) [6:2]				
Si Reg 8	(N1 - 1) [1:0]		RFREQ (integer) [37:32]					
Si Reg 9	RFREQ (integer) [31:28]				RFREQ (fractional) [27:24]			
Si Reg 10	RFREQ (fractional) [23:16]							
Si Reg 11	RFREQ (fractional) [15:8]							
Si Reg 12	RFREQ (fractional) [7:0]							
Si Reg 135	RST_REG	New Freq	Freeze M					RECALL
Si Reg 137				Freeze DCO				

Figure 2 — This drawing illustrates the frequency range that does not require a DCO Freeze operation before changing frequency. A larger change will require a DCO Freeze operation first.

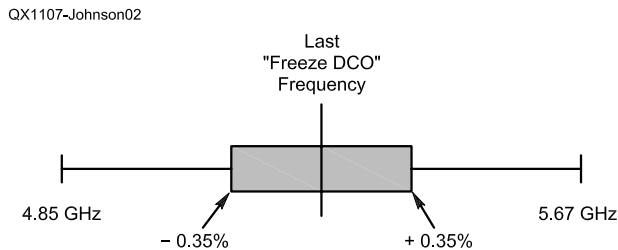
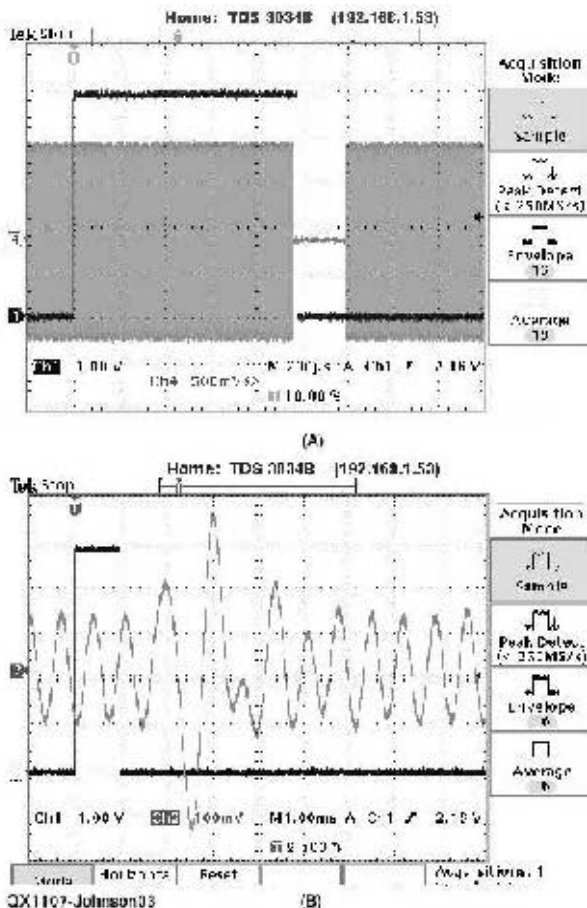


Figure 3 — Part A shows an oscilloscope display of the RF dropout following a DCO Freeze. Part B shows an oscilloscope display of the audio “pop” that follows a DCO Freeze.



changing the output frequency of the Si570, the current frequency must also be considered. Large frequency changes require the DCO to be stopped and restarted before it can jump to the new frequency while small changes do not. Freezing the DCO is done by setting the “Freeze DCO” bit (bit 4 in SiReg 137) before sending the normal frequency update registers (Registers 7 - 12) to the Si570. After the frequency update the “Freeze DCO” bit is cleared to unlock the DCO.

If the difference between the new frequency and the last freeze frequency is more than 3500 parts per million (0.35%) of the last freeze frequency, a DCO freeze is needed. Figure 2 shows the frequency range of the DCO oscillator (specified by $F_{xtal} \times RFREQ$) and the frequency range that can be covered without a freeze. If the output change is less than 0.35% from the last freeze frequency, the DCO frequency is the only value that needs to be changed for the frequency update.

Why not just do a freeze/unfreeze on every frequency update and skip the calculation to determine whether or not it is necessary? Because it can take a relatively long time (up to 10 ms) for the RF to “settle” on the new frequency and the RF output is stopped during this period. See Figure 3.

In this example, trace 1 is high during the freeze-update-unfreeze sequence (980 μ s) and trace 4 shows the RF dropout (220 μ s). The RF dropout that occurs when the Si570 is stopped and restarted at the new frequency after a DCO freeze causes an audible pop in a receiver. See Figure 3B for an oscilloscope screen shot of the audio pop. Channel 1 is high during the DCO freeze and Channel 2 is the audio. Small frequency changes without a DCO freeze do not cause the pop sound.

Freeze M

It takes a measureable amount of time

Figure 4 — Here is an oscilloscope display of the Si570 RF output at 14.025 MHz.

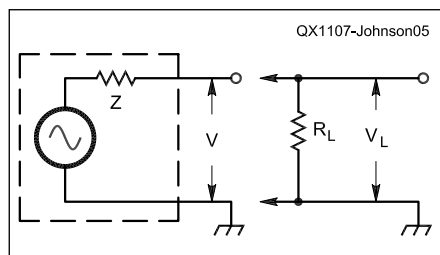
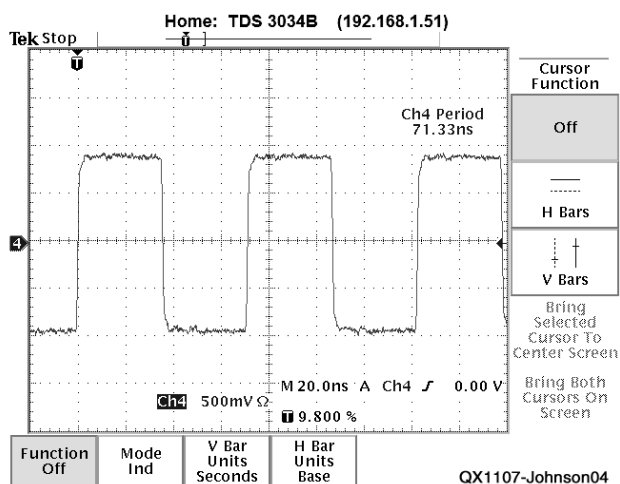


Figure 5 — A basic test circuit to measure the Si570 output impedance.

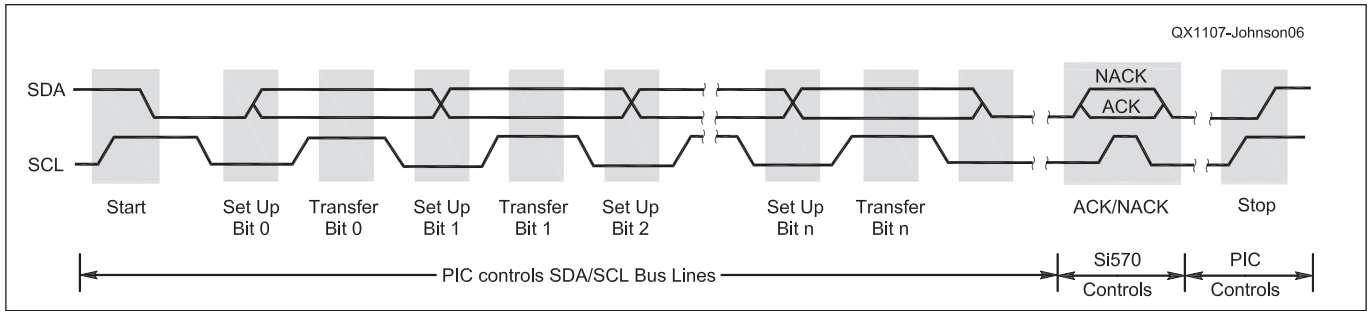


Figure 6 — The I2C data transfer timing diagram.

to send the six frequency configuration (RFREQ and loop parameter) bytes to the Si570 registers via the I2C communications link. (It takes 120 μs if sent at the maximum I2C communications link speed of 400 kHz and 667 μs in the PEgen570 application with an I2C rate of 72 kHz.) As the six bytes are being sent, one bit at a time, the Si570 is using the registers to spray RF signals at undesired frequencies. Granted, the time is short and the RF signal is often not being transmitted while the frequency is being changed so this random RF would not be going far, but it could be a significant problem for FSK (where the transmitter stays on as it shifts between the MARK and SPACE frequencies) or for other digital modes.

The FREEZE M feature solves this problem. The FREEZE M bit (Bit 5 in configuration byte 135) is designed to be set just before the frequency update is done and cleared after all six bytes are transferred. Note that this is different from the FREEZE DCO functionality, which is required when the frequency changes by more than 0.35% from the last freeze. The FREEZE DCO function will continue to be used; however, this is for the small frequency updates in which a FREEZE DCO is not needed. This new FREEZE M functionality causes the frequency update in the Si570 to be frozen until the FREEZE M bit is cleared. By then, all of the new frequency bytes are ready to be used and the Si570 jumps directly to that frequency.

Si570 RF Output and Output Impedance

The Si570 RF output is close to a square wave. An example of a CMOS Si570 running at 14.025 MHz into a 50 Ω load is shown in Figure 4. Here the output RF signal level is about 1.7 V p-p.

Calculations were done to determine the output impedance of the Si570. The basic test circuit is shown in Figure 5.

First the output voltage, V , is measured with no load resistor. This is the same as the source voltage, since there is no current through Z at this time. Then a shunt resistor with known resistance is placed across

the output and the voltage, V_L , is measured. Using the following equations, the output impedance is calculated.

$$I = V / (Z + R_L)$$

$$V_L = R_L \times I$$

$$V_L = R_L \times V / (Z + R_L)$$

$$Z = R_L \times ((V - V_L) / V_L)$$

An 18 Ω load resistor in the test circuit produced the following results:

$$V = 3.8 \text{ V}$$

$$V_L = 3.4 \text{ V}$$

$$Z = 18 \times ((2 - 1.2) / 1.2) = 12 \Omega$$

This means that a 38 Ω series resistor could be used to match the Si570 RF output to a 50 Ω load.

I2C Communications

The control interface to the Si570 is an I2C-compatible 2-wire bus for bidirectional communication. The I2C address for an Si570 is always 55 (hex). Since the slave address for I2C is a 7 bit field, the most significant bit is truncated and the direction bit (0 for a Write operation) is placed in the least significant bit of this byte. For a Write com-

mand to the Si570, the bit order is as shown in Table 2. The operation and timing of the two I2C signals on the bidirectional bus is illustrated in Figure 6.

When the source device and the destination device are communicating via the bidirectional I2C protocol, and they are operating with different voltage levels, hardware circuitry is necessary to translate the voltages. Many different schemes have been devised but a very simple and effective method, without the need for direction control signals, is described in the I2C Bus specification. With a single source (a PIC microcontroller) and a single destination (an Si570) the level shifting mechanism is as shown in Figure 7.

The level shifter consists of one discrete N-channel enhancement MOSFET for the serial data SDA bus line and one for the serial clock SCL bus line. The MOSFET gates are connected directly to the lowest supply voltage. The sources of the two MOSFETs are connected to the SDA and SCL bus lines on the 3.3 V device and the MOSFET drains are connected to the SDA and SCL bus lines

Table 2
The I2C bit order.

Start	Slave Adr + Dir	Ack	Data	Ack	Data	Ack	Stop
	1010101 0		xxxxxxx		xxxxxxx		

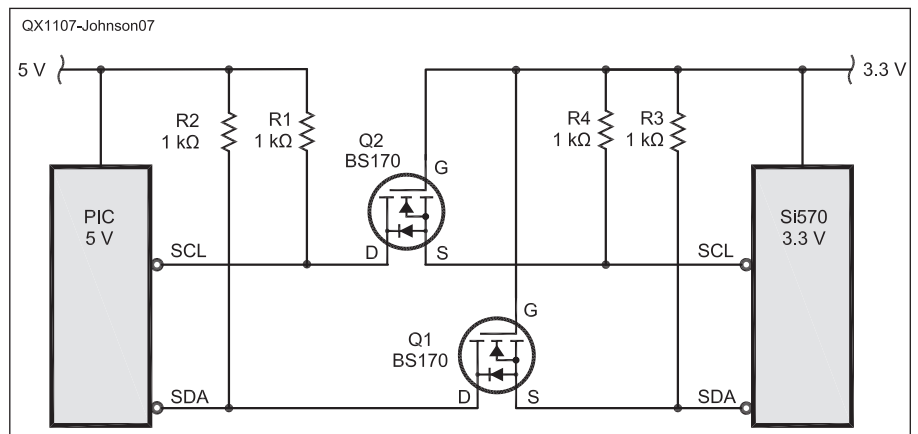


Figure 7 — This circuit shows an I2C level shifter.

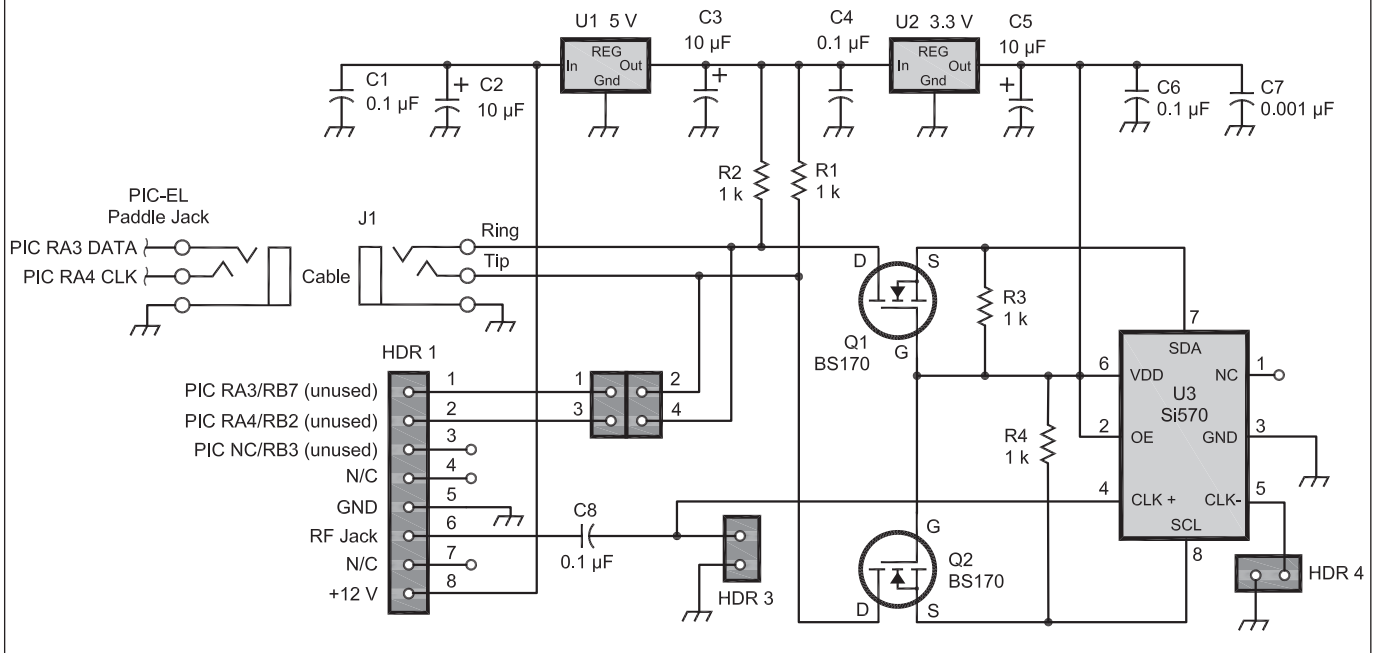


Figure 8 — The Si570 daughtercard schematic diagram.

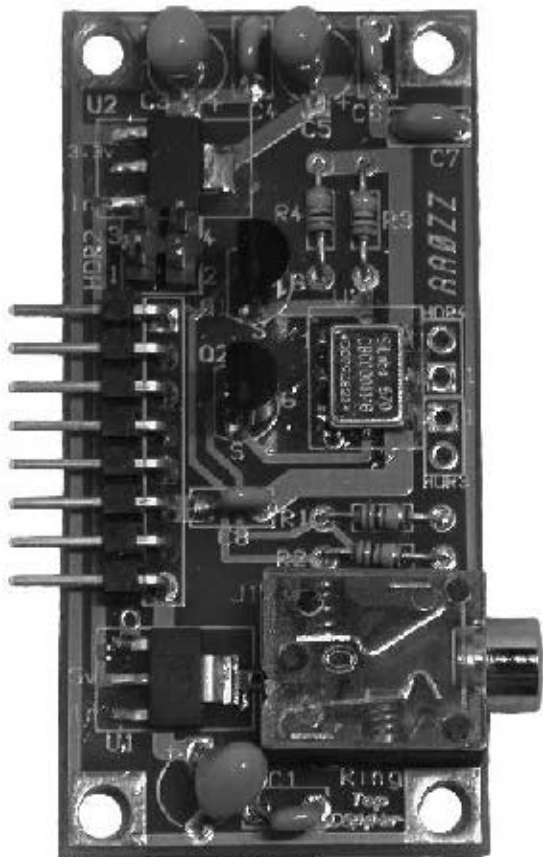


Figure 9 — This photo shows the Si570 daughtercard.

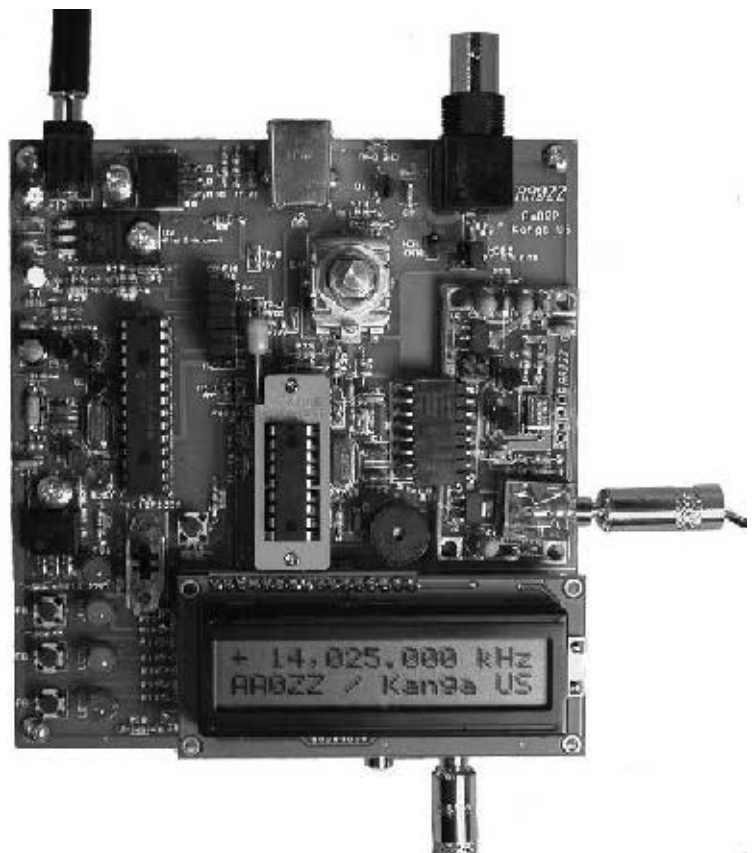


Figure 10 — Here, the Si570 daughtercard is plugged into the PIC-EL III board.

on the 5 V device. Each of these BS170 MOSFETs has an internal diode between the drain and source.

When neither device is pulling down a bus line (either SDA or SCL), the bus lines on the 3.3 V side are pulled up by the pull-up resistors R3 and R4 to 3.3 V. Since the gate and the source voltages of both MOSFETs are at 3.3 V, the V_{gs} voltages are below the turn-on threshold voltages so neither MOSFET is conducting. This allows the bus lines at the 5 V side to be pulled up by the pull-up resistors R1 and R2 to 5 V. The bus lines of both sides are HIGH but at different voltage levels.

When the 3.3 V device pulls down a bus line (SDA or SCL) to a LOW level, the source of the MOSFET also becomes LOW

while the gate stays at 3.3 V. As V_{gs} rises above the threshold, the MOSFET starts to conduct. The bus line on the 5 V side is also pulled down to a LOW level by the 3.3 V device via the conducting MOSFET. Both sides of the bus lines are LOW and at the same voltage level.

When the 5 V device pulls down a bus line (SDA or SCL) to a LOW level, the source of the MOSFET is also pulled to a LOW level via the drain-source diode internal to the MOSFET. As the source is pulled down, V_{gs} passes the turn-on threshold and the MOSFET starts to conduct. The bus line of the 3.3 V side is then further pulled down to a LOW level of the 5 V side via the conducting MOSFET. Both sides of the bus lines are LOW and at the same voltage level.

Si570 Daughtercard

The daughtercard schematic is shown in Figure 8. It has two voltage regulators. One converts 12 V to 5 V and the other converts 5 V to 3.3 V. Why not just bring a 5 V line from the PIC-EL to the daughtercard and avoid the 12 to 5 V regulator? Two voltage regulators are used because the PIC-EL daughtercard connector was designed to deliver 12 V for a DDS-30/60 daughtercard from the American QRP Club (www.amqrp.org), and the goal of this project was to use the existing PIC-EL circuitry without making hardware modifications.

Other versions of the Si570 have higher frequency limits but with reduced amplitude output. The spec sheet for the CMOS version

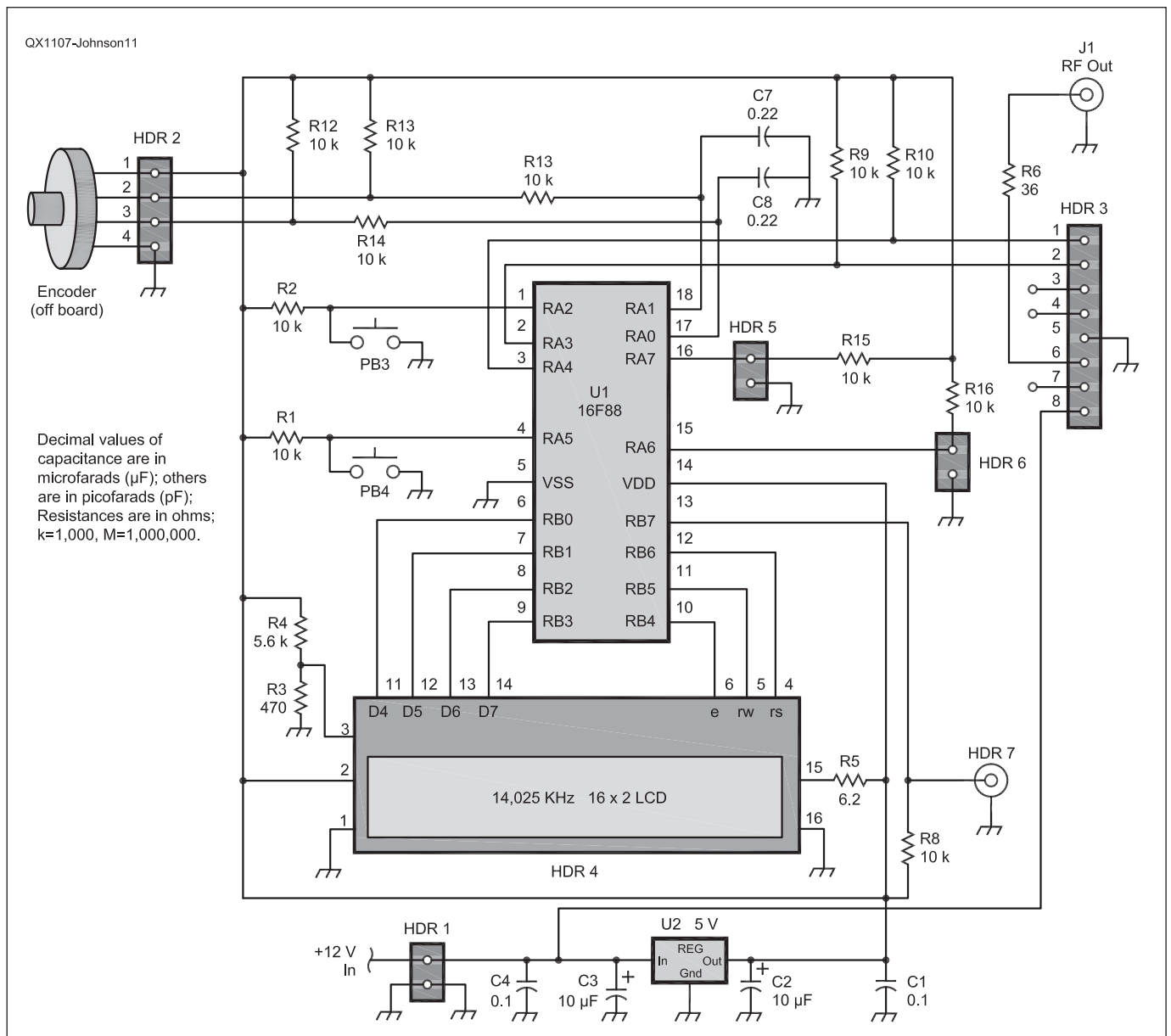


Figure 11 — This circuit is the Si570 control board schematic diagram.

says it operates between 10 and 160 MHz, but some users report it can be used between 3.5 and 240 MHz.

The daughtercard can be used in many different platforms. I will describe a couple of examples.

Daughtercard with PIC-EL

One platform for the Si570 daughtercard (Figure 9) is the AA0ZZ PIC-EL board (Figure 10). The PIC-EL board provides a very convenient platform for experimenting with the software to operate the Si570. I described the PIC-EL board in several *QST* articles.²

The Si570 daughtercard was designed to fit into an 8-pin socket on the PIC-EL board that was originally designed to accommodate an AmQRP DDS-30 or DDS-60 daughtercard. The DDS daughtercard operates with three control lines. The Si570 daughtercard is simpler in that it operates with two communications lines. The communications scheme used by the Si570 is I²C and that means the lines are both bidirectional. This presents a problem for the PIC-EL, since two of the three PIC lines that go to the daughtercard interface are also shared by the LCD and the other line is shared with the programmer. This sharing of pins prevents two-way communications via I²C with these lines. The workaround is to use an external cable to connect the daughtercard to the PIC-EL's paddle jack. The paddle jack connects to different PIC pins and these pins are only shared with PIC-EL Pushbuttons 2 and 3. These two pushbuttons cannot be used when operating the Si570 daughtercard but otherwise the lines work well for I²C communications.

The header (HDR2) on the daughtercard is a 2×2 connector block that is not used when the daughtercard is used in a PIC-EL with the external cable.

Daughtercard with Control Board

The Control Board schematic is shown in Figure 11.

When the daughtercard is used with a dedicated control board instead of a PIC-EL, then header HDR2, the 2×2 connector block, is put into use and the external cable from the stereo jack on the daughtercard to the driver platform is not needed. Two jumpers are installed in this header block (1 to 4 and 2 to 3) to route the I²C communications through the 8-pin interface connector.

The current required by the Si570 daughtercard alone is about 100 mA and the total current required by the daughtercard and the Control Board with LCD active is about 160 mA.

PEgen570 Software Application

The sample application software for the AA0ZZ Si570 daughtercard is called

PEgen570. It runs on a simple, inexpensive 16F88 PIC in the PIC-EL board. There are several reasons why the 16F88 was selected for this application instead of the PIC-EL standard 16F628A:

1) Compared to the 16F628A, the 16F88 has twice as much FLASH memory (for program instructions), 50% more data memory (for variable storage and tables) and twice as much EEPROM memory (non-volatile storage).

2) The 16F88 has an 8 MHz internal oscillator while the 16F628A has a 4 MHz internal oscillator. The extra speed is helpful.

Obviously, the user interface in the PEgen570 app is much simplified from the user interface in my IQPro DDS VFO but the application was simplified such that it could be developed and debugged on the PIC-EL board.³

Figure 12 shows an oscilloscope snapshot of the start of an I²C communication sequence in which the control board is sending a frequency update to the daughtercard. The I²C communications sequence begins with the falling edge of the SDA line (Channel 2) while the SCL line (Channel 1) is high. The next bits show the beginning of the 55 (hex) device address (lower 7 bits) as described in the I²C Communications section. The clock rate in this implementation is 72 kHz. Since the Si570 can handle speeds up to 400 kHz, this rate is well below the limit.

Frequency Selection Method

The methods for selecting N1, HS_DIV and calculating RFREQ for every frequency update are many. They can also be very time consuming, so optimization is especially important for a small microcontroller. For this reason, the following scheme was developed.

1) Create a list of pairings of all valid N1

and HS_DIV values. Calculate the frequency ranges that can be reached with each of these pairings. The total set of ranges must cover the intended operational range (10 MHz to 157 MHz). Since there are 65 valid N1 values and 6 valid HS_DIV values, there are 390 valid pairings, so there are 390 valid frequency ranges in this working table.

2) Examine the working set of pre-calculated frequency ranges for the N1 and HS_DIV pairings and select the minimum number of frequency ranges (bands) that can span the intended operational range of 10 to 157 MHz without gaps while starting and ending on MHz boundaries. Look for the bands with the widest frequency spans while also looking for the lowest N1 values and highest HS_DIV values. The total number of bands is limited by the size of a microcontroller memory bank (96 bytes) and each band entry requires 4 bytes, so 24 bands are possible.

3) Create a table that contains entries for the lowest frequency of each of the 24 bands.

4) Create a table of 1 byte entries for the selected bands, with each entry being constructed by multiplying the selected N1 by the HS_DIV value and then dividing the product by 2. If the N1 and HS_DIV pairings selected in Step 2 do not fit into 1 byte after they are multiplied and divided by 2, then rework the band selection tables. This may force the selection of some non-optimal N1 and HS_DIV pairings. It also limits the total operational range.

Note that no significant figures are lost in dividing the N1 and HS_DIV product by 2, since each valid N1 is an even number (or 1). The RFREQ calculations will take into account the fact that this division by 2 has taken place.

5) Construct the table, which contains entries combining Fxtal with N1 and HS_

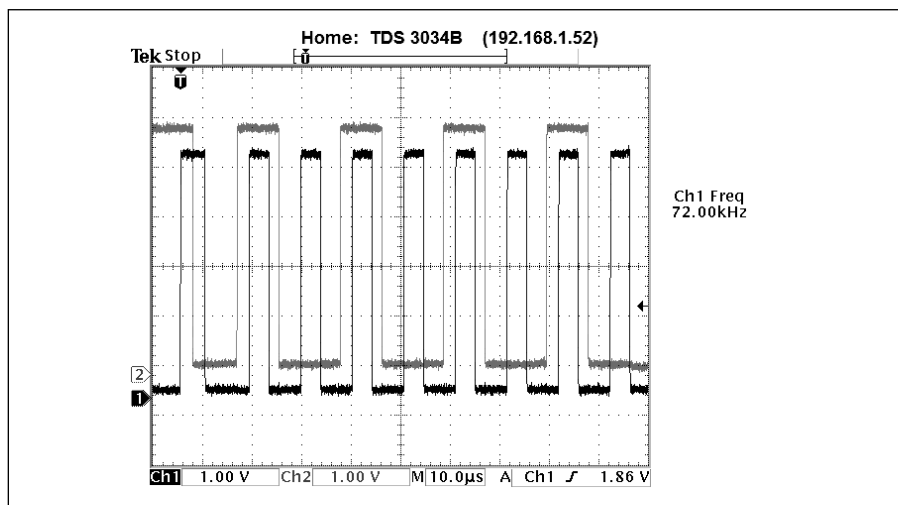


Figure 12 — This oscilloscope display shows the I²C communications, with SDA/SDC signals in the PEgen570 software application.

DIV for the corresponding frequency bands. Each entry will be $F_{xtal} / (N1 \times HS_DIV)$.

6) To calculate RFREQ for a given frequency, retrieve the appropriate table entry containing $F_{xtal} / (N1 \times HS_DIV)$ and divide the desired output frequency by this value. The result of this division must be a 10 bit integer and a 28 bit fraction.

7) Position N1, HS_DIV and RFREQ in the command packet to be sent via I²C to the Si570 control registers. To be exact, store $(N1 - 1)$ instead of N1 and store the 3 bit

index corresponding to the selected HS_DIV value.

This scheme provides a relatively quick Si570 frequency update with some table look-ups and a single division. This single mathematical operation is not a simple one, however, since it divides a 40 bit integer value by a 32 bit integer value and results in a 10 bit integer and a 28 bit fraction positioned such that the five bytes can be directly loaded into the Si570 registers.

DCO Freeze Handling

Earlier in the article, I described the Si570 requirement for a DCO freeze when updating the frequency, if the frequency has moved by more than 3500 ppm (0.35%) from the last freeze frequency.

The software keeps track of the frequency at which the last freeze operation was done. If the difference between the new frequency and the last freeze frequency is more than 0.35% of the last freeze frequency, the freeze

Table 3
RFREQ in Si570 Registers

Register	Bit 7	Bit 6	Bit 5	Bit 4	Bit 3	Bit 2	Bit 1	Bit 0	Hex
Si Reg 7	X	X	X	X	X	X	X	X	0xXX
Si Reg 8	X	X	0	0	0	0	1	0	0x02
Si Reg 9	1	1	0	1	1	1	1	0	0xDE
Si Reg 10	0	1	0	1	1	0	1	0	0x5A
Si Reg 11	1	0	0	0	1	1	0	1	0x85
Si Reg 12	0	1	0	1	0	1	0	0	0x55
SiReg135									
SiReg137									

HS_DIV_Index [2:0]
(N1 - 1) [6:0]
RFREQ-integer [37:28]
RFREQ-fractional [27:0]

Table 4
RFREQ, HSDIV and N1 in Si570 Registers

Register	Bit 7	Bit 6	Bit 5	Bit 4	Bit 3	Bit 2	Bit 1	Bit 0	Hex
Si Reg 7	1	1	1	0	1	0	0	0	0xE8
Si Reg 8	0	1	0	0	0	0	1	0	0x42
Si Reg 9	1	1	0	1	1	1	1	0	0xDE
Si Reg 10	0	1	0	1	1	0	1	0	0x5A
Si Reg 11	1	0	0	0	1	1	0	1	0x85
Si Reg 12	0	1	0	1	0	1	0	0	0x55
SiReg135									
SiReg137									

HS_DIV_Index [2:0]
(N1 - 1) [6:0]
RFREQ-integer [37:28]
RFREQ-fractional [27:0]

Table 5
RFREQ Extracted From Nonvolatile Memory

Register	Bit 7	Bit 6	Bit 5	Bit 4	Bit 3	Bit 2	Bit 1	Bit 0	Hex
Si Reg 7	0	1	0	1	0	0	1	1	0x53
Si Reg 8	1	1	0	0	0	0	1	0	0xC2
Si Reg 9	1	0	1	0	0	0	0	0	0xA0
Si Reg 10	0	1	0	1	0	0	0	0	0x50
Si Reg 11	1	1	1	0	1	0	0	1	0xE9
Si Reg 12	1	1	1	1	1	1	0	1	0xFD
SiReg135									
SiReg137									

HS_DIV_Index [2:0]
(N1 - 1) [6:0]
RFREQ-integer [37:28]
RFREQ-fractional [27:0]

and unfreeze operations are done along with the frequency update. Rather than doing another large division operation, the actual calculation is performed in a simplified manner by determining whether or not the new DCO frequency ($F_{xtal} \times RFREQ$) has moved by more than 0.35%. Since F_{xtal} is a constant, the worst case is found by taking the lower limit of the integer portion of the $RFREQ$ (42) and multiplying by 0.35%.

$$42 \times 0.35\% = 0.147$$

Then, if the software determines the new $RFREQ$ is changed by more than the constant 0.147 from the last freeze, a new freeze is done.

Major Subroutines of PEGen570

The frequency selection scheme that is used in PEGen570 was described earlier. This routine is called when a frequency update is needed. The job of this routine is to calculate the 38 bit $RFREQ$ value with a 10 bit integer portion and a 28 bit fractional portion.

$$RFREQ = (F_{out} \times HS_DIV \times N1) / F_{xtal}$$

For quick calculation in a small microcontroller, the combination of factors HS_DIV , $N1$, and F_{xtal} are scaled, combined and placed in a table indexed by the frequency band number. Now, instead of multiplying F_{out} by $(HS_DIV \times N1) / F_{xtal}$, a table look-up is done and a single division operation is performed in which F_{out} is divided by the reciprocal.

$$RFREQ = F_{out} / (F_{xtal} / (HS_DIV \times N1))$$

This division is a 40 bit by 32 bit operation.

(Note: Typical 32 bit by 32 bit integer division routines result in an integer with the remainder truncated but this division routine performs additional cycles through the division mechanism in order to calculate and retain the fractional portion also.)

Sample calculation:

$$F_{out} = 14,025,000 \text{ (D60128)}$$

Hex)

$$F_{xtal} = 114,285,000 \text{ (6CFD9C8)}$$

Hex)

$$HS_DIV = 11 \text{ (D Hex)}$$

$$N1 = 34 \text{ (22 Hex)}$$

$$RFREQ \text{ (scaled by } 2^{28}) =$$

$$2DE5A8555 \text{ (Hex)}$$

The $RFREQ$ value is scaled by 2^{28} . The integer portion is 2D (Hex) and the fractional portion is E5A8555 (Hex). The $RFREQ$ value is scaled in this manner so that it is ready to be loaded into the Si570 registers as shown in Table 3.

Later, when the HS_DIV and $N1$ values are manipulated into the required form (HS_DIV_Index and $N1 - 1$) and added to the Si570 registers, the result is shown in Table 4.

The Si570 band tables for PEGen570 are described in Table 6. The entries of the table are pre-calculated using the nominal value for the Si570 internal crystal frequency

(114.285 MHz). The table entries, combining the crystal frequency with other parameters needed to generate RF in that frequency range, are stored in the PIC EEPROM and are loaded into the PIC volatile memory at power-up. This nominal frequency is almost never perfect, of course, but the Si570 is calibrated in the factory to use corrected parameter values in order to produce the default start-up output frequency of exactly 10.00 MHz. (Other Si570 part numbers use different start-up frequencies.)

By holding Pushbutton 3 down during power-up, the application is directed to retrieve the parameters from the Si570 non-volatile EEPROM memory. The software then does a "reverse calculation" to find the actual Si570 crystal frequency as determined by the factory to produce 10.00 MHz. After the actual crystal frequency is determined, the table entries are recalculated and copied back to non-volatile EEPROM. When Pushbutton 3 is released, the PIC restarts and populates the tables with the newly calculated values.

The SetupFxtal(•) routine is called at calibration time only. It retrieves the Si570 registers from the part, extracts the HS_DIV , $N1$, and $RFREQ$ values, and uses this formula to find the calibrated crystal frequency as determined during manufacturing. The default frequency for the Si570 being used in this project (570CAC000107DG or 570CBC000107DG) is 10.0 MHz.

Normal frequency formula: $F_{out} = (F_{xtal} \times RFREQ) / (HS_DIV \times N1)$

Rearranged to give: $F_{xtal} = (F_{out} \times HS_DIV \times N1) / RFREQ$

The following steps are taken:

- 1) Extract HSDIV_Index from the Si570 words and convert to HS_DIV .
- 2) Extract $(N1 - 1)$ from the Si570 words and convert to $N1$.

3) Extract $RFREQ$ from the Si570 words.

4) Multiply HS_DIV by $N1$.

5) Divide $RFREQ$ by $(HS_DIV \times N1)$.

6) Divide by default F_{out} (10,000,000).

As an example, Table 5 shows values as extracted from one Si570 with a 10 MHz start-up frequency.

The values of the fields of the registrations shown in Table 5 are as follows:

Extracted HS_DIV Index = 2 so HS_DIV is 6.

Extracted $(N1 - 1) = 4F$ (hex) which is 79 (dec) so $N1 = 80$ (dec).

Extracted $RFREQ$ Integer = 2A (hex) or 42 (dec).

Extracted $RFREQ$ Fractional = 050E9FD (hex).

Note that $RFREQ$ is scaled by 2^{28} . The decimal value can be determined by converting the entire $RFREQ$ value to decimal and then dividing by 2^{28} .

$$RFREQ = 2A050E9FD \text{ (hex)} =$$

11,279,591,933 (dec).

$$11,279,591,933 / 2^{28} = 11,279,591,933 / 268,435,456 = 42.0197.$$

The CalDivide routine is used in the SetupFxtal routine. It performs this calculation:

Calculate F_{xtal} with this formula:

$$F_{xtal} = (F_{out} \times HS_DIV \times N1) / RFREQ$$

Form used by routine:

$$F_{xtal} = (F_{out} / RFREQ) \times HS_DIV \times N1$$

This requires a 40 bit by 40 bit division followed by a 32 bit by 8 bit multiplication. To retain important significant figures, F_{xtal} is scaled by multiplying it by 256 before the division, so F_{out} must also be scaled by 256 before performing the calculation.

$$F_{xtal} \times 256 = (10,000,000 \times 256) \times (6 \times 80) / 42.0197$$

$F_{xtal} = 114.231984$ MHz (compare to 114.285 MHz nominal) Note that this F_{xtal} value, extracted from one sample Si570, is only 0.05% from nominal.

This F_{xtal} value, along with corresponding HS_DIV and $N1$ values from the band tables (described later), is then used to recalculate all values in the HSN1FX table in EEPROM. This table is copied from EEPROM to working (SRAM) memory at power-up so calibrated values will be used for all subsequent $RFREQ$ calculations.

Si570 Bands

The PEGen570 software is implemented with 24 frequency bands. (Note that these do not correspond to amateur bands.) Most of the parameters that the Si570 requires to produce the desired output RF signal are in tables in program memory. These program memory tables cannot be modified with program instructions. These tables are used by the application by using the band number as an index.

One table is located in the PIC data memory, and can be modified. This table is populated by extracting values from EEPROM upon power-up. This table consists of 24 entries, each entry containing a starting frequency requiring 4 bytes. This means that the 24 band table requires 96 bytes of memory. Since the maximum size of any single bank of data memory in the 16F88 (or any "16F" PIC for that matter) is 96 bytes, this determines the maximum number of bands that can easily be handled in the PIC. With additional overhead the size could be expanded and then the upper frequency could be increased. The CMOS version of the Si570, however (the version that the daughtercard is designed to use), has a maximum frequency of 160 MHz. This means the current 96 byte table with an upper limit of 157 MHz is reasonable for this Si570 version. The lower limit of the Si570 is 10 MHz and the 96 byte table also handles this limit.

The 24 PEGen570 bands were created by

Table 6
PEgen570 Bands

BAND	Frequency Range	BAND	Frequency Range	BAND	Frequency Range	BAND	Frequency Range
0	10 - 11 MHz	6	19 - 21 MHz	12	36 - 41 MHz	18	81 - 90 MHz
1	11 - 12 MHz	7	21 - 23 MHz	13	41 - 47 MHz	19	90 - 101 MHz
2	12 - 13 MHz	8	23 - 25 MHz	14	47 - 54 MHz	20	101 - 111 MHz
3	13 - 15 MHz	9	25 - 28 MHz	15	54 - 61 MHz	21	111 - 128 MHz
4	15 - 17 MHz	10	28 - 32 MHz	16	61 - 70 MHz	22	128 - 135 MHz
5	17 - 19 MHz	11	32 - 36 MHz	17	70 - 81 MHz	23	135 - 157 MHz

examining the Si570 spec sheet and making calculations with a spreadsheet based on the Si570 parameter requirements. Without getting into the esoteric requirements of the Si570 frequency generating parameters and the formula involving several specific “multipliers,” the Si570 internal crystal frequency and the desired output frequency, the frequency range of each band was calculated. The table was generated in such a way that the major parameters for each band can be pre-calculated and retrieved from tables when changing frequency. This greatly minimizes the number of complex calculations that must be performed for each frequency change.

The 24 PEGen570 bands are defined in Table 6.

Several tables were constructed, ready for quick access by the frequency update routines. Each table has one entry per band (24 entries).

There is one table in EEPROM with each 4 byte entry containing a combination of HS-DIV, N1 and Fxtal. The table is initially populated with the default crystal frequency (114.285 MHz) but this table is updated during calibration with the actual crystal frequency that is measured and stored in the Si570 during manufacture.

Entries are constructed and scaled in this manner:

$$\text{HSN1FX} = (\text{Fxtal} / (\text{HS_DIV} \times \text{N1})) \times 256$$

At first glance it would appear that one byte is wasted per entry since multiplying by 256 appears to be simply shifting the original number by 1 byte. It is not that simple. The division operation results in a fractional quotient so multiplying by 256 by continuing the division for 8 additional steps preserves important significant figures of the fractional remainder. Subsequent calculations compensate for this scaling factor.

Example: The entry for Band 0 (covering 10 - 11 MHz) is:

$$\text{HSN1FX0} = (114,231,984) / (46 \times 11) \times 256 = 57,793,256 \text{ (dec)} = 371DAE8 \text{ (hex)}$$

Note that with the nominal crystal frequency the default entry would have been:

$$\text{HSN1FX0} = (114,285,000) / (46 \times 11) \times 256 = 57,820,079 \text{ (dec)} = 37243AF \text{ (hex)}$$

There is one table in volatile memory (SRAM). This table is identical to the

HSN1FX table in EEPROM. Accessing EEPROM during program execution is relatively slow so this 24 entry table is copied from EEPROM to fast-access program memory at power-up time (4 bytes per entry).

These tables have one entry per band in program (FLASH) memory.

1) SiBandTable — A table containing the lower limits (in MHz) of the frequencies for each band (4 bytes per entry).

2) BandN1Minus1 — A table containing the selected N1 value for each band (1 byte per entry).

3) BandHSDIVIndex — The selected HSDIV Index for each band (1 byte per entry).

4) BandHSNID2 — The selected values of HSDIV and N1 multiplied together and divided by 2 (1 byte per entry). No significant figures are lost in dividing the HS_DIV and N1 product by 2 since each selected N1 is an even number.

User Interface

The user interface for the PEGen570 application is very simple. It uses two push-buttons, an encoder, and a 2-line by 16-character LCD. A simple menu for changing configuration is activated via the two push-buttons.

The “Reset” pushbutton on the PIC-EL board is configured (via the CONFIG statement in the source code) such that it does not perform a microprocessor reset when pressed but to operate as a normal I/O pin instead. This made the pushbutton available for operation and it is needed. To clarify this change in usage, the pushbutton will be referred to as Pushbutton 4 rather than

the Reset pushbutton. This means that the PIC-EL board must be powered down and up after loading new software into the PIC before the new program will start executing. Simply moving the slide switch from PGM position to RUN position does not start the PEGen570 program.

Pushbutton 3 and Pushbutton 4 are the two operational pushbuttons. When running the Si570, each time Pushbutton 3 is pressed and released, the tuning digit that is currently being modified by turning the encoder is increased by one digit. It can be advanced up to the 1 MHz position. Similarly, each time Pushbutton 4 is pressed and released, the tuning digit that is currently being modified by turning the encoder is decreased by one digit. The digit that is currently being modified by the encoder is underlined.

When the program is running, pressing and holding Pushbutton 3 for longer than 2 seconds stores the current frequency in EEPROM. This frequency is used as the start-up frequency on subsequent power-ups.

Menu

A simple menu is used for changing mode between upper and lower sideband (USB, LSB, CW+ or CW-). Then the user can turn FSK on or off.

The menu is activated by holding Pushbutton 4 while pushing Pushbutton 3 and then releasing them both. The current mode is shown in character position 1 of line 1 of the LCD. Now, tapping Pushbutton 3 allows the user to toggle through the four sideband options, with the display showing U, L, + or -. Tapping Pushbutton 4 leaves this portion of the menu. Then FSK mode may be



Figure 13 — The first line of the LCD shows RFREQ.

enabled. The current FSK state is displayed (either F or blank) in character position 1 of line 1 of the LCD. Tapping Pushbutton 3 toggles FSK mode between on and off. Tapping Pushbutton 4 once again exits the menu.

Sideband Select Relay

An external latching relay is engaged or disengaged as the sideband is changed in the menu. PIC output ports RA6 and RA7 attach to HDR6 and HDR5 (pins 15 and 16) respectively. As the sideband is changed in the menu, either RA6 or RA7 is driven high with an 8 ms pulse (with the opposite side being held low) to engage or disengage the external latching relay. The recommended latching relay (TQ2-L-5V — DigiKey part 255-1004-5-ND) requires 14 mA at 5 V for 3 ms plus contact bounce time. The latching relay is intended to enable the proper I and Q phases of the transmitter and/or receiver to set the correct sideband.

Sidetone During Receive (or FSK Shift)

Header HDR7, attached to PIC input port RB7, is monitored by the software to deter-

mine whether or not to shift the frequency by the sidetone amount if FSK is not active, or to shift the frequency by the FSK shift size if FSK is active. In CW+ or CW- mode, HDR7 is expected to be set to a low state by exter-

nal transmit/receive circuitry during receive operations and to a high state during transmit operations. The software continually monitors the signal at HDR7 and, when it is detected to be low while in CW- mode, shifts

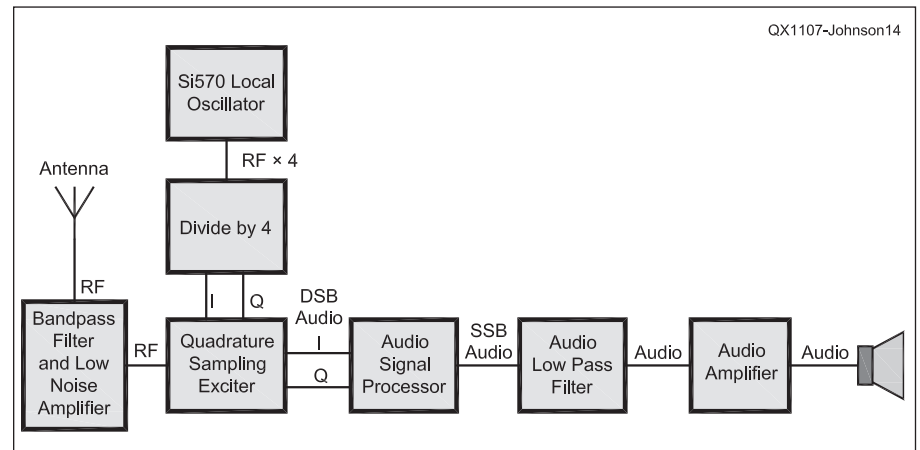


Figure 14 — This block diagram represents a CW or SSB Receiver.

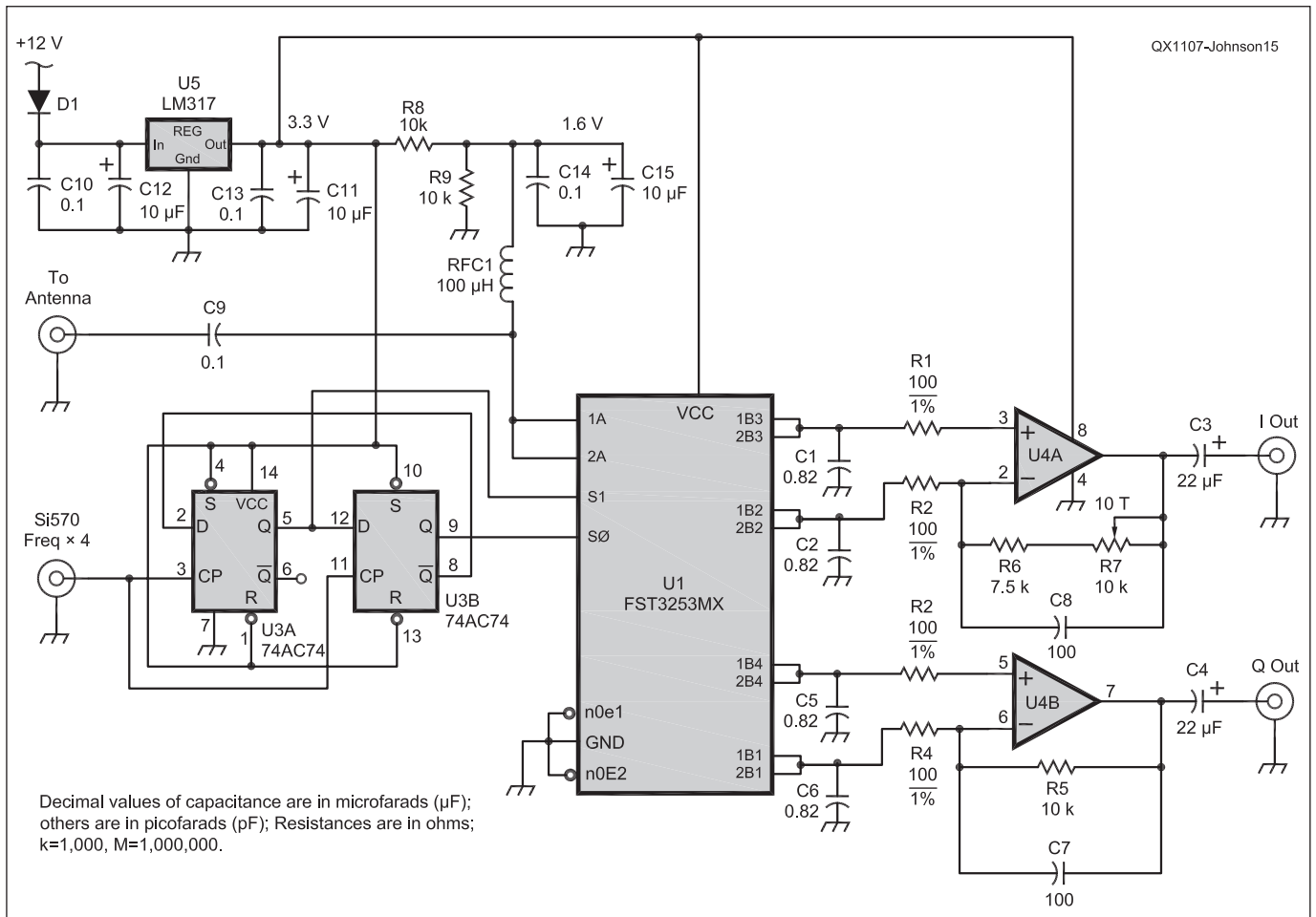


Figure 15 — Here is the schematic diagram of a receiver using the Si570 P-PLL and a PC for audio processing.

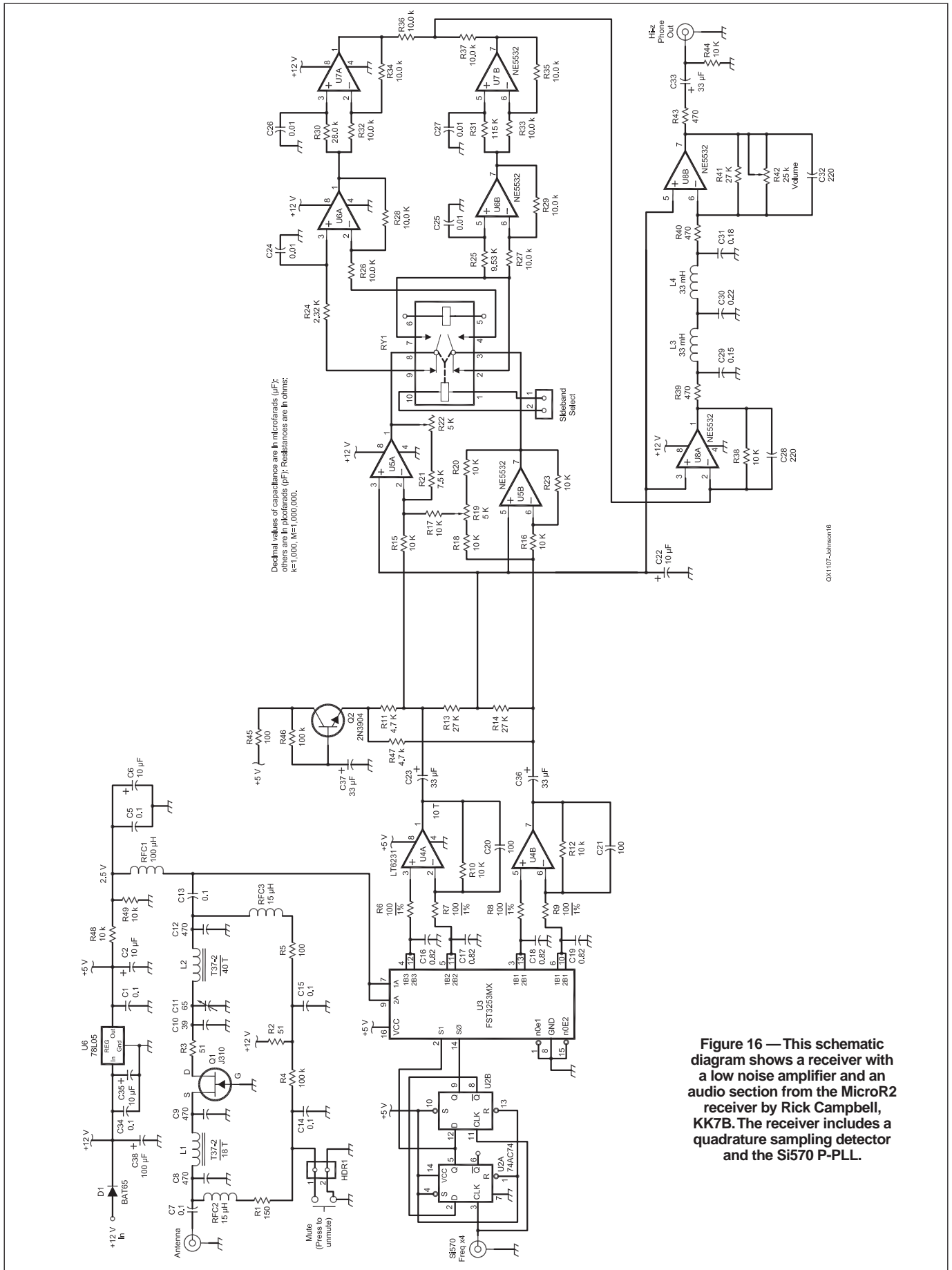


Figure 16 — This schematic diagram shows a receiver with a low noise amplifier and an audio section from the MicroR2 receiver by Rick Campbell, KK7B. The receiver includes a quadrature sampling detector and the Si570 P-PLL.

OX1107-Johnson16

the frequency down by 600 Hz from the nominal, displayed frequency. If the mode is CW+ and HDR7 is set LOW (receive), the frequency is shifted up by 600 Hz from the nominal, displayed frequency. In either case, whenever HDR7 is detected to be HIGH, indicating Transmit operation, the frequency will be set back to the nominal frequency that is displayed on the LCD.

When FSK mode is activated via the menu, the frequency is set to the displayed frequency when the signal on HDR7 is HIGH (the MARK frequency) and is shifted down by 170 Hz when the signal on HDR7 is LOW (the SPACE frequency).

How fast does it switch? The software looks at the signal on HDR7 often enough

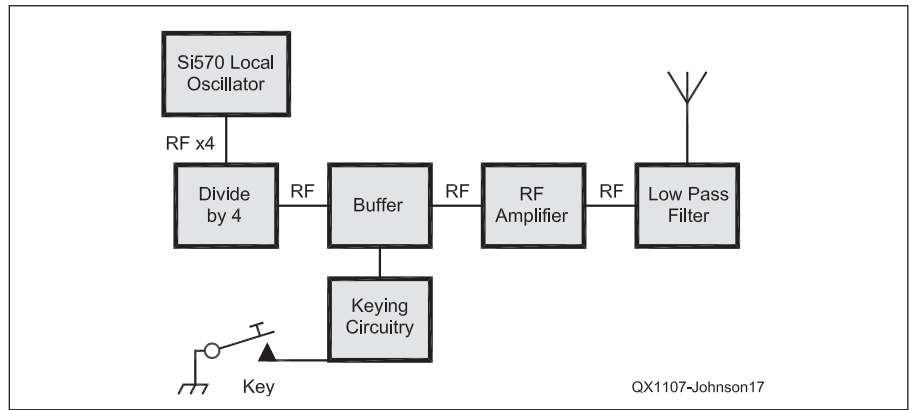


Figure 17 — A 40 m CW Transmitter is shown in this block diagram.

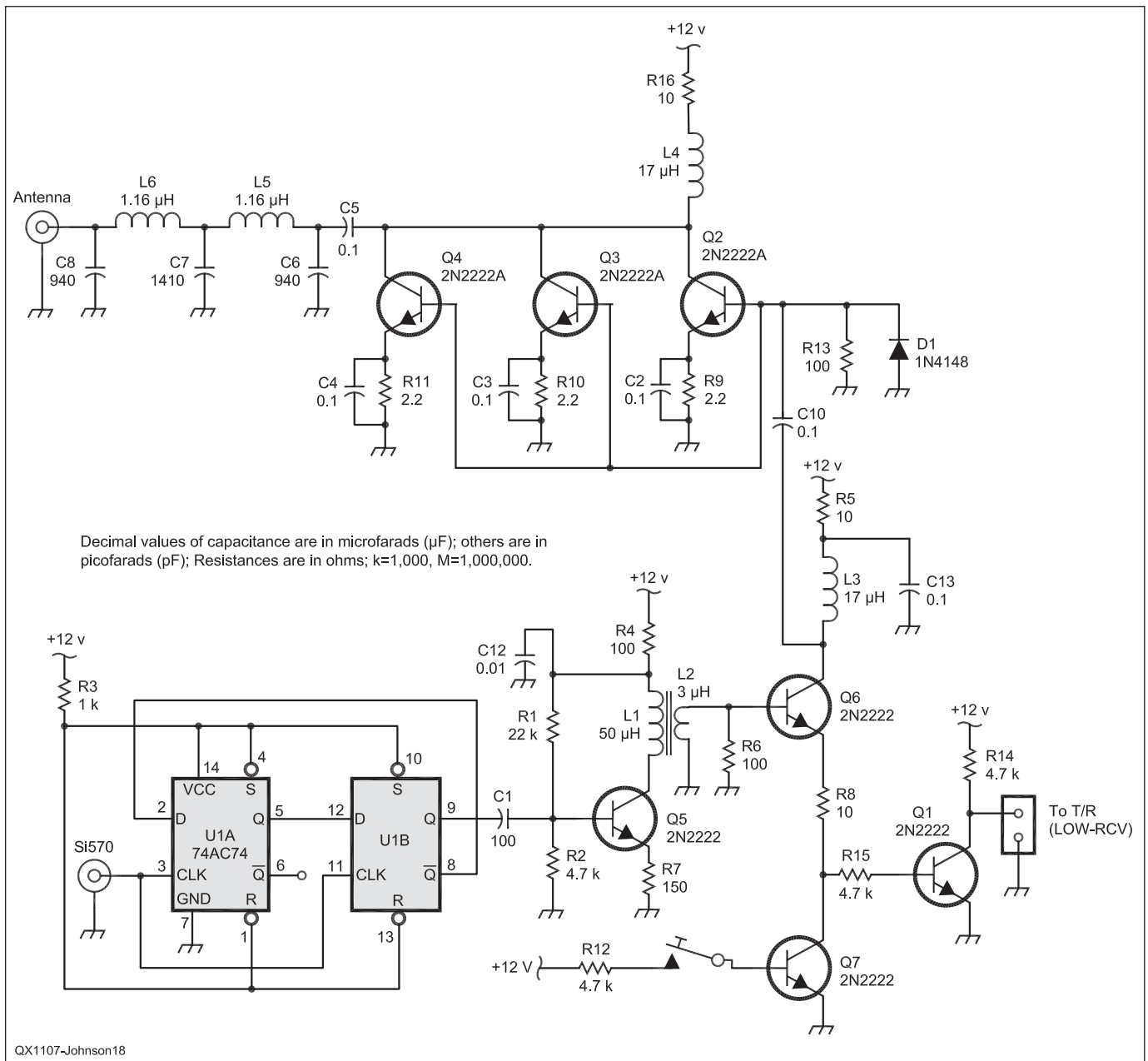


Figure 18 — This schematic diagram shows a 40 m CW Transmitter that uses the Si570 P-PLL as the local oscillator.

to detect and change the frequency within 1.6 ms of HDR7 changing state. That's fast enough for QSK.

Liquid Crystal Display

The first line of the LCD shows the current frequency. The second line is for debug purposes and when debug mode is enabled, shows the hex digits for the six Si570 frequency-specifying registers (SiReg7 through SiReg12) starting at LCD position 1. The current band number is displayed in positions 15 and 16 of line 2.

The PEGen570 application can be configured to display the Si570 frequency or it can be configured to display the Si570 frequency divided by two or four. The divide-by-four option is useful when the signal generator is being used as a signal source for a QSD/QSE ("Tayloe") mixer. The circuitry for these mixers usually divides the input frequency by four so this software option allows the LCD to display the mixer's operating frequency.

FSK Operation

PEGen570 has the capability of running in FSK mode as well. When FSK mode is enabled in the software, header HDR7 on the Control Board is used for FSK modulation. When HDR7 is modulated (header pins "opened" or "shorted" by external hardware circuitry) the frequency is shifted from MARK (nominal frequency) to SPACE (170 Hz below nominal displayed frequency). When HDR7 is set high (not shorted to ground) the software will command the Si570 to generate RF at the MARK frequency and when HDR7 is set low (shorted to ground) the software will command the Si570 to generate RF at the SPACE frequency.

If the user is not interested in FSK operation, header HDR7 is available for re-commissioning.

Debug Mode

If debug mode is turned on (by pressing and holding PB3 and PB4 during power-up), the Si570 registers and the current Si570 band number are displayed on the second line of the LCD, as shown in Figure 13.

Ideas for Future Modification

The source code of this software is available for download from the ARRL QEX website, for experimenters to examine, change and extend to accommodate personal preferences.⁴ A couple of items are easy to imagine:

1) Make the CW sidetone frequency changeable. Currently the sidetone frequency is fixed at 600 Hz. (600 Hz is added to or subtracted from the base frequency during receive operation and the base frequency is restored during transmit operation.)

2) Display additional information on the LCD: receive versus transmit, sidetone and so on.

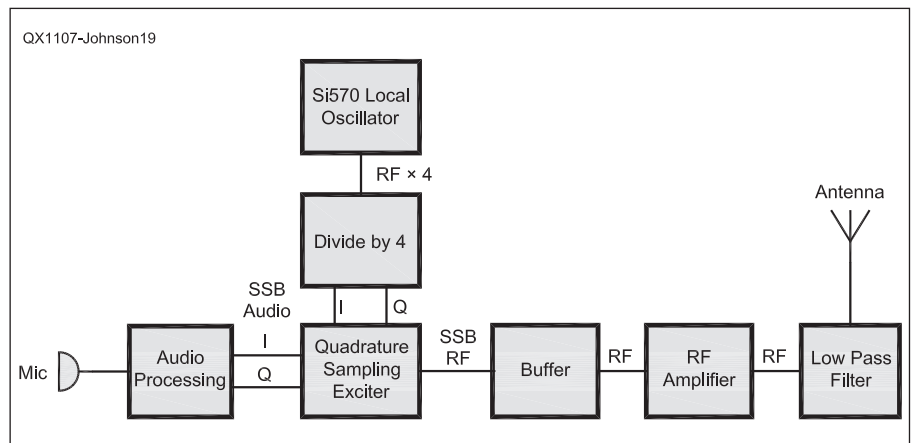


Figure 19 — Here is a block diagram of a 40 m SSB Transmitter that uses the Si570 P-PLL as the local oscillator.

3) Startup frequency is now saved in EEPROM. Add code to save other current settings.

4) Personalize line 2 of the display with the operator's call sign.

Example Receivers and Transmitters Using the Si570 Programmable PLL

Figure 14 shows a block diagram and Figure 15 is a schematic diagram for a receiver that uses the Si570 P-PLL and a QSD to produce I and Q audio signals for processing in a PC with software such as the Rocky SDR software for the SoftRock radio.^{5,6}

Figure 16 shows the schematic of the Si570 LO and a QSD combined with a MicroR2 low noise amplifier and audio processing section designed by Rick Campbell, KK7B.⁷ (Also see Note 1.)

Figure 17 is a block diagram showing the Si570 LO and a QSD in a 40 m CW transmitter. (See Note 1.) Figure 18 is the corresponding schematic diagram. Figure 19 is a block diagram of a 40 m SSB transmitter using the Si570 programmable PLL.

Conclusion

The Si570 programmable PLL from Silicon Labs opens up a myriad of new possibilities for Amateur Radio experimenters to explore. I hope this article has given you some ideas. To continue the discussion, please join us on the PPLL-VFO YAHOO group (www.groups.yahoo.com/group/ppll-vfo). Kits are available from Bill Kelsey, N8ET, at Kanga US; web page (www.kangaus.com) or e-mail him at kanga@kangaus.com. For questions, comments, source code and schematics see the YAHOO group or my web page, www.cbjohn.com/aa0zz, or contact me at aa0zz@arrrl.net. Happy experimenting!

Craig Johnson, AAØZZ, lives in St. Paul Minnesota. He has a Bachelor's degree in Electrical Engineering and a Masters degree in Business Administration. He worked for Unisys for 35 years on the design and development of large computers, and then switched to working with microprocessors — hardware as well as software — in the development of medical devices and "smart" weapons for the military.

Craig earned his first Amateur Radio license in 1964, at the age of 14. He credits ham radio with sparking his interest in electronics, and pointing him toward a career in electrical engineering. For several years Craig led a team of Volunteer Examiners and helped hundreds of people in the St. Paul area earn or upgrade their licenses. He still serves as a VE on occasion. He is an active member of the Minnesota QRP Society and QRP ARCI.

Craig is married and has three children. All five members of his family are licensed Amateurs. Craig enjoys CW, operating QRP, DXing and contesting. He is happiest, however, when he is tinkering, building or experimenting with new designs, circuits and software. His current interests are centered around projects that use micro-controllers, direct digital synthesis and digital modes. He holds seven US Patents for his work in computer hardware and software.

Notes

¹Gerald Youngblood, AC5OG, "A Software-Defined Radio for the Masses, Part 1", QEX, Jul/Aug 2002, pp 18-20.

²Craig Johnson, AAØZZ, "Learning to PIC with a PIC-EL — Parts 1 and 2," QST, May 2007 and June 2007 and "Pickle with a USB Interface," QST, Feb 2010.

³Craig Johnson, AAØZZ, "The IQPro: A High Performance Quadrature DDS VFO" QEX, May/June 2006, pp 8-22.

⁴The author's program source code is available for download from the ARRL QEX website. Go to www.arrrl.org/qxfiles and look for the file 7x11_Johnson.zip.

⁵Alex Shovkoplyas, VE3NEA; www.dxtatlas.com/Rocky/

⁶Tony Parks, KB9YIG; www.kb9yig.com/

⁷Rick Campbell, KK7B, "The MicroR2 — an Easy to Build 'Single Signal' SSB or CW Receiver", QST, Oct 2006.



A 10 MHz to 6 GHz Power Meter

This power meter, based on a Mini-Circuits ZX47 power detector, gives a direct display of -55 to +10 dBm power levels.

I was building the Modularized Spectrum Analyzer described by Scotty Sprowls. For detailed information about this spectrum analyzer, see www.scottyspectrumanalyzer.com. I ran into a problem when I needed to align the analyzer. We are talking here about frequencies in the low gigahertz range. My frequency meter goes up to 3.5 GHz and would give a frequency reading but no indication of the power level involved. My 100 MHz scope couldn't cope and was useless. I needed two kinds of measurements:

- Relative ones: Am I getting any gain or loss? How much? Is the signal getting from point A to B?

- Absolute ones: Am I getting the 10 dBm I need from the phase locked oscillators (PLOs)? Remember that when making absolute measurements a sine wave shape is assumed. Also, *all* of the power coming out of the device must be measured: placing the probe in parallel when the device is delivering power to another device will not measure the true output. Most likely, and assuming 50 Ω impedances, it will measure 50% of the power. Use a pigtail as shown attached to the meter in Figure 1.

A Big Problem

With tiny (and I mean *tiny*) surface mount components, taking your eyes from the circuit to glance at a meter a foot or two away may result in the measuring probe slipping away, with disastrous effects; if not to the electronics, perhaps to yourself due to the adrenaline jolt. When measuring voltages I could bring my handheld DVM very close to the point of measurement to see the results, but not my heavyweight HP 435B power meter. I needed a hand-held device with local readout. This is particularly important in today's crammed circuits where you don't dare to glance away from the point of mea-



Figure 1 — The finished assembled power meter.

surement for fear of the probe slipping.

The solution

I was looking for a way to enhance the "Pocket dBm RF Power Meter" by Steve Whiteside, N2PON in the August 2008 issue of *QST*, so it would measure into the gigahertz range. During that search I discovered the Mini-Circuits power detectors. See



Figure 2 — A Mini-Circuits ZX47 -40+ power detector module.

Figure 2. The Mini-Circuits ZX47 power detectors measure RF power from 10 MHz to 8 GHz and, depending on the detector chosen, -50 dBm to +15 dBm, displaying the results directly in dBm. This is especially convenient because with its small size, the readout can be at the place of measurement.

These devices are very linear, have a wonderful dynamic range and are tiny. Besides, their data sheets include response curves that allow for a close calibration without the need for an external reference. Figure 3 shows the output voltage versus input power response curves for the ZX47 -40+ power detector. I ordered one of them and ran a few tests to verify how close the response was to the published curves and found a general agreement of between 1 and 2 dBm. The detectors are not cheap (about \$90 each) but they beat by a mile (and in some cases parsecs) the cost of commercial units.

Among other things, the combination

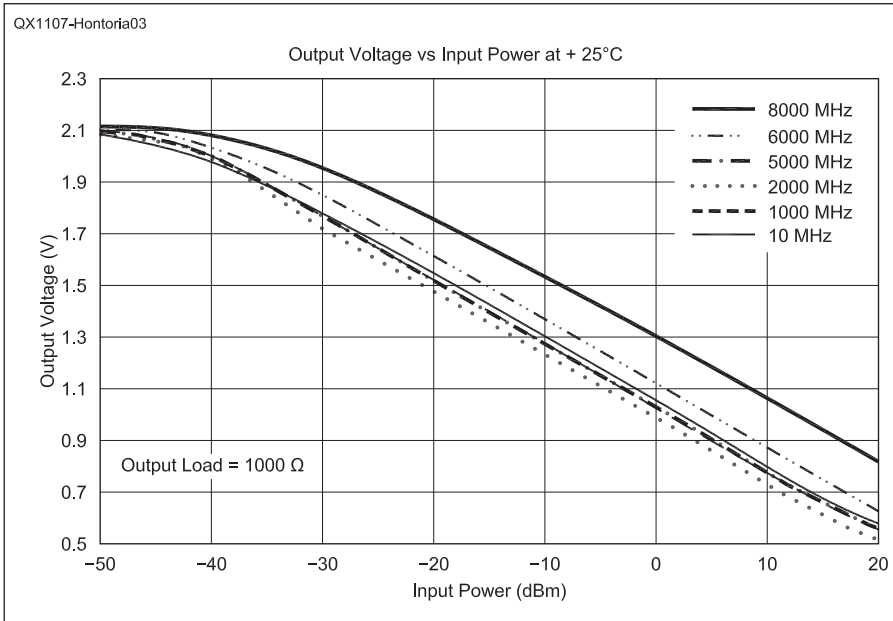


Figure 3 — This graph shows the ZX47 –40+ power detector output voltage versus input power at 25°C. This graph is reproduced from the Mini-Circuits data sheet for the detector.

of a VFO at 1013.3 MHz and this meter allowed me to set up the spectrum analyzer's cavity band pass filter to a loss of –10 dB in no time flat.

Mini-Circuits offers four detectors in its ZX47series. The linear span is approximately as follows :

Model 60: –55 to +0 dBm

Model 55: –50 to +5 dBm

Model 50: –45 to +10 dBm

Model 40: –40 to +15 dBm

These ranges are good up to 6 GHz, but beyond that the range is smaller. Their output voltage is 0.6 to 2 V. Since its high power range may be increased by using an attenuator, my favorite is Model 60.

The schematic shown in Figure 4 is quite simple: one potentiometer sets the slope and the other sets the intercept of the response curves. Since — up to 6 GHz — the linear portions are essentially parallel, the slope pot is set once and left alone. As Figure 3 shows, the 8 GHz output voltage curve is quite noticeably different than the lower frequency curves, and would require a different calibra-

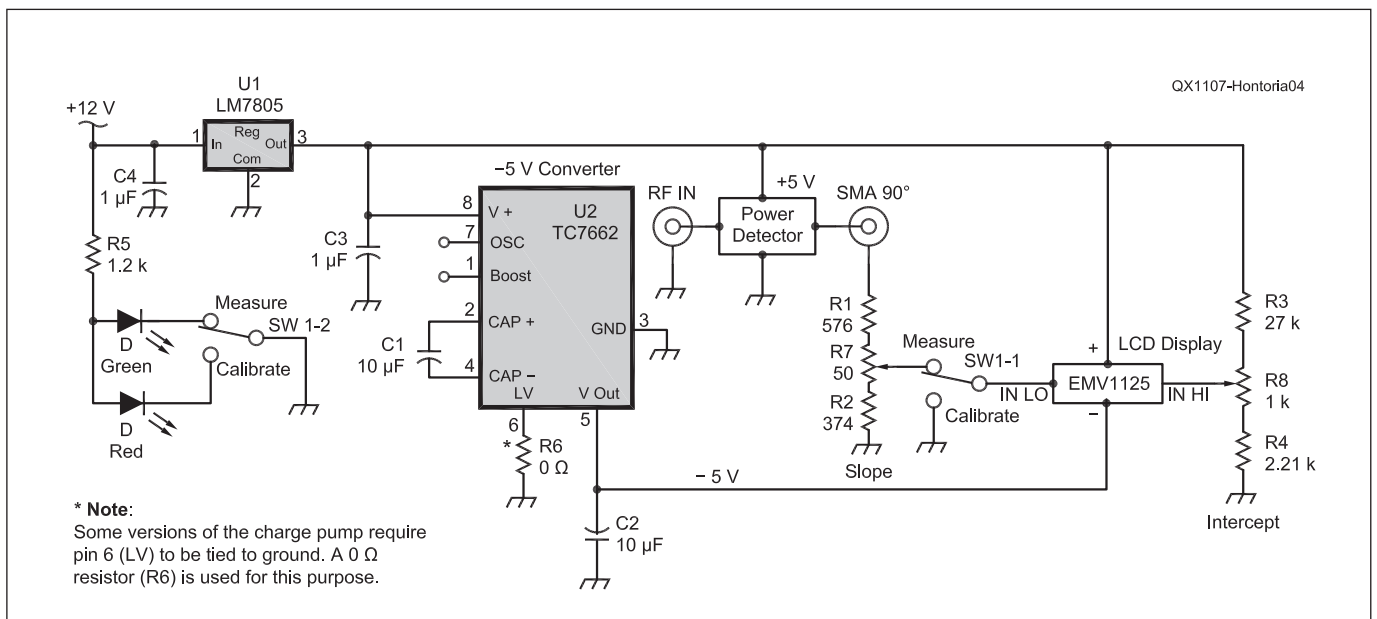


Figure 4 — The schematic diagram of the power meter shows how simple this circuit is. Potentiometer R7 sets the detector slope for the LCD voltmeter and R8 sets the display intercept. Once the slope is set no further adjustments are needed to that control. The intercept potentiometer is adjusted for the appropriate frequency range.

Parts List

C1, C2	10 μ F, 16V SMT 0805 Ceramic (Mouser 81-GRM21BR61C106KE15 or equiv)	R3	27 k Ω
C3, C4	1 μ F, 16V, 5% SMT 0805 Ceramic (Mouser 81-GRM21BR71C105JA1K or equivalent)	R4	2.21 k Ω
Enclosure	Hammond 1590A (Mouser 546-1590A)	R5	1.2 k Ω
Lascar LCD	Lascar EMV1125 LCD voltmeter (Jameco 2113201)	R6	0 Ω (jumper, if needed)
LED	Panasonic bi-color, LN11WP23 (Digikey P391-ND)	R7	50 Ω (Mouser 652-3314G-1-500E) (Digikey 3314G-1-500ECT)
Power Detector	Mini-Circuits ZX47 –40+	R8	1 k Ω (Mouser 774-296UD102B1N)
Power Jack	Switchcraft 722A EG2209A (Jameco 281851)	SW1	DPDT E-Switch EG2209A (Mouser 612 EG2209A)
Resistors	SMD 0805, 1%	SMA 90°	Amphenol 132112 male/female elbow (Mouser 523-132112)
R1	576 Ω	U1	78M05 DPAK_3 (Mouser 863-MC78M05CDTG)
R2	374 Ω	U2	Charge pump voltage converter, Maxim ICL7662EBA+ (Digikey)



(A)



(B)

Figure 5 — My original unit. The left wall in Part A has the 12 V jack. There is a 7805 voltage regulator bolted to the box floor underneath the circuit board and secured by the screw at the upper left corner which holds both the 7805 and the circuit board in place. The IC visible on the circuit board is a charge pump device to get the -5 V needed for the LASCAR LCD voltmeter. The latest version of the meter has moved all the components to the circuit board, which has simplified the wiring. Part B shows the front of the box, with the LCD voltmeter, the Calibrate/Measure switch, the intercept potentiometer control and the bi-color LED.

tion. The intercept is a function of the frequency and is set at the time of calibration or simply taken from the Mini-Circuits curves.

The user interface includes a Lascar EMV 1125 LCD digital voltmeter, a bicolor LED (red when the switch is in calibration mode, green when in measurement mode) and the offset potentiometer. A calibration table is pasted to the face of the box (not seen in any of the pictures). The offset potentiometer is set to the value in the table, which corresponds to the frequency of the signal being measured.

The meter requires an external supply from 12 to 20 V dc. Because of the sensor current draw (about 120 mA), no attempt has been made to use batteries.

Figure 5 depicts my original unit. The left side of Part A has the 12 V jack. There was a 7805 voltage regulator bolted to the box floor underneath the circuit board and both the regulator and circuit board were secured by the screw visible at the top left corner of the circuit board. The IC visible on the circuit board is a charge pump to get the -5 V needed for the Lascar LCD voltmeter. I have built a newer version and have moved all the components to the printed circuit board. That has simplified the wiring. Figure 6 is a picture of the inside of the newer version.

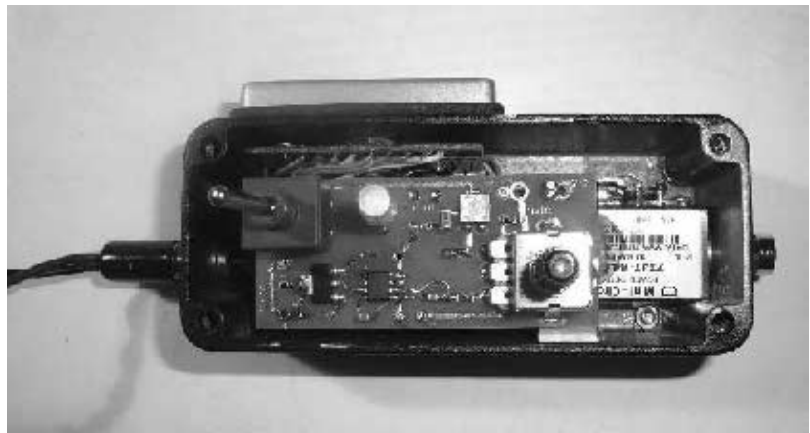


Figure 6 — A look inside the newest version of the meter. The trimmer is the slope setting and the miniature potentiometer is for the intercept setting. Note the glob of glue on the right securing the board to the detector.

Construction Notes

I used a Hammond 1590A cast aluminum enclosure, and had to remove some material from the corners to make room for the Mini-Circuits sensor, as shown in Figure 7. I center punched the area and then used my drill, being careful not to engage it and go through the wall. The probe SMA hole offset is to provide clearance for the LCD in the other side of the box. Not shown here, there was a hole drilled on the box “floor” to secure one of the legs of the sensor.

Look again at Figure 6. Some versions of the 7662 charge pump require that the LV pin (pin 6) be tied to ground to ensure a negative



Figure 7 — I used a Hammond 1590A cast aluminum enclosure and had to remove some material from the corners to make room for the Mini-Circuits sensor. I center punched the area and then used my drill, being careful not to engage it and go through the wall. The probe SMA hole offset is to provide clearance for the LCD in the other side of the box. Not shown here, there was a hole drilled on the box “floor” to secure one of the sensor legs.

5 V output of the same level as the positive input. Version 1.3 of the circuit board, which is the one shown in Figure 6, requires installing a wire jumper to ground. Circuit board version 1.4 has provision for a 0 Ω resistor (R6) if needed.

Figure 8 shows the Lascar LCD voltmeter control board on the inside of the Hammond project case, with the circuit board and power detector ready to be installed. Notice that the wires from the display feed through a hollow stud on the back of the display, and they attach to a row of holes along the top of the control board and to the switch and R8 on the circuit board.

Figure 9 shows the bottom of the circuit board, with a 90° angled SMA male to female connector between the detector output and main circuit board. I used a ¼ inch length of 141 coax between the SMA female end and the circuit board. Do not solder the coax to the SMA connector until you are sure everything fits correctly.

Figure 10 is the circuit board artwork. Note that this is a double sided circuit board, with the traces on top of the board outlined in black and traces on the bottom of the board shown in lighter gray.

The circuit board file was created using *ExpressPcb*. Because *ExpressPcb* requires a minimum board size of 3.8 × 2.5 inches, builders may want to join with a few others to make the price more attractive (a good club project?) or to include boards for other projects with the order. An alternative is to redo the design using *Eagle*.

A color copy of this artwork, along with the *ExpressPCB* file is available for download from the ARRL *QEX* files website: www.arrl.org/qexfiles. Look for the file [7x11_Hontoria.zip](#).¹

Drilling the Enclosure Cover

The potentiometer requires a ⅜ inch hole. The LED I used requires ⅜ inch and the switch needs a ¼ inch hole for the shaft. Remember: “Measure thrice, drill once.” Refer your measurements to the centers of the enclosure screw holes, not to its walls. Then, transfer those measurements to the cover.

Setting Up the LASCAR LCD Voltmeter

The EMV1125 doesn't require a split rail power supply. It can happily run from a single rail. Under these conditions, however, the signal must be left floating (totally isolated) from the power supply and link L2 ties the floating signal (INLO) to a reference voltage (Com, held 2.8 V below V+). Since in the power meter the signal is not floating, **link L2 must be cut**. Leaving this link will basi-

cally short GND to V+, damaging the meter. Figure 11 shows the LCD voltmeter control board, with the connections to the display.²

The meter is thus operated from a ± 5 V split-rail supply. In order for the LCD to read 2 V full scale the Ra (910 kΩ) and Rb (100 kΩ) resistors must be installed and **link La must be cut**. To set the decimal point so that the meter reads directly in dBm, the decimal link DPI must be shorted out.

Last, but not least, measure the input voltage at IN-HI with an accurate DMM

and adjust CAL for the same reading on the Lascar display.

Preliminary Calibration

The preliminary calibration uses the Mini-Circuits data sheet curves. A more precise calibration will require comparison with another power meter. The following is how the preliminary calibration is performed.

If using the Lascar EMV1125, set it up in accordance with its data-sheet and the instructions above. If using any other meter,

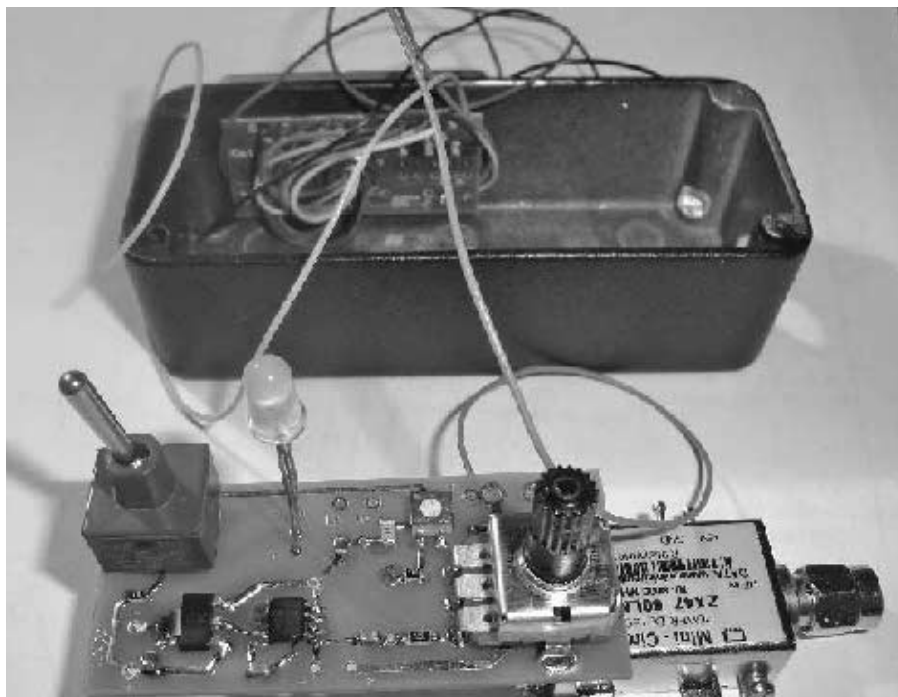


Figure 8 —The LCD voltmeter comes with fairly long wires, which I used to connect it to the circuit board.

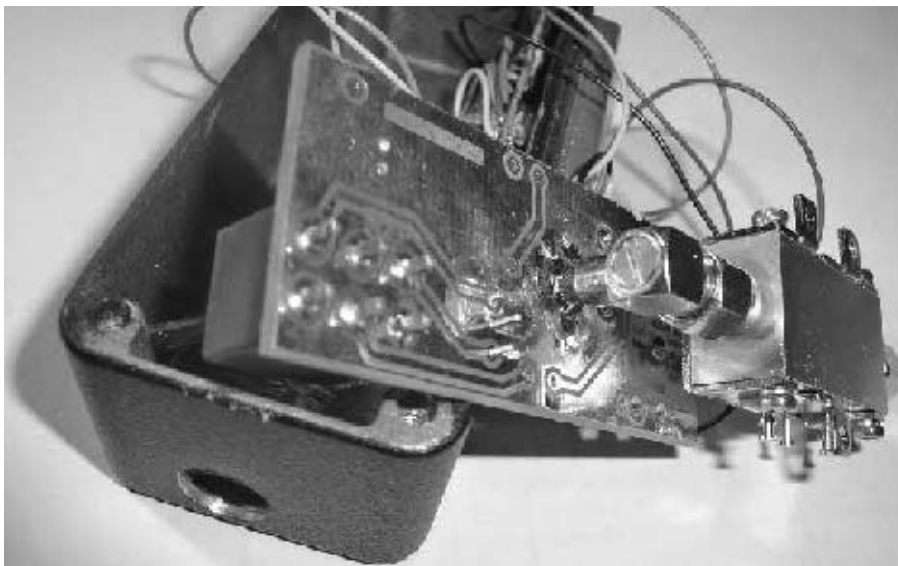


Figure 9 — I had to insert a ¼ inch length of 141 coax into right angled SMA connector, to provide clearance between the detector and the circuit board. The coax (shield and center conductor) should not be soldered to the SMA until the very end.

¹Notes appear on page 21.

Table 1
Calibration Factors

Frequency Range MHz	Calibration Factor
10	47.4
50	43.9
100	47.9
200	44.2
300	44.1
400	43.8
500	44.5
600	44.3
700	46.1
800	44.0
900	52.0
1000	49.9
1050	48.1

(My signal generator does not go any further)

set it up to display 2 V, but move the decimal point to one decimal digit.

Refer to the schematic diagram in Figure 4. It refers to the designation of the potentiometers. This preliminary calibration procedure is based on setting the slope with R7 and the intercept with R8.

1) Set the switch to “Calibrate” position, to ground the EMV 1125 input line; the bicolor LED should turn to red. Do not connect any signal to the RF input of the ZX47. Turn on the power supply.

2) Use a DMM to measure the voltage at the ZX47 output (the top of resistor R1). Suppose you measure 2.17 V

3) Adjust the slider of the slope potentiometer R7 (the small trimmer on the circuit board) and measure the voltage at the arm. For this example you should measure $2.17 \text{ V} \times 0.4 = 0.868 \text{ V}$.

4) I used the Model 40 Mini-Circuits detector, so I used the curves shown in Figure 3, reproduced from Mini-Circuits data sheet.

Use a signal generator to inject a 10 MHz signal to the ZX47 –40+ RF input. Ideally, the signal level should be in the center of the range, which for the Model 40 is around –15 dBm. In any case, do not exceed the upper limit for the ZX47 detector you are using. Read the voltage at the input side of R1. Suppose you read 1.38 V.

5) Look at the Figure 4 graph. The thin black line corresponds to 10 MHz and 1.38 V corresponds to –14 dBm.

6) Set the switch to the “Measure” position; the bicolor LED will be green. Adjust the intercept potentiometer (R8) until you get the same dBm reading on the Lascar display. Return the switch to “Calibrate” and make a note of the reading on the display. That is your set point at 10 MHz.

7) Set the switch to “Measure” again, and you are ready to start measuring power in the 10 MHz range. You can now experiment

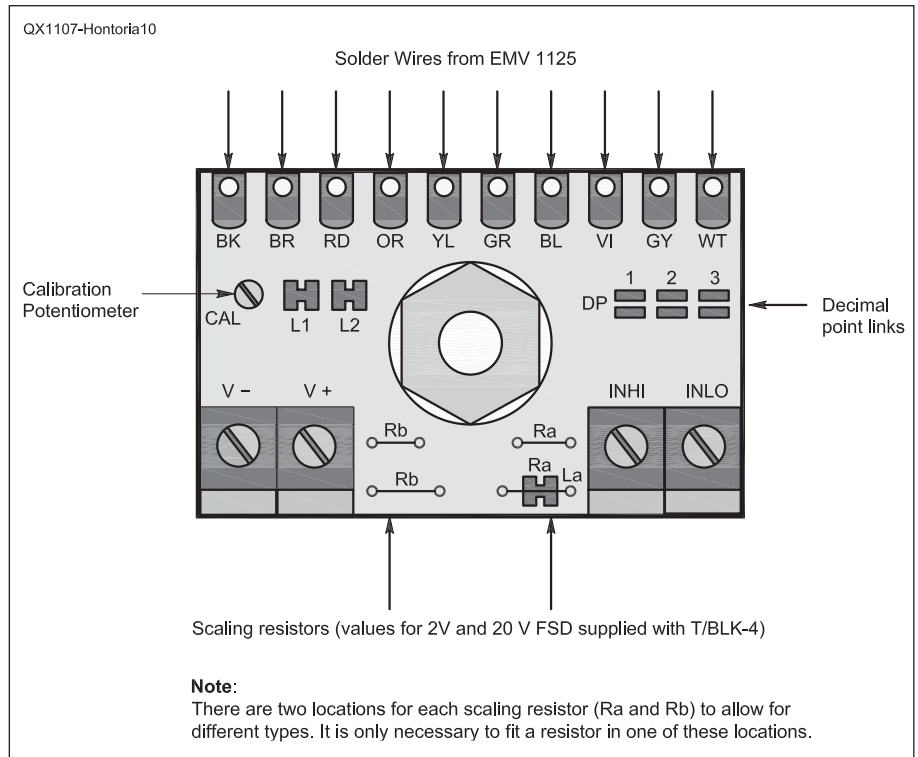


Figure 10 — This control board is part of the Lascar voltmeter. The wires from the display connect to the top row of holes.

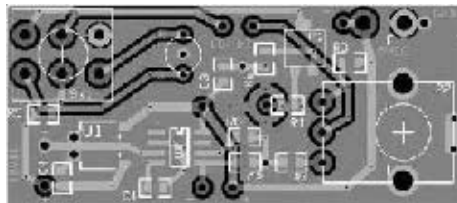


Figure 11 — This is the circuit board artwork. The board is 2.4 × 1 inch.

with different frequencies and levels. For example, my set point at 50 MHz is 44.7, and at 1000 MHz it is 43.8. These set points are the equivalent of calibration factors used in other instruments. Table 1 shows the calibration table for my meter.

Background

With the Model 40, the response equation at 10 MHz is: $\text{dBm (10 MHz)} = 42 - (40 \times V)$. For example, a sensor voltage output of 1.3 V corresponds to a power input of $42 - (40 \times 1.3) = 42 - (52) = -10 \text{ dBm}$ at 10 MHz (the thin black line on Figure 3). For other frequencies, the response equations are:
 $\text{dBm (1000 MHz)} = 41.7 - (40 \times V)$
 $\text{dBm (2000 MHz)} = 39.25 - (40 \times V)$
 $\text{dBm (6000 MHz)} = 44.7 - (40 \times V)$
 $\text{dBm (8000 MHz)} = 52 - (40 \times V)$

Since the lines are essentially parallel (with the exception of the 8 GHz line) the slope has been set as a constant at 40. The intercepts are frequency dependent, how-

ever. Based on the Mini-Circuits graphs, the Model 40 power sensor should provide fairly close results to the above formulae between –35 and +15 dBm.

Jim Hontoria, WIJGH, received his first Amateur Radio license in Spain at age 16. Residing in New York since 1979, he is a deep water sailor by inclination and a (now semi-retired) mining engineer by profession. He earned a US Amateur Radio license in 2006 and became an Amateur Extra in 2007. His interests include all digital modes and radio-related instrumentation. Jim is an avid experimenter and builder.

Notes

¹A color version of the circuit board pattern, along with the ExpressPCB circuit board file is available for download from the ARRL QEX files website: www.arrl.org/qexfiles. Look for the file **7x11_Hontoria.zip**.

²Figure 10 is from the Lascar Electronics (4258 W 12 Street, Erie PA 16505) EMV 1125/2 data sheet. Displays are available from Jameco Electronics.



Filter Synthesis using Equal Ripple Optimization

The author describes the filter design optimization technique used by his Lowpass Filter Designer software.

Modern filter design was a direct result of the availability of significant computer power. Prior to the introduction of the personal computer, this power was not available to most engineers, so filter design usually meant pulling out a book full of normalized filter design tables, and denormalizing the information for impedance and frequency, to arrive at the desired filter design. With the availability of significant computing power on a desktop computer, programs quickly became available for designing the simpler filter characteristics: Butterworth and Chebyshev, along with a few others. Eventually the program *Filsyn* became available on the personal computer, enabling the design of complex filter characteristics, but at a hefty price.¹ Today, a number of free and moderately priced programs are available for the synthesis of a variety of filter characteristics.^{2,3}

To my knowledge, all of these programs synthesize the more complex filter characteristics (those incorporating finite frequency zeros in the stopband) by forming an input and output impedance (or admittance) function, and extracting element values from one or both ends, while simplifying the impedance (or admittance) function as each element value is extracted. This technique has been improved over the years, incorporating frequency translation to reduce error accumulation, and is the accepted method to synthesize filters today.⁴

While techniques have been developed for synthesizing desired filter responses using iterative techniques rather than element extraction, it does not appear that any filter

design program has ever made use of these techniques.⁵ The normal procedure for an iterative approach to filter design has been to design a filter with characteristics close to those desired, then use the optimizer in an analysis program along with an appropriately defined error function, to drive the filter response towards the desired characteristics. Defining the error function can be problematic. There is a tradeoff in which characteristics should take priority in the optimization procedure. In general, the performance of a simple optimization like this is not very efficient, and there is no guarantee that the optimization procedure will locate the best match to the desired performance goals. The recent series of *QEX* articles on unequal-ripple low-pass filters has rekindled my interest in developing an iterative technique for the realization of optimum frequency response characteristics in a filter.^{6,7,8}

Is Optimization the Optimum Solution?

Optimization techniques have been studied in detail over the years, as the computer has made possible the repeated calculation of mathematical functions hundreds, thousands or even millions of times.^{9, 10, 11} Perhaps it was believed that optimization techniques, along with the extraordinary improvement in computational speeds, would ultimately lead to the ability to solve any problem by using optimization techniques. To my knowledge, that has never happened.

The typical optimizer works with an error function that is defined by the user. Consider for an example an amplifier for the 6 meter band. We'd like to maintain an equal ripple response over the entire band, while obtain-

ing the maximum possible rejection at the second harmonic. The lowest frequency for the second harmonic would be 100 MHz. We'd normally want to extend the passband beyond the limits of the 6 meter band, to simplify tuning, and avoid the increased loss that occurs near the band edges. Let's define the desired equal ripple passband as extending from 40 to 65 MHz. The lowest frequency second harmonic will still be at 100 MHz.

In order to implement the optimization procedure, we need to define an error function that increases as the ripple exceeds some specified value anywhere in our defined passband of 40 to 65 MHz. The error function must also increase as the stopband attenuation at 100 MHz drops. The optimizer would sweep the filter over the passband, looking for the worst case ripple point, and then perform a single analysis at the specified stopband frequency, to determine the error function value for these present element values. The goal of the optimizer is then to modify the element values in such a way as to reduce that error function. In the process, the optimizer is blind as to which part of the error function is causing the error function to increase. This is partially addressed by adding weights to the various parameters that are making up the error function. For example, the ripple might be weighted much greater than the stopband rejection, because it's more important to avoid exceeding the maximum allowable passband ripple, while obtaining the greatest stopband attenuation possible with the specified passband ripple. The optimizer will then tend to reduce the ripple to the maximum allowable as a primary goal. Improving the stopband performance becomes a second-

¹Notes appear on page 29.

ary goal. The search for an optimum solution may be random, or it may be guided by partial derivatives, guiding the optimization by their knowledge of how the error function responds as various elements are varied. My limited experience with optimizers has shown them to be of limited effectiveness, which perhaps explains why optimizers are not universally available in analysis programs.

Getting to the Root of the Problem

A problem that is addressed in most books on numerical methods is finding the location of a root of an equation. One of the techniques presented is the Newton-Raphson method.¹² This technique involves a calculation of the original function, as well as one or more derivatives of the function. For our purposes we'll consider using only the first derivative. With simple functions, the derivative may be known, but the Newton-Raphson method is equally applicable where the function and its first derivative can be determined numerically. A simple example of the Newton-Raphson method is the calculation of the square root. Since we're looking for a zero, we have to write an equation where the square root represents a zero of the equation, as shown in Equation 1.

$$f(x) = x^2 - a \quad [\text{Eq 1}]$$

We're looking for the value of x corresponding to the root or zero of the expression $f(x)$, which is obviously the square root of a . Without going into details, the Newton-Raphson method can be used with an initial approximation to the value of x , to arrive at a better approximation of x . This improved approximation to x is obtained by a recurrence relation, an expression that is used repeatedly to obtain the new, improved approximation from the previous approximation. The recurrence relation for the Newton-Raphson method is defined in Equation 2.

$$x_{n+1} = x_n - \frac{f(x_n)}{f'(x_n)} \quad [\text{Eq 2}]$$

If we substitute Equation 1 into Equation 2, and define the difference between our present approximation x_n , and our new approximation x_{n+1} , as Δx , we obtain Equation 3 as our expression for computing the change in the approximation of x .

$$\Delta x = -\frac{x^2 - a}{2 \cdot x} \quad [\text{Eq 3}]$$

Note that the numerator here is just the error in the expression $f(x)$, which is the error in the expression defining the square root. As x approaches the desired square root of a , this error value, and therefore the delta value, will

go to zero. As an example, if we set a to 10, looking for the square root of ten, and start with an initial guess for x of 1, we get the following series of approximations for the square root of ten:

1.0, 5.5, 3.659, 3.196, 3.162
After four iterations we have achieved the square root of ten to three decimal places.

So what does this have to do with filters? Fortunately, this is just a very simple example of the Newton-Raphson method. In particular, this is an example with a scalar function. The Newton-Raphson method works equally well with vector functions — with a system of equations. If we can define a vector expression involving the filter response, where the desired solution is a zero of that expression, we can use the Newton-Raphson method to obtain an approximation to that zero using an iterative technique. As with the example with the square root, the more times we iterate, the closer we will get to the actual root.

We'll define the frequency response of the filter as $H(f)$, where f is the frequency of the signal applied at the filter input.¹³ In general, we don't attempt to derive the expression for $H(f)$. Rather we employ some form of analysis routine that takes the input frequency, f , applies it to the defined network, and calculates the gain (or loss) of that circuit (and possibly the phase delay as well) from the input to the output of that circuit — a filter in this case. This could be a nodal analysis routine. In our case it will be a simple ladder analysis routine, as the filter topology we'll be considering will be a ladder network. Although we may not have a definition for $H(f)$, we do have a way to calculate $H(f)$, which is all we need to put the Newton-Raphson method to work here.

Our goal is to use the Newton-Raphson method to drive the passband ripple to a specified level. Note the difference here from the simple optimization where the goal was to reduce the ripple to a maximum value in the passband. In our procedure we're setting the ripple maximums to a specified value. The end result will be the same, but this procedure carries more information along with it. In the case of a symmetrical filter, we are concerned only with the maximum ripple points in the passband (more on this later) — these would be the ripples in the passband, the upper passband ripple cutoff frequency, and in the case of the unequal ripple filter, also the lower passband ripple cutoff frequency. We'll define these frequencies as the critical frequencies. In a symmetrical filter the number of critical frequencies is one more than half the number of elements. For example, if the filter has 7 elements, there will be 4 critical frequencies. For a true low-pass response this will be the three maximum ripple points in the passband, and the low-pass filter ripple

cutoff frequency. Considering Equation 4, $g(f)$ is defined so that when the response of $H(f)$ drops by the specified ripple, a_r , $g(f)$ is zero, just what we need for the Newton-Raphson method.

$$g(f) = H(f) - a_r \quad [\text{Eq 4}]$$

Permit just a bit of sloppy discussion here. $H(f)$ and $g(f)$ must both represent vector functions. In particular, each function is defined at four frequencies, the critical frequencies defined above. It is at these four frequencies that we are seeking the roots, forcing the function $H(f)$ to drop by the specified ripple amount. Note that both $H(f)$ and $g(f)$ are also functions of the element values in the filter. In fact, it is these element values that we are seeking to modify by employing the recurrence relation. If we want to be mathematically correct, Equation 4 should be written as shown in Equation 5.

$$g(E) = h(E) - a_r \quad [\text{Eq 5}]$$

Here the variable E is understood to be a vector, the element values that we are optimizing — in the case of this seven element symmetrical filter, E will consist of four independent values. While $H(f)$ is a function of the frequency, we're actually dealing with a related function, $h(E)$ here, that is not a function of frequency. That's because $h(E)$ returns the filter response at the critical frequencies, but doesn't care what those critical frequencies are. In the case of the ripple cutoff frequency, this frequency is a constant, not a variable. The ripple at this constant frequency is a function of the element values. In the case of the ripples in the passband, $h(E)$ returns the ripple maximum values, regardless of at what frequency they occur. The function $h(E)$ says, "Given these element values, E , what ripple does the filter deliver at the specified ripple points? I don't want to know anything about the frequency!"¹⁴ We need $H(f)$ to determine this, but $h(E)$ is blind to what these frequencies are. Given $h(E)$, we can calculate the derivatives required in the recurrence relation by perturbing the element values and observing the effect on $h(E)$.

Note that the definition of ripple that we are using is upside down. That is, the filter response $H(f)$ drops by the ripple amount at the point where we say that the ripple has reached a maximum value of a_r . While this would probably cause a mathematician to cringe, we'll just keep on referring to ripple and attenuation as positive values, realizing that they are actually negative values when evaluating $H(f)$ or $h(E)$.

This technique has been developed by S. B. Cohn.¹⁵ Better yet, it's described in the book *Generalized Filter Design by Computer*

Optimization, written by Djurdj Budimir.¹⁶ This technique uses the Newton-Raphson method to drive the passband ripple to a specified equal value ripple within the defined filter passband. The expression we defined in Equation 5 is a vector function, developing the signed deviation from the desired ripple goal at each maximum ripple point in the passband (including passband edges), and possibly the signed deviation from zero at the zeros of attenuation in the passband. We'll define the result, $g(E)$, as the error function. The numerical result will be the error vector for the given element values. As in the solution for the square root, this error vector will approach zero as the element values converge on the correct values.

Two Filter Topologies

As mentioned above, we'll be evaluating the filter response at the maximum ripple points within the passband, and possibly the zero points as well. The question of when to evaluate the zeros of attenuation in the passband involves the circuit topology. If the filter is symmetrical, we don't evaluate the zeros. If the filter is not symmetrical, we do evaluate the zeros. The reason is simple — as long as the filter remains symmetrical, the passband zeros will remain zero. You can't have it any other way. And attempting to optimize them will result in an unsuccessful procedure. So then, we'll need two procedures for driving the filter response towards the desired response. One is designed for symmetrical filters, evaluating the passband response only at the maximum ripple points, and adjusting the elements in pairs (except for the center

element). The other is designed for non-symmetrical filters; it looks at both the maximum ripple points, and the zeros of attenuation, and adjusts each element in the filter.

The immediate question raised by this division of labor is, "What filter parameters will result in a symmetrical filter?" The first requirement is that the order of the filter be odd. If the order is even, the topology isn't even symmetrical — if the first element is a shunt capacitor, the last element will be a series inductor. For our purposes we'll consider only filters with an odd number of elements. A second requirement is that the input and output impedances be equal. This would normally be the case in an RF filter, but a special case might occur where the filter is driven by a transistor. In this case we might want to design the filter with a specified load impedance, perhaps 50 Ω , but the source impedance would approach infinity, because of the current source drive. A filter with unequal source and load impedances will not be symmetrical.

In some cases a finite stopband zero is created in the low-pass filter by placing a capacitor in shunt with the center inductor. This will not affect the symmetry of the filter. If a single stopband zero is associated with an element that is not in the center of the filter, however, that filter will not be symmetrical. For our purposes, any stopband zeros will be realized by placing a capacitor in shunt with one of the series inductors in the low-pass filter. In a three section low-pass filter this will be in shunt with the center inductor, and the filter remains symmetrical. If the filter has, for example, five sections, the center element is a shunt capacitor and symmetry

cannot be maintained if a stopband zero is incorporated into an existing inductor in the design. If more than one stopband zero is incorporated, the filter will never be symmetrical. In summary, any of the following conditions will result in a non-symmetrical filter in our design.

- 1) The input and output impedances differ (designed for a current source at the input.)
- 2) There is a single zero in the stopband, and the center element is not an inductor.
- 3) There are two or more zeros in the stopband.

Our procedure seems to be pretty straight forward. (Let's consider the symmetrical case here, and remember that the non-symmetrical case is a bit more complicated). We evaluate the filter response at the maximum ripple points to obtain our error vector — the signed deviation from the desired ripple goal at each of the critical frequencies. This is the error vector that will appear in the recurrence relation, equivalent to the numerator in the recurrence relation for the square root problem. We then perturb each of the element values, one at a time, to obtain new error vectors, used to calculate the partial derivatives of the response at each of the maximum ripple points as each element is varied (more about this later.) This gives us a square matrix of partial derivatives that appears in the recurrence relation. The error vector and matrix of partial derivatives will allow us to calculate an improved approximation for the element values. It sounds simple enough — well, with enough programming. But there is one immediate problem: in general, aside from the passband edges where the frequency of maximum ripple is defined by specification,

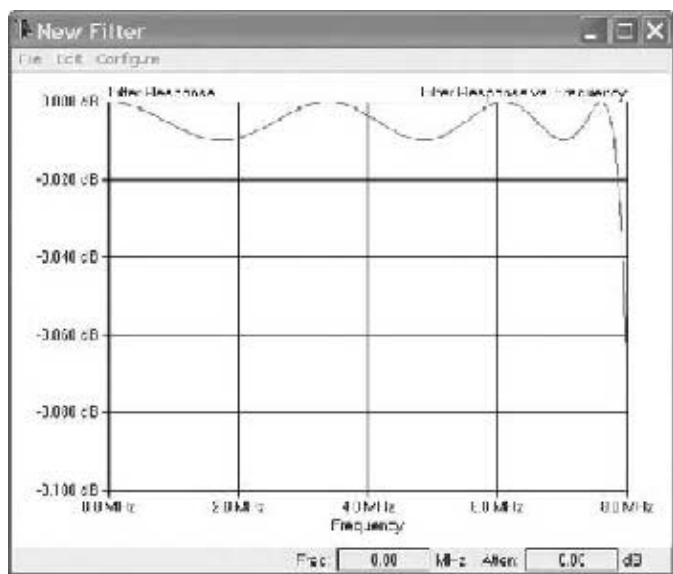


Figure 1 — The initial Chebyshev design provides an equal ripple response in the passband.

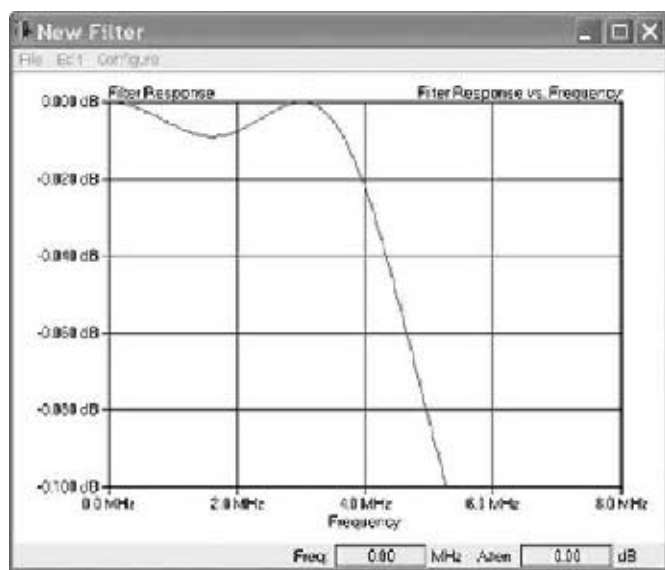


Figure 2 — Inserting the stopband zero destroys the passband response.

we don't know at what frequencies those ripple maximums occur. In order to locate those ripple maximums, we first have to sweep the passband response of the filter. But the element values must then be close enough to assure that the passband ripples are present. It appears that we've reached the proverbial catch 22 here — we can't synthesize the filter unless the ripples are present, and the ripples won't be present until the filter has been synthesized. The way we work around that problem is to first create a standard Chebyshev design, which achieves an equal ripple response in the passband. This establishes the ripples required for calculating the error vector and matrix of partial derivatives. We'll then modify the filter slowly, while maintaining the ripples in the passband by optimizing the element values with the recurrence relation.

Taking a Closer Look

Again, consider the symmetrical case. Let's say we want to design a seventh-order unequal-ripple low-pass filter for use on the 40 meter band. We'll specify a passband of 6.5 to 7.8 MHz, allowing an extra 500 kHz on either side of the band. And we'd like to include a single stopband zero at twice the center frequency of the 40 meter band (14.3 MHz) to aid in second harmonic rejection. We'll specify a maximum passband ripple of 0.01 dB. The basis for the design will be a 0.01 dB Chebyshev low-pass filter with a ripple cutoff frequency of 7.8 MHz. The initial response of the Chebyshev design, shown in Figure 1, displays the desired passband ripple of 0.01 dB, as requested, dropping below 0.01 dB at the specified passband cutoff frequency of 7.8 MHz. The first

thing we're going to do is to introduce the 14.3 MHz stopband zero, by placing a capacitor in parallel with the series inductor present in the center of this filter network. The value of the capacitor is calculated to provide a trap at 14.3 MHz in conjunction with the inductor value dictated by the Chebyshev filter design. We don't have to perform those calculations; we have computer code to accomplish this.

Attempting to incorporate the 14.3 MHz zero by simply adding a capacitor across the center inductor has introduced an unacceptable degradation of the passband response, as displayed in Figure 2. Only the lowest frequency ripple maximum is still visible in the passband plot. But we need to maintain the ripples in order to calculate the error vector. The way we resolve this is to start pushing the zero frequency up by reducing the value of the shunt capacitor, while continuing to sweep the passband, until the ripple response is again acceptable. Figure 3 shows the passband response with the stopband zero pushed out to 107 MHz. The ripple is only slightly perturbed by the presence of the zero. The program code will now sweep the passband response locating the four critical frequencies — the three frequencies where the ripple reaches a maximum, along with the attenuation at the specified ripple cutoff frequency of 7.8 MHz. The ripple goal (0.01 dB) will be subtracted from the filter response at these four frequencies to arrive at four components of the initial (unperturbed) error vector. As can be seen from the plot, the first two errors will be small, while the third ripple point and cutoff frequency errors will be larger. Since this is a symmetrical filter, the element values will now be perturbed in pairs. First the shunt input and output capacitors (C1

and C7) will be perturbed, and another error vector will be formed with the perturbed element values, allowing the calculation of the partial derivatives (in conjunction with the unperturbed error vector) at these four ripple points with respect to C1 and C7. (Note that the frequencies of the ripples may change slightly — we're looking for the ripple peaks, and are not concerned with the exact frequencies, so long as the analysis is performed at those peaks.) This procedure will then be repeated for L2 and L6, C3 and C5, and finally with the value of L4 perturbed by itself. This will result in four error vectors with perturbed element values, allowing us to calculate 16 partial derivatives, consisting of the four ripple points with respect to each of the four perturbations. With these numerical results we can solve for the Δ values for the elements to arrive at a better approximation to the ripple goal.

After this first iteration the passband ripple response of the modified filter, with the zero inserted at 107 MHz should be vastly improved. But we're not going to sit still and watch perfection arrive. The program will calculate the new element values, and then move that zero down a bit closer to the specified frequency, which will again increase the ripple error in the passband. The program has the goal of moving that zero frequency down, continuing to degrade the ripple response as fast as the iterations improve it. Eventually the zero will reach the specified frequency of 14.3 MHz, and the element values will have been modified to maintain an acceptable ripple performance. The resulting filter response is shown in Figure 4.

With the zero inserted into the filter, we need to start implementing the lower

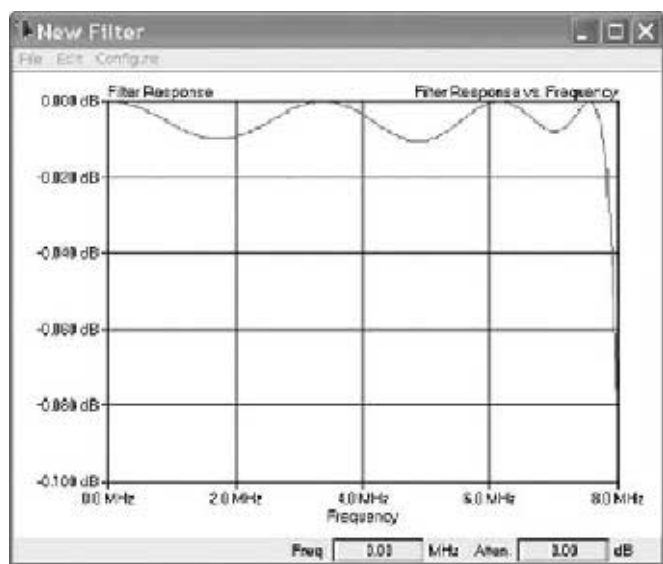


Figure 3 — The stopband zero is pushed up in frequency until all the ripples are restored.

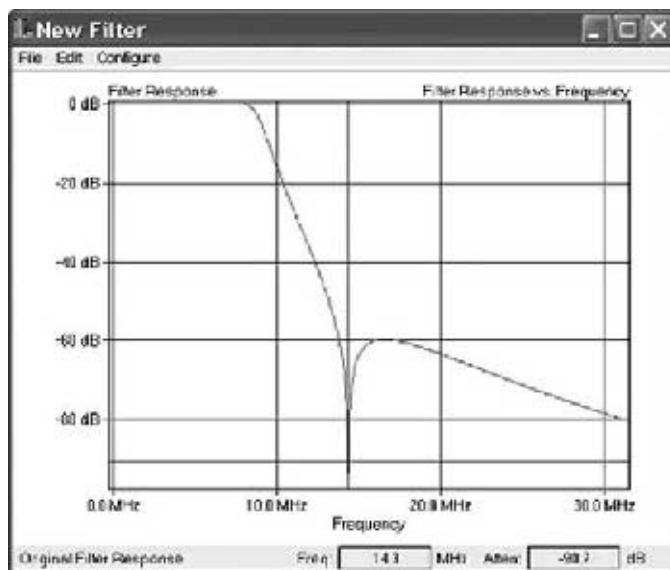


Figure 4 — The iterations are completed when the stopband zero is present with an equal ripple passband.

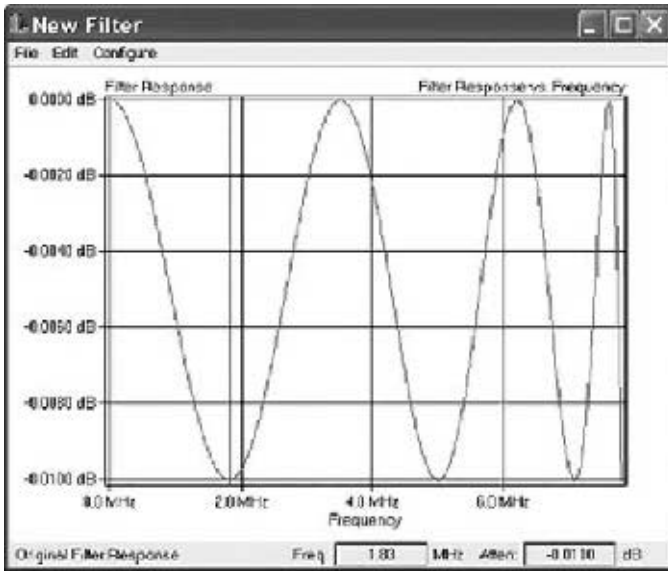


Figure 5 — The first ripple maximum becomes the initial lower ripple cutoff frequency.

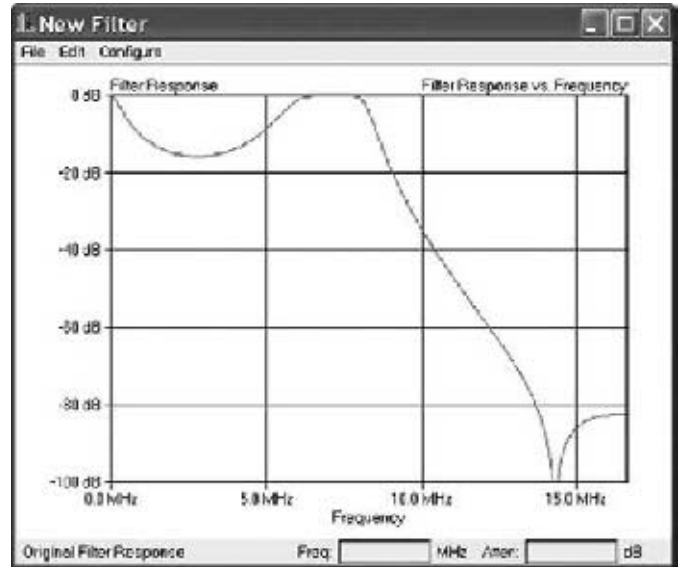


Figure 7 — After moving the lower ripple cutoff frequency up, the filter design is completed.

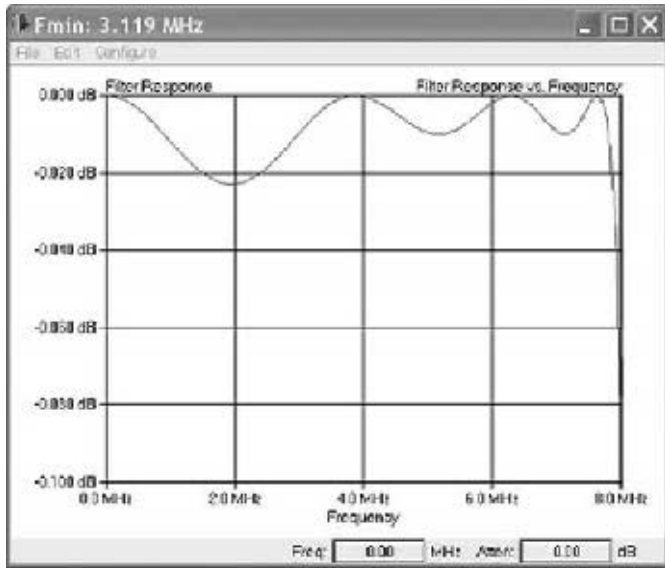


Figure 6 — As the lower ripple cutoff frequency is pushed up, the first ripple grows.



Figure 8 — The main window allows the user to specify the filter parameters.

passband ripple cutoff frequency. We'll be taking the first ripple in the passband and increase the ripple magnitude, which will also push this first ripple up in frequency, to establish a lower frequency ripple cutoff for the filter. The passband response given in Figure 5 shows that the first ripple maximum occurs near 1.83 MHz. This, then, is where the application will initially place the lower ripple cutoff frequency, where it has already reached the maximum ripple value. We'll then start pushing that cutoff frequency up, maintaining the ripple value at that cutoff frequency (which will in turn force the magnitude of the first ripple to continue to grow), at the upper passband cutoff frequency, and

at the two remaining ripple maxima in the passband. The same procedure will be followed, forming the unperturbed error vector, the four perturbed error vectors, and calculating the 16 partial derivatives to allow the program to improve the element values, while continuing to move this lower passband cutoff up in frequency.

In Figure 6 we see the results of several iterations of pushing this lower cutoff frequency up. The lower ripple has increased to just over 0.02 dB, pushing the lower ripple cutoff frequency (where the first ripple level is equal to the specified ripple goal) to just over 3 MHz. The program will continue to move the lower cutoff frequency up, evalu-

ating the ripple error at the two passband ripple cutoff frequencies and the two ripple points, until the lower passband ripple cutoff frequency reaches 6.5 MHz. A few more iterations will achieve an acceptable ripple performance in the new filter passband. Eventually the desired filter response is achieved, as displayed in Figure 7.

The Nonsymmetrical Case

If the filter is not symmetrical, the optimization procedure becomes more complicated. We not only evaluate the response at the maximum ripple points (including the passband limits), but also at each of the zeros of attenuation in the passband (minimum rip-

ple points). If the filter is terminated in equal impedances on the two ends, the response at these zeros can never have a positive deviation, only a negative one (loss.) If the filter is synthesized with a current source at the input, the zeros of attenuation in the passband take on a somewhat different flavor. The error function is still defined by how far these points deviate from zero, but in the case of a current source drive, the deviation can be of either sign. The response at the load can actually increase beyond the “zero” attenuation level defined by the response at dc, where the low-pass filter effectively disappears from the circuit. For each pass we have to sweep the filter response to locate the frequencies of both the ripple maximums and minimums. In this case, for a filter with n sections, we evaluate the filter response at n points, corresponding to the maximum and minimum ripple points, and optimize all element values, solving n equations in n unknowns. As we mentioned earlier, multiple zeros in the stopband will result in a filter that is nonsymmetrical. In this case we’ll move all these stopband zeros up proportionally the same amount, until the passband

ripple is acceptable, and then move them all back together, proportionally again, while optimizing the element values, until they arrive at the specified frequencies. The process with the non-symmetrical filter is essentially the same as in the symmetrical case, but will take longer because of the increased number of variables (element values) and equations (critical frequencies.)

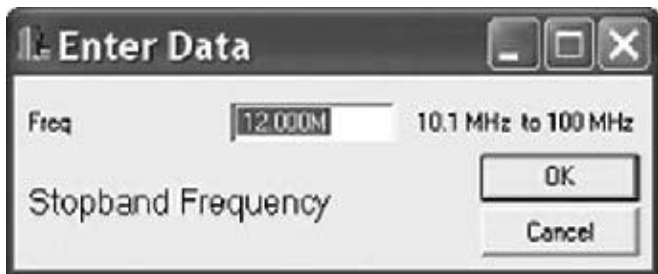


Figure 9 — Defining an elliptic filter requires a specification of the minimum stopband frequency.



Figure 10 — The application can calculate and insert zeros required for an elliptic filter.

The Mechanics

The first requirement for implementing the Newton-Raphson method for an iterative technique to synthesize the low-pass filter is the ability to evaluate the filter response as a function of frequency. We obtain our initial element values from a Chebyshev design with the same ripple and ripple cutoff frequency. The passband is then swept to locate the minimum and maximums of the filter response and the critical frequencies as we defined them earlier. A parabolic curve fit is used to improve our approximation of each critical frequency from the discreet points used in the analysis. The signed error from the desired ripple response is then calculated and saved at each of these critical frequencies as the error vector. These error vectors will be used in the recurrence relation, as well as to determine the partial derivatives.

Each of the elements to be varied (in pairs for the symmetrical filter, and individually for the nonsymmetrical filter) is then perturbed, and the process repeated, to determine the partial derivatives of the filter response at each critical frequency with respect to each element varied. These are then combined to create the square matrix of partial derivatives, known as the Jacobian. The Jacobian is defined in Equation 6.

$$\begin{matrix} \frac{\partial E_1}{\partial y_1} & \frac{\partial E_1}{\partial y_2} & \dots & \frac{\partial E_1}{\partial y_m} \\ \frac{\partial E_2}{\partial y_1} & \frac{\partial E_2}{\partial y_2} & \dots & \frac{\partial E_2}{\partial y_m} \\ \dots & \dots & \dots & \dots \\ \frac{\partial E_m}{\partial y_1} & \frac{\partial E_m}{\partial y_2} & \dots & \frac{\partial E_m}{\partial y_m} \end{matrix} \quad [\text{Eq 6}]$$

where E_i is the filter response at the i^{th} critical frequency, and y_k is the k^{th} independent element value. We’ll denote the Jacobian by the letter J . The error vector (unperturbed) is denoted by the letter e . We’re looking for the correction vector — the Δ values for the elements, which we’ll denote as Δ . Once the error vector, e , and the Jacobian, J , are formed, we need to find a solution for Δ in the matrix equation shown in Equation 7.

$$J \cdot \Delta = e \quad [\text{Eq 7}]$$

It’s not quite as simple as the scalar case used to approximate the square root. The most obvious path would be to find the inverse of the Jacobian matrix, and post multiply by e to obtain the Δ vector, but that makes the calculation more difficult than is required. A more efficient technique is to solve for the Δ vector using Gaussian elimination with back substitution.¹⁷ The Δ vector is then added to a vector of the element values being optimized, to obtain an improved approximation to the desired filter response. Move the zero frequencies in the stopband down a bit, or raise the lower passband cutoff frequency a bit, and do it all over again until we arrive at the desired characteristics, and an acceptable ripple in the passband.

A Test Vehicle

All this sounds great in theory, but does it work? In order to answer that question I developed a program to perform this optimization using the Newton-Raphson method. The installation files and com-

plete documentation for *Lowpass Filter Designer* are available for download at the ARRL *QEX* files website.¹⁸ The program starts with a Chebyshev filter, and then performs optimization to incorporate stopband zeros, and then a second optimization procedure to move the lower passband ripple cutoff frequency up.

Figure 8 shows the user interface for this program. There are edit

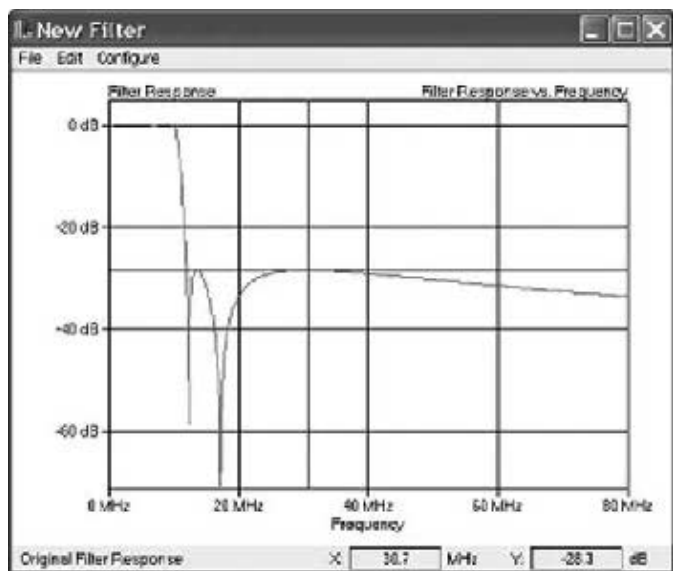


Figure 11 — The elliptic response is shown after completing the optimization cycle.

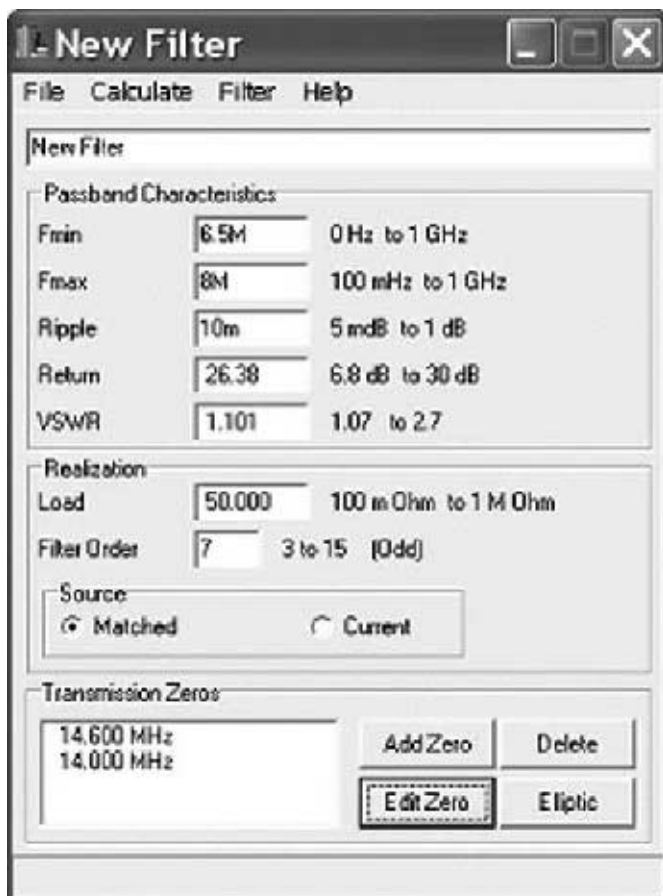


Figure 12 — Defining the filter parameter for an unequal ripple filter with two stopband zeros.

boxes for the lower passband ripple cutoff frequency (F_{min}), upper passband ripple cutoff frequency (F_{max}), and passband ripple. The Ripple can also be specified in terms of the minimum return loss (Return), or maximum VSWR (VSWR). The user can also specify the filter order, the load impedance (which is defaulted to 50 Ω here), and whether the source impedance is matched to the load impedance, or alternatively, the filter can be designed to be driven by a current source. At the bottom of the user interface is an area for entering finite stopband zeros. Pressing the “Elliptic” button will set the lower passband ripple cutoff frequency to zero, and insert the correct zero frequencies for an Elliptic response into the Transmission Zeros list.

As an example, we can set F_{max} to 10 MHz and press the Elliptic button. The program will respond by opening a dialog requesting the minimum stopband frequency for the elliptic function filter, as shown in Figure 9. Entering a value of 12 MHz, and pressing the OK button will insert the correct zero frequencies to obtain an Elliptic filter response with a ripple cutoff frequency of 10 MHz, and a minimum stopband frequency of 12 MHz, as shown in Figure 10. Selecting the Calculate | Response menu item will then begin the optimization process with zeros as defined for an Elliptic response. During the optimization procedure, the caption bar displays the progress of moving the zeros down to the desired frequency. After completing the optimization, the filter response is displayed in Figure 11.

As another example, design an unequal ripple filter with a lower passband frequency of 6.5 MHz, and an upper passband frequency of 8 MHz. We’ve increased the number of sections to 7, and included passband zeros at 14 MHz and 14.6 MHz to improve the second harmonic rejection. We’ve also reduced the passband ripple to 0.01 dB, as displayed in Figure 12. This synthesis takes a bit longer, and runs through two cycles. First the two stopband zeros are brought down to frequency, then the lower passband frequency is moved up until it reaches 6.5 MHz. The resultant response is then plotted in Figure 13. The desired passband response has been achieved, and the two zeros have brought the second harmonic rejection beyond 100 dB. Of course, seeing the response plotted doesn’t mean a lot if we can’t look at the element values. Selecting the Edit | Elements menu item on the response plot will bring up a window displaying the final element values, as shown in Figure 14. Notice that default values of 1 million have been added for the inductor Q_s . This has

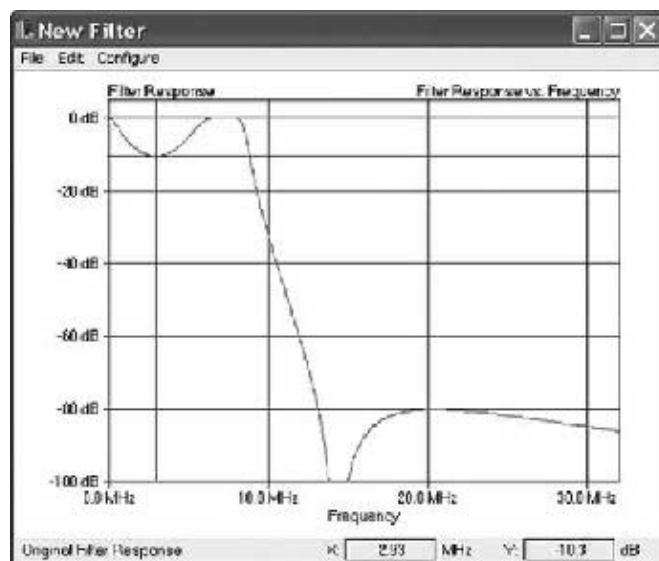


Figure 13 — The unequal ripple filter requires two iteration cycles, one to move the stopband zeros down, and the second to move the lower passband ripple cutoff frequency up.



Figure 14 — The element values can be viewed and modified from the element list window.

been done to prevent math errors that may occur when plotting the response through the stopband zeros. Alternatively you can enter realistic Qs for the inductors (capacitor Qs cannot be defined) to plot a more realistic filter response. By double clicking on any of the inductor elements, the Q entries can be changed. For illustration, we'll insert values of 200 for each of the inductors. Then by selecting the Plot | Amplitude menu item on this element list window we can plot the filter response with the degraded inductor Qs. Selecting the Configure | Passband menu item on the plot window will zoom in on the defined filter passband, as displayed in Figure 15.

The new plot shows that the filter loss reaches almost 0.2 dB at the upper end of the 40 meter band, with inductor Qs of 200. Along with the Q values, the element values can also be changed, allowing a filter response to be plotted with different element values. For example, you can enter the nearest standard value for the capacitors and re-plot the response to see how much degradation occurs by moving to a standard value. You can also "tweak" the inductor values to compensate for the standard values assigned to the capacitors.

Other Thoughts

This test application is not written as efficiently as it could be. In particular, each time an error vector is calculated, the application sweeps the passband until the final ripple maximum is located. Since the frequencies

associated with the ripple maximums do not vary significantly as the element values are perturbed, or even between successive iterations, this is clearly inefficient. If the application kept track of the frequencies it could reduce the number of points swept in each iteration. As the zeros are moved down in frequency, and as the lower passband ripple cutoff frequency is moved up in frequency, the step size is adjusted in order to maintain stability — that is to ensure that the passband ripples are not excessively degraded between cycles. No attempt has been made to optimize the speed at which these frequencies are adjusted.

It would also be tempting to modify the code so that optimization could proceed with fixed capacitor values — standard values. This would require a reconsideration of the error function. With fixed capacitor values, we no longer have the same number of variables as components in the error vector. With the three-element symmetrical filter for example, if we fix the two capacitors, we have only one variable — the inductor value. We can no longer force the two ripple points to a specified ripple value. We could, however, force the two ripple points to be equal in value, which now reduces our error function to one component, making the ripples equal. We could then solve for one variable with one equation. How this would be resolved in the higher order filters has not been considered.

Conclusion

The optimization technique proposed by

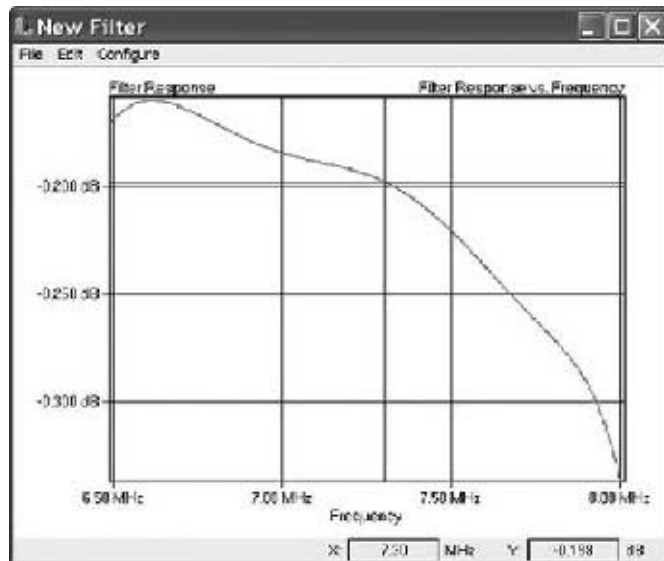


Figure 15 — Realistic inductor Q values increase the passband loss.

Cohn, and developed by Budimir does work, as verified by this test application. It's not particularly fast, but it does allow the user to specify an unequal ripple filter design, along with finite stopband zeros, and arrive at the correct element values to realize that response. The process is conceptually much simpler than extracting element values from the response, and the iterative procedure assures that errors will not accumulate. In the test application the filter can be realized with either a matched source impedance, or with a current source at the filter input. While this particular application is designed around a low-pass filter topology, the technique would be equally applicable to a bandpass topology, so long as the application has the capability to analyze the filter performance as a function of frequency. A result of this investigation has been the development of an application that should be useful in the design of equal and unequal ripple low-pass filters, with or without zeros in the stopband.

Notes

- ¹ALK Engineering, *Filsyn* filter design software: www.alkeng.com.
- ²Almost All Digital Electronics, AAE Filter Design: www.aade.com.
- ³Jim Tonne, W4ENE, *Elsie* filter design software, from www.tonnesoftware.com. The Student Edition of *Elsie* has been included on *The ARRL Handbook* companion CD for a number of years, including the 2011 *Handbook*. *The Handbook* and other ARRL publications are available from your local ARRL dealer, or from the ARRL Bookstore. Telephone toll free in the US 888-277-5289 or call 860-594-0355, fax 860-594-0303; www.arrl.org/shop; pubsales@arrl.org.
- ⁴H.J. Orchard and Gabor C. Temes, "Filter Design Using Transformed Variables," *IEEE Transactions on Circuit Theory*, Vol CT-15, pp 385-408, Dec 1968, reprinted

in *Computer Aided Filter Design*, edited by George Szentirmai, IEEE Press, 1973.

⁵Jose Luis Herrero and Gideon Willoner, *Synthesis of Filters*, Prentice-Hall, Inc, 1966.

⁶Dave Gordon-Smith, G3UUR, "Seventh-Order Unequal-Ripple SVC Low-Pass Filters with Improved Second Harmonic Attenuation," *QEX*, Jan/Feb 2011, pp 29 – 34.

⁷Dave Gordon-Smith, G3UUR, "Seventh-Order Unequal-Ripple Low-Pass Filter Design," *QEX*, Nov/Dec 2006, pp 31-34.

⁸Dave Gordon-Smith, G3UUR, "Fifth-Order Unequal-Ripple Low-Pass Filter Design," *QEX*, Nov/Dec 2010, pp 42-47.

⁹Gabor C. Temes and Donald A. Calahan, "Computer-Aided Network Optimization: The State-of-the-Art," *Proceedings of the IEEE*, Vol 53, Nov 1967, pp 1832-1863, reprinted in *Computer-Aided Filter Design*, edited by George Szentirmai, IEEE Press, 1973.

¹⁰Philip E. Gill, et al, *Practical Optimization*, Academic Press, 1981.

¹¹William H Press, et al, *Numerical Recipes in C*, Cambridge University Press, 1988, Chapter 10: "Minimization or Maximization

of Functions."

¹²William H Press, et al, *Numerical Recipes in C*, Cambridge University Press, 1988, pp 270-275.

¹³The frequency response of the filter is normally defined as $H(s)$, where s is a complex number. Since we're only concerned with the response of a filter for a sinusoidal input frequency of f , and because we won't be defining $H(s)$ as a mathematical function, we'll consider $H(f)$ instead, which is generally the solution provided by a circuit analysis program.

¹⁴In fact, this is precisely what the code does. The main code calls a subroutine that returns the ripple value at the next critical point. Except for the band edges, the main code doesn't specify the frequency, and the subroutine that finds the maximum ripple point doesn't return the frequency, only the ripple magnitude.

¹⁵S. B. Cohn, "Generalized Design of Band-Pass and Other Filters by Computer Optimization," *IEEE MTT-S International Microwave Symposium Digest*, June 1974, pp 272-274.

¹⁶Djuradj Budimir, *Generalized Filter Design*

by *Computer Optimization*, Artech House, Inc, 1998.

¹⁷William H Press, et al, *Numerical Recipes in C*, Cambridge University Press, 1988, pp 37-39.

¹⁸The author's *Lowpass Filter Designer* program is available for download at the ARRL QEX files website. Go to www.arrl.org/qexfiles and look for the file **7x11_Appel.zip**.

Gary Appel, WAØTFB, was involved in the design of radio frequency equipment for over 30 years, most recently as an RF design consultant in the Silicon Valley. Gary has been fascinated with radios for years, and was first licensed as WNØTFB in November of 1967, at the age of 14. He is a member of the ARRL and holds a BSEE degree from Washington University in St. Louis. Gary has been retired since 2008, and presently enjoys the opportunity that his retirement provides for working on homebrew projects, writing code, and swimming in the Pacific Ocean.



Array Solutions Your Source for Outstanding Radio Products

Top ranked Antenna Analyzers from Array Solutions

Announcing the **NEW** Array Solutions...

AIM *uhf* Analyzer

- Frequency range from 5 kHz to 1 GHz
- Data plots include SWR, RL, R + X, series and parallel, magnitude, phase, and more
- Dual Smith charts with rotation and 20 markers
- Plots and calibration files can be saved and used anytime in CVS and dynamic formats.
- AIM 4170C is still in production covering 5kHz to 180 MHz.



NEW!



Rig Expert Antenna Analyzers

New low-cost RigExpert AA-30 and AA-54 are powerful antenna analyzers designed for testing, checking, tuning or repairing antennas and antenna feedlines.

NEW!

Vector Network Analyzer Model VNA 2180

Measures impedance magnitude, phase and transmission parameters for antennas, filters, and discrete components - using one or two ports.

- Frequency range is 5KHz to 180MHz.
- Data plots include: impedance, SWR, return loss, S11 and S21.
- Plots can be saved for before and after comparisons.
- Dual Smith charts with zoom and rotation.
- Analog/digital I/O port for accessories.



NEW!

Other Quality Products from Array Solutions...

ACOM
Sales and Service for
Amplifiers and Accessories

Phillystran, Inc.
Official Worldwide
Phillystran Distributor

RigExpert
Analyzers and
Interfaces

Prostel Rotators
Strongest Rotators
on the Market

OptiBeam Antennas
German Engineering means
High Performance

Hof®
Surge Arrestors &
Antenna Switches



www.arrayolutions.com

Sunnyvale, Texas USA
Phone 214-954-7140
sales@arrayolutions.com
Fax 214-954-7142

Array Solutions analyzers are used by amateur, commercial, and professional broadcast engineers. See our web site for other products and additional details on these analyzers.

Transmission and Reception of Longitudinally-Polarized Momentum Waves

This introduction to vector potential radiation describes the verification of an alternative form of radiation predicted by James Clerk Maxwell's famous equations of electromagnetic radiation.

The world has been communicating with transverse electromagnetic (TEM) radio waves for more than one-hundred years. These are the waves known to radio amateurs, with the electric field, \mathbf{E} , perpendicular to the magnetic field, \mathbf{H} , and both fields perpendicular to the direction of propagation.

Research at McMaster University in Hamilton, Ontario has recently documented a new type of radiation, called vector potential (VP) radiation, which shares some similarities with TEM radiation, but is distinct in many ways:

1. Both TEM radio waves and VP waves were predicted by James Clerk Maxwell.
2. Both waves travel at the speed of light.
3. Both waves are emitted by a current-carrying wire.
4. Both wave amplitudes diminish with range as $1/\text{Range}$.

There the similarities end:

1. VP waves are longitudinal waves, much like sound waves.
2. VP waves carry no energy (The ultimate QRP). VP waves are carried by "virtual photons" rather than the real photons of radio waves.
3. VP waves carry only linear momentum. In fact, Maxwell's term for VP waves was "electro-kinetic momentum."
4. VP waves cannot be received with metallic antennas. For this reason, they have remained a mystery since Maxwell described them.
5. Since VP waves cannot be received with normal metallic antennas, they are in a fundamental way covert in nature. It is

expected that one of the first uses of VP communication will be for the military, in as much as transmissions cannot be easily intercepted.

In the years ahead, radio amateurs may play an important role in learning more about VP radiation. This article may serve as a primer.

Basic Characteristics

VP waves are emitted by all current carrying wires, in direct proportion with the current amplitude along the wire, and the length of the wire in wavelengths. In fact, a normal half-wave dipole emits VP waves along with the usual TEM radio waves. The vector potential (called \mathbf{A} in graduate electromagnetic texts), however, *is always polarized parallel with the current carrying wire*. This stands at odds with \mathbf{E} and \mathbf{H} fields, which tend to fold around a radiating wire. Most importantly, the vector potential exists *even off the ends of a dipole*, where there is no radiated \mathbf{E} or \mathbf{H} field. This makes the region off the ends of a dipole of special interest, as \mathbf{A} exists in the absence of \mathbf{E} or \mathbf{H} fields. In this region, the vector potential is polarized entirely longitudinally; in other words, in the direction of propagation.

These VP waves carry mechanical momentum. Free electrons oscillate remarkably well when they are exposed to a VP wave. How can we convert the VP wave back into an RF signal, though? Fortunately, this problem has now been solved: The solution is to use a fluorescent tube (with electronic "plasma" inside) which is folded

in the shape of the letter U. These tubes are usually sold at the hardware store for about \$6.00, for use in camping lanterns. Figure 1 schematically shows such a U tube aligned with a VP wave coming from the left side of the drawing. The VP wave travels the length of the tube, and causes an RF current to travel down the tube structure, similar to a parallel transmission line. When the RF current reaches the tube terminals (at the end of the tube), this current continues onward into a coaxial cable attached to the terminals and on to a radio receiver.

Momentum Coupling

The \mathbf{A} vector potential will couple linear momentum to free-electrons in its path. This is the basis for the detection of VP waves, and is called the Aharonov-Bohm Effect. (To learn more about the Aharonov-Bohm Effect, do a Google search on the term.) Electrons in copper and other metals can never move at velocities greater than about 3 mm/s because of crystalline lattice scattering, which becomes dominant at that velocity. This is entirely too slow to couple to vector potential radiation.

Free electrons in plasmas can easily travel at "drift velocities" of tens of kilometers per second. This makes plasma antennas a good match for vector potential wave reception. As an example, the vector potential near a half-wave dipole carrying a 10 mA rms current is about 10^{-10} webers/m (SI units). In a well designed plasma detector tube, momentum coupling for this potential (if the tube is aligned with \mathbf{A}) will yield a

free electron velocity of ± 20 m/s. Obviously, the sluggish electrons in copper cannot be expected to couple to this — metallic receiving antennas are out.

Figure 1 demonstrates the desired geometry for vector potential coupling momentum to a U-shaped plasma tube, and describes how RF current is developed in the tube terminals.

A Transmitting Antenna for 1296 MHz

This section describes the construction of a VP transmitting antenna for 1296 MHz. Since a transmitting dipole in free space will emit a large TEM RF signal, we house the transmitting element inside a circular waveguide to prevent radiation of TEM power. This shielding stops emission of TEM RF power while allowing the transmission of VP radiation through an open-ended guide. The circular waveguide shown in Figure 2 operates in the transverse magnetic TM_{01} longitudinal mode. The fields inside such circular guide are shown in Figure 3. The cutoff wavelength for this mode is 2.613 times the radius of the guide. Accordingly, a 7 inch diameter galvanized stovepipe (diameter = 17.78 cm) provides a cutoff wavelength of $\lambda_{cut} = (17.78/2) \times 2.613 = 23.23$ cm, which is a frequency of 1291 MHz.

To get maximum current on the waveguide probe (and hence maximum radiated vector potential amplitude) from a given transmitter, the probe should provide an impedance of zero ohms at the coaxial drive port. (Remember, we do not wish to radiate RF power anyway.) To get zero ohms at the drive port, with the other end of the guide as an “open circuit” for the TM_{01} mode, requires that the guide be a quarter wavelength overall from the open port to the coaxial port. For this 7 inch guide, the guide wavelength at 1296 MHz ($\lambda_0 = 23.148$ cm) is:

$$\lambda_{guide} = \frac{\lambda_0}{\sqrt{1 - \left(\frac{\lambda_0}{\lambda_{cut}}\right)^2}} = 275 \text{ cm}$$

Accordingly, the waveguide should be 69 cm in length to yield a quarter-wavelength. The coaxial probe should also be this length. It is important to keep the probe longitudinally centered in the waveguide. For this a Styrofoam strut may be used inside the guide.

Zero ohms will yield an infinite SWR on the coaxial cable leading to the transmitter. To prevent transmitter damage, use a 3 dB attenuator pad on the coaxial connection to the waveguide. (Of course, a circulator may also be used with a load on the third port.) A 3 dB pad will provide a return loss of 6 dB for an SWR of 3, which should be adequate

protection for most Amateur Radio transmitters. Be sure to use a pad rated at the full transmitter power.

To prevent minor off-axis TEM radiation, a “choke collar” may be used at the open

end of the guide. The length of the choke should be $23.148 / 4 = 5.8$ cm. This addition, although not strictly essential, will prevent currents on the inside of the waveguide from “folding around” the open end and radiating.

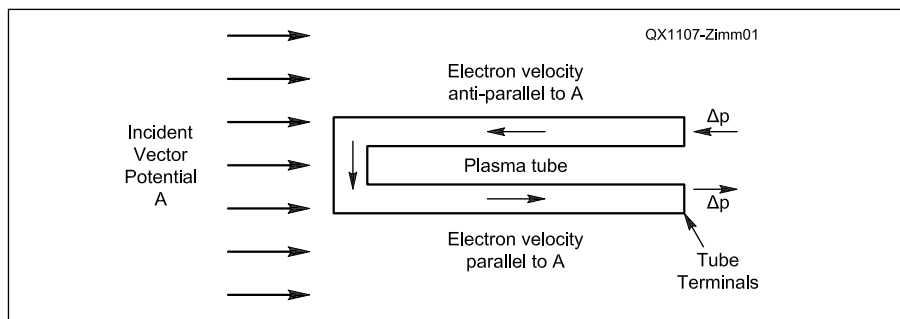


Figure 1 — In this diagram, the vector potential wave is traveling to the right towards the plasma tube (shown at an instant in time). The polarity of A is constantly oscillating at the frequency of the transmitting antenna, f . The electron dc current in the tube, provided by the tube high-voltage bias supply, travels in the direction shown by the arrows in the tube itself. At the instant shown, A is anti-parallel with the electron velocity in the top leg of the tube. This yields a momentum increment (and acceleration) to the left as shown. Likewise, in the bottom leg of the tube, A is parallel with the electron velocity, yielding momentum (and acceleration) to the right as shown. (Keep in mind that the momentum contributed to the electrons will be oscillating at frequency f .) This changing electron momentum and velocity is the detected RF current in the tube terminals.

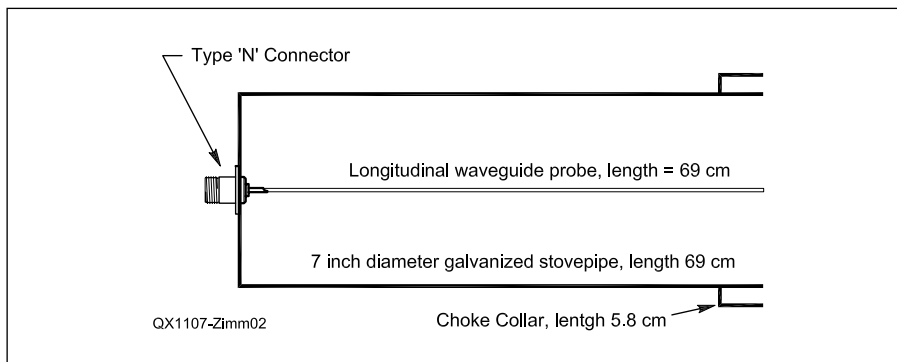


Figure 2 — This drawing shows the transmitting waveguide antenna for VP radiation at 1296 MHz.

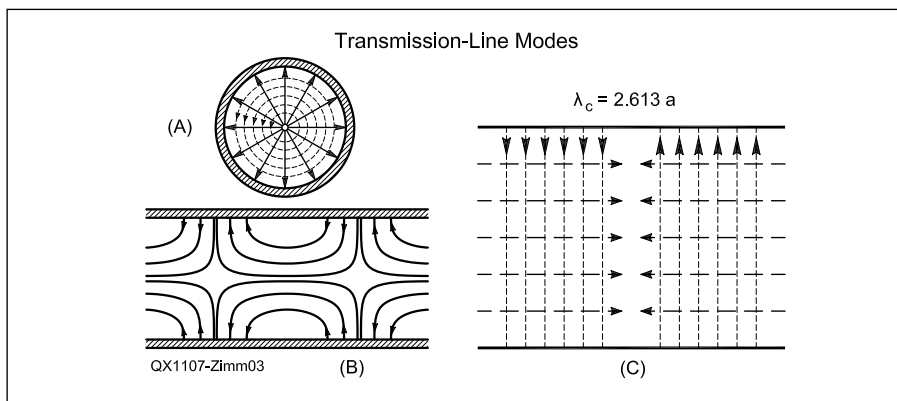


Figure 3 — The longitudinal fields inside a TM_{01} mode circular waveguide are illustrated here. The drawing is from N. Marcuvitz, *Waveguide Handbook*, MIT Radiation Laboratory Series, Vol 10, pg 68, McGraw-Hill, 1951.

A Receiving Antenna for 1296 MHz

The receiving plasma detector is made from a compact mercury-vapor fluorescent tube as found in camping lanterns. The fluorescent lamp is mounted inside the 7 inch diameter waveguide, as shown in Figure 4. At McMaster University, we use commercial waveguide with flanges; the fluorescent tube mounted on its flange is shown in Figure 5.

The U-shaped folded lamp, when ionized with direct current, provides a parallel transmission line with a characteristic impedance of 50Ω ; a perfect match to the 50Ω coaxial cable. When the longitudinal VP wave enters the waveguide, it couples a travelling wave onto the tube due to the Aharonov-Bohm effect. One leg of the tube is connected to the coaxial center conductor, while the remaining leg is grounded. (A balun could be used here, but the benefits are minor.)

The tube is operated at 200 mA dc current from a high voltage current-regulated power supply coupled to the coaxial line with a bias T. My power supply would not hold the current constant until I put a 10 W 120Ω resistor in series with the power supply. (Without the resistor, the tube flashed at a 1 Hz rate.) It is important to use a linear supply to keep bias current noise to a minimum.

The negative lead of the power supply should be connected to the coaxial center lead. About -400 V dc is momentarily required to ionize the fluorescent tube. My power supply is limited to -200 V dc. Accordingly, I went to Home Depot and purchased a battery operated fluorescent lamp for use in a closet. I wired the transformer output of this battery operated supply in series with the main power supply. By momentarily energizing the battery operated supply with a push button, the fluorescent tube will ionize, and then the direct current is regulated by the main supply and the 120Ω resistor. Note that the battery operated supply produces 500 V ac at 50 kHz . Be sure your bias T can momentarily support this large voltage or you will burn out your receiver front end.

Bias T Design

A suitable Bias T for use here is very costly if purchased commercially. Most of these bias Ts will not withstand the momentary 500 V used to ignite the fluorescent tube. This means you probably have to build your own. Figure 6 shows the location of the bias T in the receiver setup. Figure 7 presents a design based on a quarter-wave stub at 1296 MHz . In free-space, a quarter wavelength is 5.8 cm at this frequency. If built on microstrip with Teflon substrate (dielectric constant = 2.1) the stub should be 4.0 cm in length.

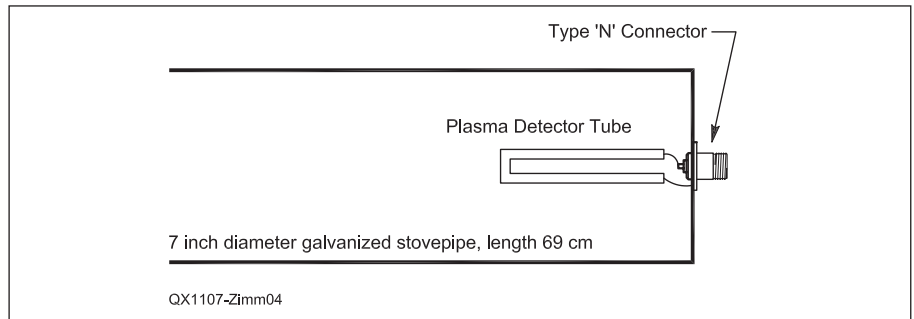


Figure 4 — The receiving waveguide antenna for VP radiation at 1296 MHz uses a camping lantern fluorescent tube. DC bias current to the plasma tube is provided by way of the coaxial cable via an inline bias T network.

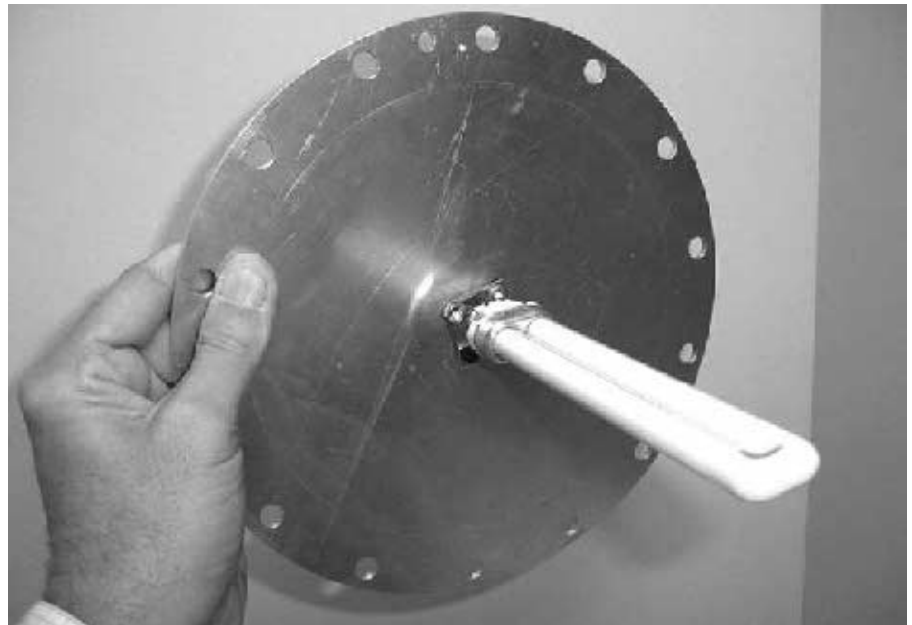


Figure 5 — Here is a photo of the fluorescent plasma detector tube mounted on a waveguide flange.

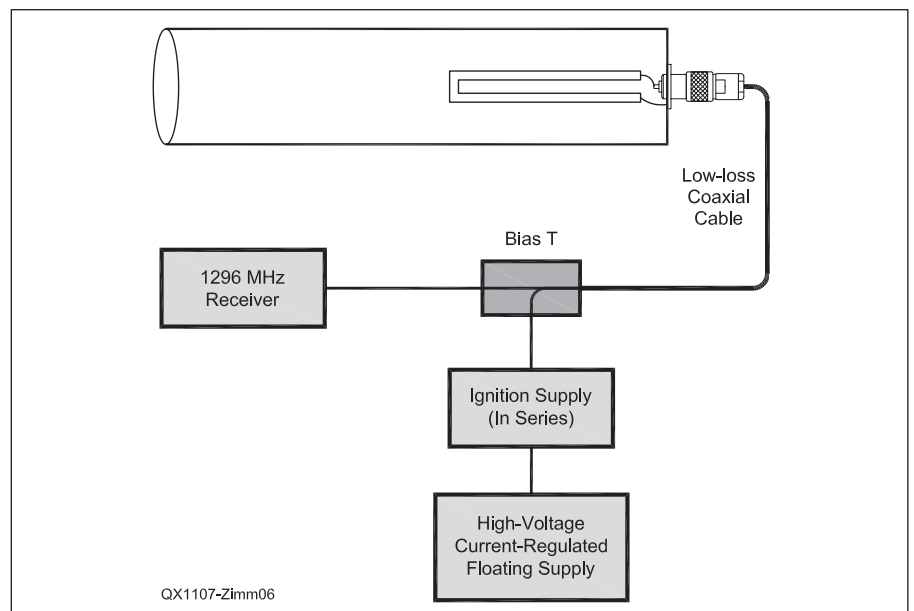


Figure 6 — Block diagram of the receiving setup. The bias T combines RF and tube bias on the single coaxial line leading to the waveguide antenna.

There are two 1000 pF capacitors in the design: one to block dc from the receiver line, and one to bypass the “cold-end” of the stub. In order to withstand the high dc voltage, these capacitors should have Teflon dielectric; for best RF performance, the capacitors should be single layer. If 0.010 inch thick Teflon film is used, a 1 square cm capacitor will yield > 730 pF, which is sufficient for the design¹.

Operating

The open-ended waveguides have an on-axis gain for VP radiation of about 3 dBi. (Additionally, there is an on-axis null for TEM radiation from the TM_{01} guide.) With a 1 W FM handheld transmitter, and a 3 dB pad, this will provide for a range of 500 meters over a clear path. For further range, you may use more drive power to yield more probe current. Alternatively, if you like sheet-metal work as I do, you can build a horn antenna for the transmitter and receiver. Figure 8 shows the 20 dBi horn I built for the receiver, which permitted a solid link at 1500 meters. If you use such horns at both the transmitter and receiver, a link range of 10 kilometers should be realized. FM is not the only mode possible — SSB or CW are certainly fine as well. Figure 9 shows Sherry Goeller, VE3DCU, operating the transmitting station on the 1500 meter link. Figure 10 is a photo of the author at the receiving site.

Summary

Fundamental advances in electromagnetics have yielded a new means of communication that small-signal microwave hams will find of interest; these waves are electro-mechanical in nature and carry no energy. Perhaps someday radio and television broadcasts will be transmitted without energy! Note that vector potential radiation requires radio frequency current into zero ohms, rather than RF power itself. This means that an intense VP wave may be transmitted without much (or any) RF power. Maybe distant civilizations are communicating with such waves right now?

There are no international regulations governing transmission of VP momentum radiation. It is prudent to operate within Amateur Radio allocated frequency bands and identify your station by call sign, however.

This work has been funded for 5 years by Dr. Natalia K. Nikolova of the Electrical

¹McMaster-Carr industrial supply house sells 0.010 inch Teflon sheet. Digi-Key Inc. sells adhesive copper foil. These materials may be used to construct the two capacitors. Use no more than a 25 W soldering iron when connecting the capacitors in the bias T circuit.

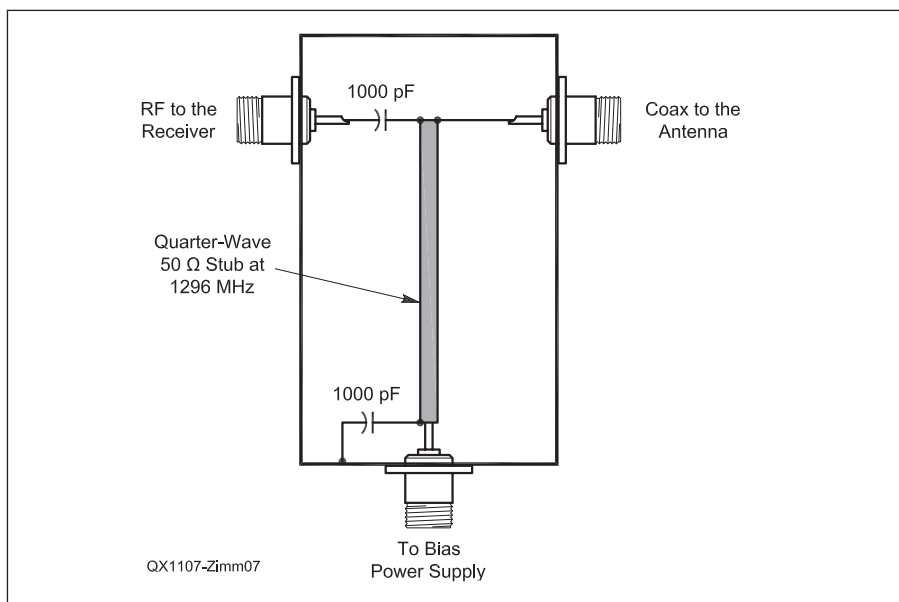


Figure 7 — Design of the bias T used to feed bias current to the waveguide antenna, and route RF back to the receiver from the antenna. The stub may be realized with microstrip. Alternatively, and perhaps easier, is to use a segment of Teflon-dielectric subminiature coaxial cable. If this is done, be sure to intimately ground the coaxial shield at both ends of the stub. Be careful to mark the ports clearly, for if the bias T is reversed your receiver will be destroyed.



Figure 8 — The 20 dBi gain conical horn built for the receiving detector is shown here.



Figure 9 — Sherry Goeller, VE3DCU, operating the transmitting momentum station on the 1500 m link. Note that the coaxial cable is connected to the rear of the waveguide.



Figure 10 — The author, NP4B/VE3RKZ, on the receiving end of the 1500 m momentum link. Note that the receiving horn had to be aimed at VE3DCU on top the bluff for satisfactory reception. The coaxial cable exits the waveguide from the rear; inside the waveguide is a small U-shaped fluorescent tube aligned with the waveguide center axis.

Engineering and Computer Department at McMaster University, Hamilton, Ontario, Canada, to whom the author is most grateful.

This report is based on the scientific paper: *Macroscopic Aharonov-Bohm Effect at L-band Microwave Frequencies*, Modern Physics Letters B, Vol 25, No. 9, April 2011, pp 649-662. PDF reprints are available from the author.


Robert Zimmerman obtained his Novice license in 1965 at the age of 13. Being very timid as a youth, the entire year passed without his making a QSO. Upon receiving his General license, his ham radio efforts began in earnest.

Zimmerman has spent his entire career as an RF engineer. In 1979 he joined the engineering staff at Arecibo Observatory, designing cryogenic low-noise preamplifiers for the telescope. Later, at the NASA Goddard Spaceflight Center, he was a design engineer on the Mars Observer spacecraft.


Zimmerman holds an extra-class license, NP4B, and a Canadian advanced-class license, VE3RKZ. He enjoys 40 meter PSK31 and SSB. Presently he lives in the hills overlooking Arecibo, Puerto Rico. He may be reached at: HC 3 Box 21829, Arecibo, Puerto Rico 00612.




NATIONAL RF, INC.




VECTOR-FINDER
Handheld VHF direction finder. Uses any FM xcvr. Audible & LED display
VF-142Q, 130-300 MHz \$239.95
VF-142QM, 130-500 MHz \$289.95



ATTENUATOR
Switchable, T-Pad Attenuator, 100 dB max - 10 dB min BNC connectors
AT-100, \$89.95



**TYPE NLF-2
LOW FREQUENCY
ACTIVE ANTENNA
AND AMPLIFIER**
A Hot, Active, Noise Reducing Antenna System that will sit on your desk and copy 2200, 1700, and 600 through 160 Meter Experimental and Amateur Radio Signals!
Type NLF-2 System: \$369.95



DIAL SCALES
The perfect finishing touch for your homebrew projects. 1/4-inch shaft couplings.
NPD-1, 3 3/4 x 2 3/4, 7:1 drive \$34.95
NPD-2, 5 1/8 x 3 3/8, 8:1 drive \$44.95
NPD-3, 5 1/8 x 3 3/4, 6:1 drive \$49.95

NATIONAL RF, INC
7969 ENGINEER ROAD, #102
SAN DIEGO, CA 92111

858.565.1319 FAX 858.571.5909
www.NationalRF.com

Extended Bandwidth Crystal Ladder Filters With Almost Symmetrical Responses

Learn about the design of a class of crystal filters capable of providing wider bandwidths and more symmetrical responses than conventional crystal ladder filters, while still retaining much of the inherent simplicity.

The Dishal LSB form of ladder filter, shown in Figure 1, is a very simple and convenient configuration for producing a crystal filter with exceptional ultimate attenuation and an excellent shape factor when the order is high and the bandwidth narrow, but for low orders and wide bandwidths the filter response becomes very asymmetric and the close-in attenuation on the low frequency side is quite poor. This is well illustrated by the response of a 4 pole, 5 MHz, 1 dB-ripple Chebyshev LSB crystal ladder filter with a bandwidth of 5 kHz, which is indicated by the solid black curve in Figure 2. The parallel resonance caused by the static capacitance (C_0) produces a null above the passband for each crystal in the filter, and this gives quite a good rate of attenuation on the high side of the response at the expense of quite a bit of degradation on the low side. The more symmetrical dashed curve shows how the response would look if C_0 didn't exist. The interval between the crystal series resonance and the parallel resonance due to C_0 is known as the pole-zero (PZ) spacing, and depends on the crystal frequency as well as the ratio of the motional capacitance, C_m , to C_0 . It limits the maximum bandwidth that is achievable with a standard crystal ladder filter at any frequency. The PZ spacing for AT-cut fundamental crystals can be less than 2 kHz at 1 MHz, but gets progressively wider as the crystal frequency increases, to the point where fundamental operation gives way to overtone. It then gets quite restricted again because the motional capacitance of a crystal in one of its overtone modes is very much smaller than it is at the fundamental resonance, yet the value of C_0 remains the same. This switch to overtone operation is

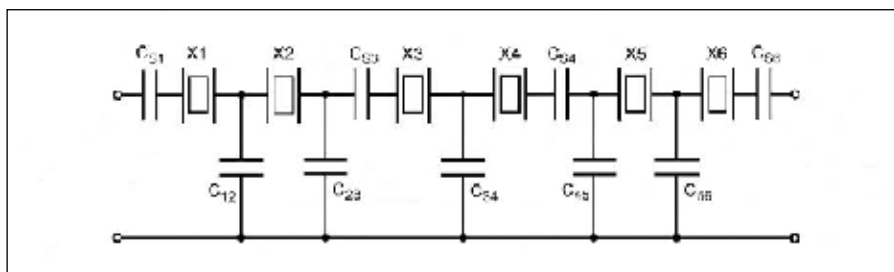


Figure 1 — Circuit of a standard 6-pole Dishal LSB crystal ladder filter (more identical crystals with their associated series tuning and shunt coupling capacitors can be added between X3 and X4 to increase the order of the filter).

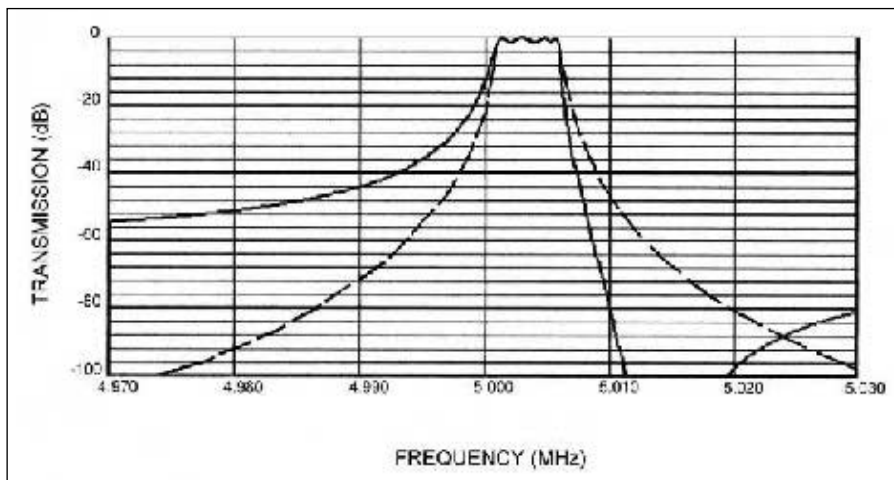


Figure 2 — Frequency response of a standard 4-pole, 5 kHz wide, Dishal LSB crystal ladder filter (solid curve) compared with the response of an ideal filter of the same bandwidth made with crystals that have no C_0 (dashed curve).

determined by production yield, and usually occurs above 25 MHz. Thinner fundamental crystals can be made, but the technology and expertise of individual crystal manufacturers varies and so do the decisions they make

about what constitutes an economical yield.

Crystals for the same frequency made by different manufacturers can also vary widely in their PZ spacing. For example, some 6 MHz HC-49/U crystals obtained by the

author from one manufacturer had a PZ spacing of around 8 kHz with a motional capacitance, $C_m = 0.008$ pF, while those from another had a PZ spacing of over 17 kHz with $C_m = 0.022$ pF. Generally, those crystals with a higher value of C_m at any given frequency will have a greater PZ spacing because the stray capacitance in the leads, mounting and base are a smaller proportion of the total parallel static capacitance of the crystal. Low-profile and surface-mount crystals tend to have smaller values of C_m than the larger HC-49/U, HC-18/U and HC-25/U types, though C_m can vary somewhat from manufacturer to manufacturer even with these.

Wide or extended bandwidths might be considered to be anything from slightly above 0.3 to more than 0.4 of the PZ spacing for crystal ladder filters. The presence of C_0 is responsible for the disproportionate reduction in the value of the coupling capacitors required to achieve bandwidths that are an ever greater proportion of the PZ spacing. The ultimate attenuation well away from the passband depends on both the ratio of C_0 to the coupling capacitor values and the number of stages (crystals) used in the filter. Consequently, the ultimate attenuation of a Dishal LSB crystal ladder filter decreases as the bandwidth is increased or the order reduced. How wide a simple low-order Dishal LSB crystal ladder filter can be made is heavily dependent on how poor a response can be tolerated. Dishal LSB ladder filters with bandwidths of over 0.6 PZ can be produced, but their ultimate attenuation might be considered far too low and the asymmetry of their response so poor that they are not worth using in practice. Extra LC tuned circuits in the IF stages can help improve the ultimate attenuation, but the only way to tackle asymmetry and poor close-in attenuation is to change the order, or the configuration of the filter.

Restoring Symmetry

Fortunately, there are two relatively simple hybrid forms of the crystal ladder filter that can provide almost symmetrical responses, and slightly wider bandwidths than the standard Dishal LSB form for the same maximum value of coupling capacitor. These hybrid forms, which are illustrated in Figures 3 and 4, can be used with any number of poles, but filters with 4, 5 or 6 poles benefit the most from them. The inductor across each end crystal in Figure 3 could be used solely to cancel out C_0 , but that would still leave some asymmetry because of the nulls just above the passband caused by the uncompensated C_0 of the two inner crystals. Crystals compensated by parallel inductors still produce nulls, but they are spaced well away from the passband and have little effect

on the close-in response unless their L/C ratio is very low. The spacing of these nulls from the crystal frequency for the case where C_0 is tuned to the same frequency can be predicted by Equation 1.

$$\Delta F_n = \pm 0.5 F_R \sqrt{\frac{C_m}{C_p}} \quad [\text{Eq 1}]$$

where:

C_m is the motional capacitance of the crystal, C_p is the total capacitance across the crystal, which includes C_0 and any additional capacitance used for tuning or the self-capacitance of the coil, and F_R is the resonant frequency of the crystal.

Smaller values of inductance than that required to tune C_p to resonance at the crystal frequency cause the null on the low side of the passband to move closer and the one above it to move further away. If the value of the parallel inductor is chosen carefully, a couple of nulls on the low side can be produced by the end crystals to even up the response of a simple 4-pole ladder filter built according to the circuit in Figure 3. This usually requires a value of around 0.5 to 0.6 L_p , where L_p is the value of inductance required for parallel resonance at the crystal frequency. The main disadvantage of this form of hybrid ladder filter is the fact that the end sections degenerate to a low-pass form at lower frequencies, and compromise the overall ultimate attenuation. The fact that only the two end crystals are affected by this

degenerative behavior does mean that the loss of ultimate attenuation is less important as the order of the filter increases and more ultimate attenuation is accrued.

In Figure 4, the end crystals are incorporated into half-lattice sections with 1:1 transformers and interfaced to the rest of the ladder filter by the correct choice of C_{S1} , C_{S4} , C_{12} and C_{34} . In order to create suitably spaced nulls on the low side of the passband, the neutralizing capacitors, C_n , are made larger than that required to just compensate for C_0 . Values of C_n between 2 and 3 times C_0 usually provide adequate symmetry. Because C_n is fed with an anti-phase signal at the input, it contributes approximately $2C_n$ to the coupling between the end crystals and the adjacent inner crystals. Therefore, the value of the coupling capacitors used for C_{12} and C_{34} in a 4-pole ladder filter with half-lattice end sections needs to be reduced by $2C_n$ to allow for this. Obviously, the value of C_{12} can never be less than $2C_n$, so this creates an upper limit to the bandwidth that can be achieved with this form of modified ladder filter. The hybrid ladder filter with half-lattice end sections is by far the best configuration as far as ultimate attenuation and a clean response is concerned, but using these is only convenient if matching transformers are a natural requirement of the design anyway. Ratios other than 1:1 can be used for the end transformers, of course, but any changes here must be taken into account when a suitable

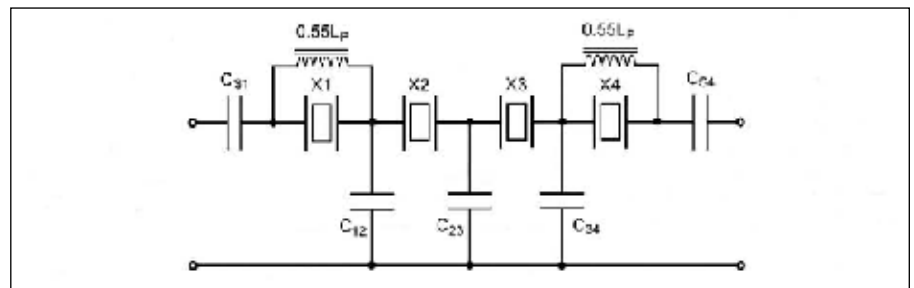


Figure 3 — First type of symmetrical hybrid crystal ladder filter using 0.55 L_p inductors across the end crystals. (L_p is the value of inductance that resonates with C_0 and its own capacitance at the crystal frequency.)

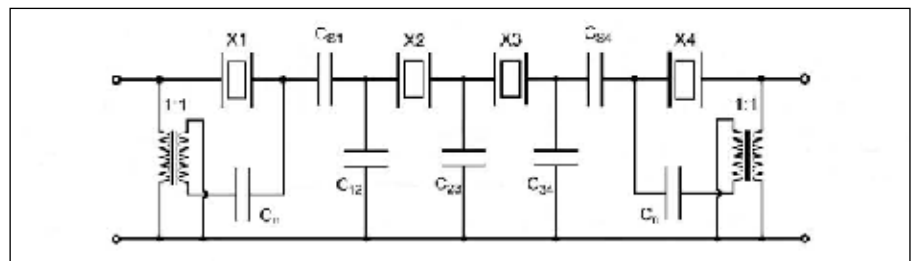


Figure 4 — Second type of symmetrical hybrid crystal ladder filter using half-lattice end sections. (C_n generally needs to be 2 to 3 times the value of C_0 to achieve reasonable symmetry.)

value is chosen for C_n .

Both of these forms of hybrid ladder filter cause the effective motional parameters of the end crystals to be different from those of the inner crystals, and interfacing the end sections to the inner part of the filter to produce a particular desired response requires a knowledge of how the different circuit topologies affect the behavior of the crystals.

Effect of Parallel Reactance on Crystal Behavior

In addition to creating a transmission zero at the anti-resonant frequency (parallel resonance), C_0 also causes the effective motional capacitance and inductance of each crystal to vary within the PZ interval between its resonant and anti-resonant frequencies. This is the reason why the termination resistance and coupling capacitor values of conventional Dishal crystal ladder filters do not vary linearly with bandwidth. They would if C_0 didn't exist. The effect of C_0 can be cancelled around the series resonance of the crystal by tuning it out with a parallel inductor of the right value (L_p). The standard k and q figures can then be used to calculate the termination resistance and coupling capacitor values using the actual measured motional inductance and capacitance of the crystals directly without any modification. Doing this for a 5 kHz, 1 dB-ripple ladder filter using perfect lossless 5 MHz crystals, each with their static capacitance, C_0 , tuned to resonance at 5 MHz by a parallel inductor, produces the design shown in Figure 5. Compare the termination and coupling values of this filter with the one in Figure 6 using identical crystals, where the effect of C_0 has not been cancelled. Both these designs exhibit perfect Chebyshev passband responses with 1 dB of ripple, and have the same bandwidth. It can be seen from the increased value of the termination resistance in Figure 6 that the effective motional inductance of these crystals with uncompensated static capacitance is 1.88 times that of the compensated crystals. Also, the coupling capacitor values indicate that the effective motional capacitance of the crystals is smaller than the actual measured value by 0.532 (the reciprocal of 1.88).

A third 1 dB Chebyshev design with four transmission zeroes created on the low-frequency side of the filter response by using a smaller value of parallel inductance ($0.55 L_p$) across each of the crystals is shown in Figure 7. This over compensates for the effect of C_0 and produces a null on the low side of resonance, separated from it by about the same interval as the anti-resonant frequency due to C_0 would have been above it. In this case, the termination resistance for the same bandwidth and response is lower than that of the filter made with compensated crystals

shown in Figure 5, reflecting a lower effective motional inductance, and the coupling capacitor values are larger, reflecting a higher effective value of motional capacitance for crystals with remnant parallel inductance.

When all crystals in a ladder filter have the same effective motional inductance and capacitance, the standard k and q figures can be used to calculate the termination resistance and coupling capacitor values with these effective motional parameter values. When crystals with different kinds of parallel reactance are combined in hybrid designs, however, the end crystals have a lower effective motional inductance than the inner crystals, and only approximations to the equal-ripple Chebyshev response can be achieved in practice. This is really only an academic point because component tol-

erances and crystal losses cause deviations from the ideal Chebyshev response anyway. In fact, since these ideal responses are always compromised in practice, it can be beneficial to use unequal-ripple filter designs that produce lower ripple in the outer regions of the passband to achieve a broader and flatter response after the effects of crystal loss and component tolerances have been taken into account. This is a similar idea to the quasi-equiripple (QER) type of filter described in the 2011 *ARRL Handbook*,¹ but instead of just equalizing the major valleys of an unequal-ripple response, any other convenient unequal-ripple form that provides a wider, flatter passband is considered acceptable as well.

¹Notes appear on page 44.

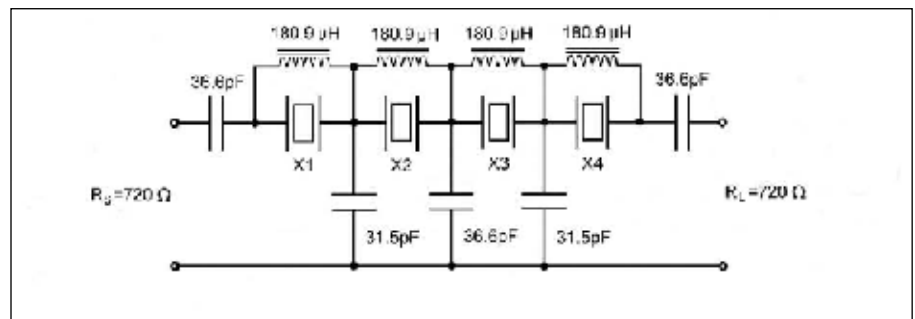


Figure 5 — A 4-pole, 1 dB-ripple Chebyshev crystal ladder filter design with the C_0 of each crystal tuned to resonance at the crystal frequency (5 MHz) — equivalent to no C_0 at all.

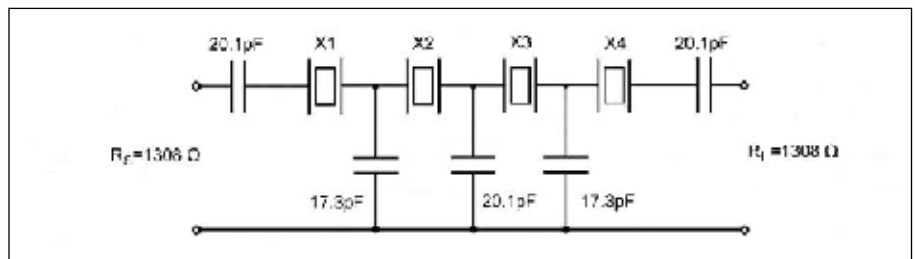


Figure 6 — A standard 4-pole, 5 MHz, Dishal LSB crystal ladder filter design using the same crystals and with the same bandwidth and pass-band ripple as the filter shown in Figure 5.

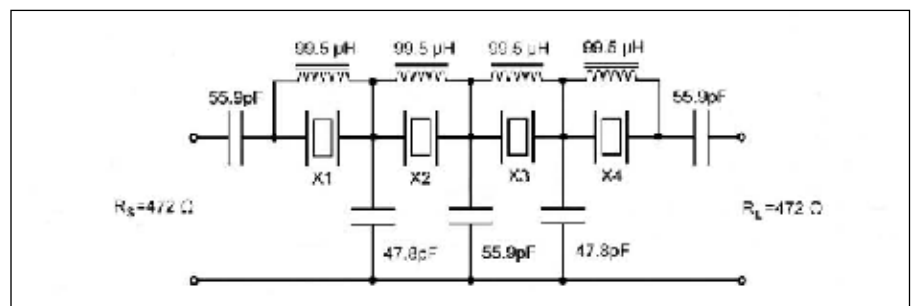


Figure 7 — A 4-pole 1 dB-ripple 5 MHz crystal ladder filter design with each crystal over-compensated by $0.55 L_p$ inductors so that four nulls are placed on the low side of the response to produce a USB image of the standard Dishal LSB ladder filter response (crystals and bandwidth are the same as in Figures 5 and 6).

Effective Motional Capacitance

The way in which the effective motional capacitance, C_{mf} , of a crystal varies with frequency for the case where C_0 provides the only parallel reactance is shown in Figure 8. In this graph, the ratio of the effective motional capacitance, C_{mf} , to the measured value, C_m , is plotted against the -3 dB bandwidth of the filter normalized in terms of the PZ spacing. This is done for design convenience and to make it universally applicable. It allows the effective motional capacitance of the inner crystals to be estimated for any hybrid design up to a bandwidth limit of 0.4 PZ. Extrapolation can be used for greater bandwidths if only rough estimates are sufficient.

Figure 9 indicates the effective motional capacitance versus the normalized bandwidth for crystals in half-lattice end sections or with $0.55 L_p$ parallel inductors. In the case of the former, the anti-phase signal fed through C_n makes it appear like a parallel inductor. When C_n is larger than the value of C_0 , the effective motional capacitance of the crystal increases, just as it does for values of parallel inductance that are less than L_p . At any bandwidth the effective motional capacitance for values of C_n between $2C_0$ and $3C_0$ can be found by linear interpolation between the two curves in Figure 9.

Also included on the same graph is a curve for the variation of the effective motional capacitance with a parallel inductor of $0.55 L_p$ ($r = 188$). Here $r = C_p / C_m$ and 188 is about the lowest ratio that is likely to be found in practice. Generally, because of the self-capacitance of the parallel inductor, this ratio will be greater, and usually comes out nearer 260. The L/C ratio of the parallel inductor and capacitor has an effect on both the position of the nulls and the value of the effective motional parameters. The $C_n = 3 C_0$ curve for half-lattice end sections also works quite well for parallel inductors of $0.55 L_p$ when they have a C_p / C_m ratio of around 300, so it can be used as the other limit for interpolation between $r = 188$ and $r = 300$ at any value of normalized bandwidth.

Designing Equal-Ripple Hybrid Filters

Approximations to the equal-ripple Chebyshev response can be achieved using either of the 4-pole hybrid crystal ladder filter circuits presented in Figures 3 and 4. First, however, the normalized bandwidth must be determined. The PZ spacing between the resonant and anti-resonant frequencies is given by:

$$PZ = F_R C_m / (2C_0) \quad [\text{Eq } 2]$$

When calculating the true PZ spac-

ing, allowances must be made for the stray capacitance between the electrodes and the case, which no longer contributes to C_0 if the crystal metal case is grounded. If PZ is measured, allowances must be made for both C_{case} and the measurement jig stray capacitance. Once the bandwidth has been established in terms of the true PZ spacing, the graphs in Figures 8 and 9 can be used to determine the

effective motional capacitance that should be used for the inner and outer crystals, and the coupling between them can be calculated from

$$C_{12} = C_{34} = F_C (C_{mf1} \times C_{mf2})^{1/2} / (k_{12} \times BW_3) \quad [\text{Eq } 3]$$

Where:

C_{mf1} and C_{mf2} are the effective motional

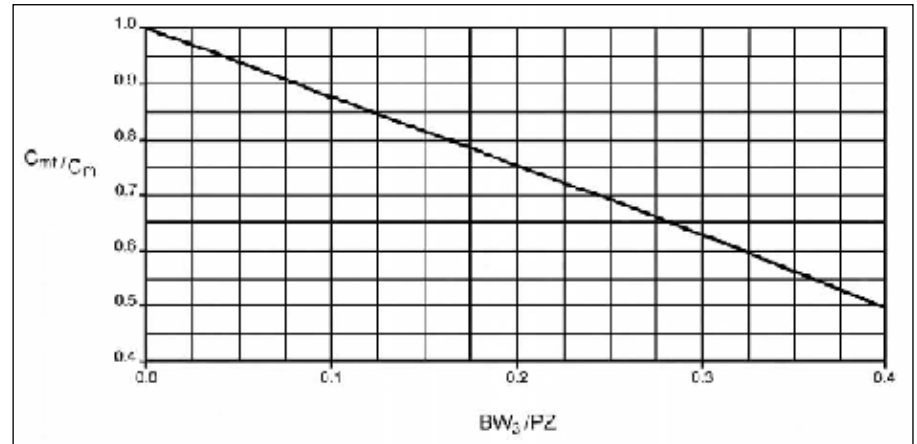


Figure 8 — Effective motional capacitance of hybrid ladder filter inner crystals (with parallel C_0) versus normalized bandwidth.

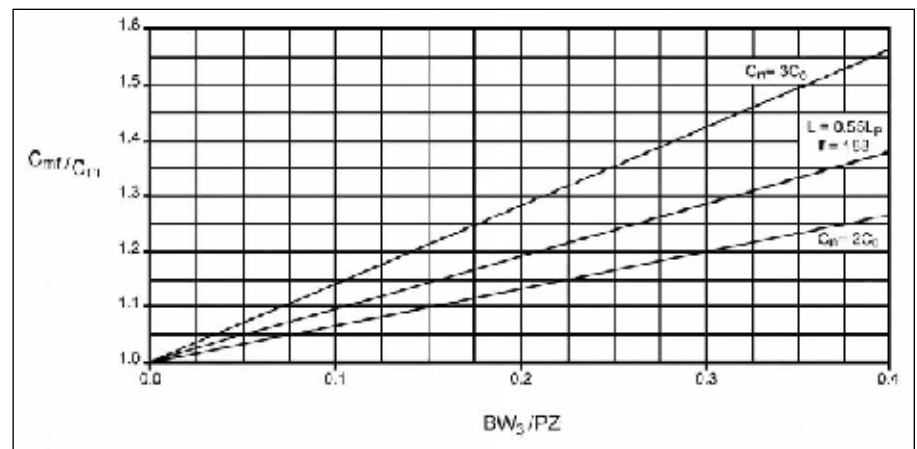


Figure 9 — Effective motional capacitance versus normalized bandwidth for end crystals used in hybrid ladder filters with either $0.55 L_p$ parallel inductors or half-lattice sections.

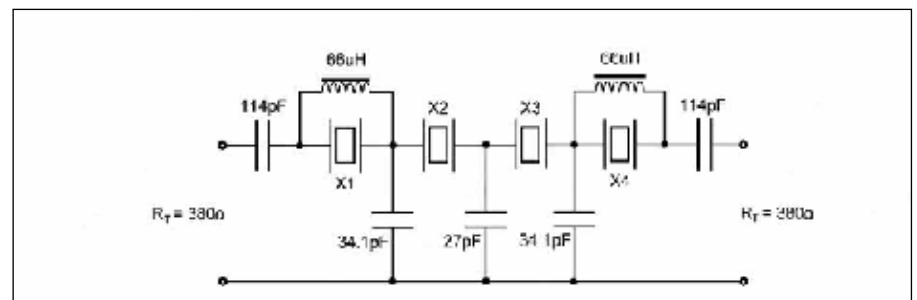


Figure 10 — Circuit of symmetrical 6.146 MHz hybrid crystal ladder filter of the first type with a 0.9 dB-ripple Chebyshev response.

capacitances of the end and inner crystals, respectively; F_C is the center frequency of the filter and BW_3 is the -3 dB bandwidth.

Usually, the exact center frequency is not known at this stage in the design process, and it's often more convenient to use the frequency marked on the crystals, instead, because the difference is usually negligible. The calculation of the termination resistance also needs to take into account the reduced motional inductance of the end crystals. The ratio of the effective motional inductance to measured motional inductance at any bandwidth is the reciprocal of the number given for C_{mf} / C_m in Figure 9. The standard k and q figures for Chebyshev designs can then be used with the effective values of motional inductance and capacitance to calculate rough values for the filter components. The design can then be optimized using a circuit analysis program to find the precise values required for an equal-ripple response.

An approximation to a 0.9 dB Chebyshev design for the first type of hybrid ladder filter using standard 6.144 MHz crystals is presented in Figure 10. The crystals X1 thru X4 have $C_m = 0.02131$ pF, $L_m = 31.503$ mH and $C_0 = 3.8$ pF with their cases grounded — this removes $C_{case} / 2$ from C_0 , and adds $2C_{case}$ to the coupling capacitance. The filter has a -3 dB bandwidth of 5.76 kHz and the effective motional inductance of the end crystals is about 0.71 of the measured value. Note the relative values of C_{12} and C_{23} . Normally, C_{12} would be smaller than C_{23} in a conventional Dishal LSB design with a Chebyshev response. In this case, however, it's the other way around, and the apparent anomaly comes about because C_{mf1} is more than twice C_{mf2} at this bandwidth, and C_{12} is worked out using the geometric mean of the two, whereas C_{23} is between the two inner crystals and its calculation is based solely on C_{mf2} . Figure 11 shows a plot of this hybrid crystal ladder filter, which looks quite acceptable within ± 200 kHz of the center frequency. The end sections degenerate into low-pass filters, however, at lower frequencies, and compromise the ultimate attenuation. As can be seen in the wider plot of this filter shown in Figure 12, there is a broad peak centered on about 3.3 MHz, which rises to 23.5 dB down on the passband level.

An example of an equal-ripple design using the second form of hybrid ladder circuit is presented in Figure 13. This is an approximation to a 0.2 dB Chebyshev design and has a bandwidth of around 6 kHz. It uses the same type of 6.144 MHz crystals as the previous design. The effective motional inductance of the end sections is closer to $0.77 L_m$ in this case, and the design value of C_{12} is, therefore, slightly smaller at 29.8 pF.

The actual value of C_{12} (and C_{34}) used in the circuit has been reduced by 16.4 pF to allow for the contribution from $2C_n$. This design has a stop-band attenuation of over 65 dB and a 6/60 dB shape factor of around 3. Theoretically, a 0.2 dB Chebyshev design without any added transmission zeroes would have a shape factor of around 4, but in

practice the degradation caused by the presence of C_0 in a standard 4-pole Dishal LSB ladder filter of the same bandwidth produces such a slow tail-off on the low side that a measurement of the response width at the -60 dB level becomes almost pointless, and the shape factor works out to be a staggering 21.7! So, it can be seen that the hybrid

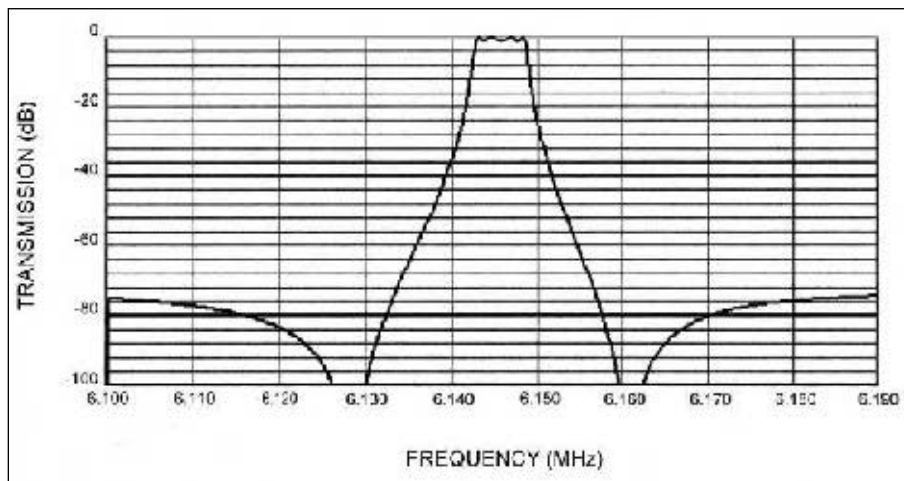


Figure 11 — Close-in frequency response of the symmetrical 0.9 dB Chebyshev hybrid crystal ladder filter of the first type (circuit shown in Figure 10).

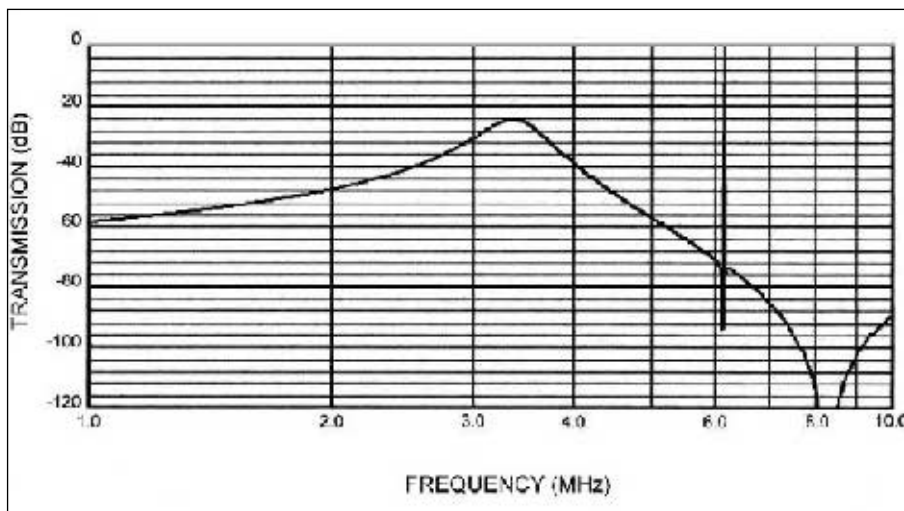


Figure 12 — Wider frequency response of the symmetrical 6.146 MHz hybrid crystal ladder filter in Figure 10, showing the broad low-frequency spurious response caused by the degeneration of the end sections to low-pass circuits.

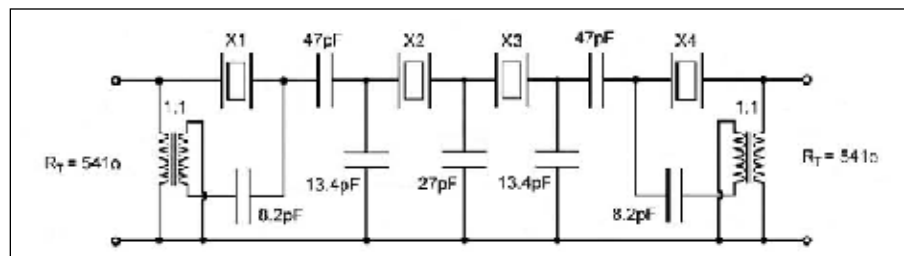


Figure 13 — Circuit of the second type of hybrid crystal ladder filter with a 0.2 dB-ripple Chebyshev response centered on 6.146 MHz.

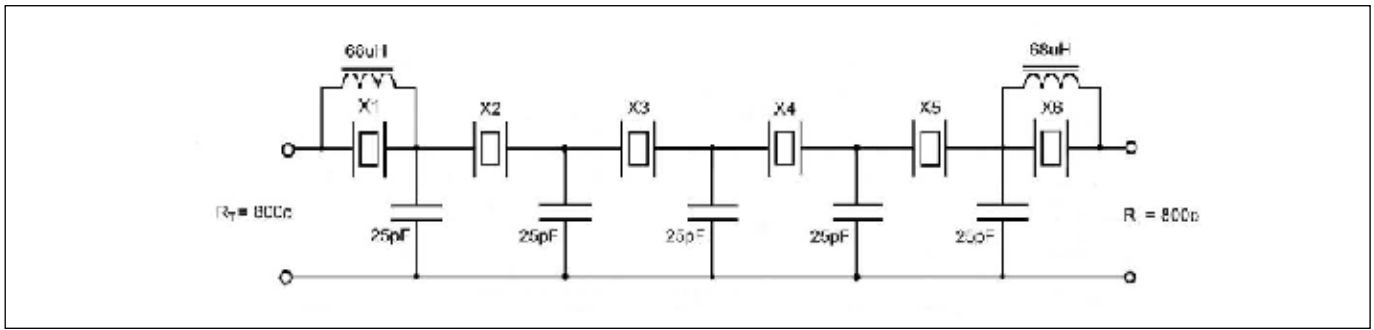


Figure 14 — Circuit of 6-pole hybrid AM crystal ladder filter of the first type using 6.144 MHz crystals (HC-18/U type).

version makes a big difference in the transition band on the low side of the response of a low-order crystal ladder filter. This design is much cleaner than the first type of hybrid ladder filter and doesn't suffer from degradation of the stop-band attenuation at lower frequencies.

There is one very significant difference between both of these forms of hybrid ladder filter and regular ladder filters, and that is the requirement for mesh frequencies to be staggered by a certain amount on either side of the interface between crystals with different effective motional parameters. In regular Dishal ladder filters, the crystals all have the same effective motional parameters and their meshes are tuned to the same frequency to produce the correct response. In hybrid ladder filters, the amount by which the mesh frequencies of individual crystals need to be staggered is dependent on both the bandwidth and the ratio of their effective motional capacitances. For example, the design shown in Figure 13 requires the inner crystals to be $0.083 BW_3$ high of the filter center frequency, and the end crystals to be an equal amount below it.

Variations on the QER Type of Filter

Although it can be very pleasing to design and use an almost symmetrical 4-pole hybrid crystal ladder filter with an equal-ripple Chebyshev response, the complications introduced by the mix of different motional parameters make this type of response considerably less attractive than some unequal-ripple types. Designing equal-ripple ladder filters with crystals that have different motional parameters becomes more difficult as the order increases, so there is good reason to consider other types of response for hybrid ladder filters, particularly those using more than four crystals. Very satisfactory passband shapes can be achieved with slightly simpler circuitry if unequal-ripple responses are used. These can be much easier to design and implement because no series tuning capacitors are required and the same value of coupling capacitor is used throughout the

filter, whatever the order. One unequal-ripple response that is ideally suited to designs using crystals with different motional parameters is the QER type. There are other closely related responses that provide quite acceptable passbands with motional parameter ratios in excess of 2.

Over the bandwidth range 0.25 to 0.31 PZ, the ratio of C_{m1} to C_{m2} varies from about 1.8 to 2.2 in nearly symmetrical hybrid ladder filters, and this is close enough to 2.0 to give a QER response. Above this range, the ripple in the middle of the response tends to be greater than it is towards the outer edges, but this still produces quite a wide, flat passband with the number of central ripples increasing with the order of the filter. Compared with Chebyshev and Butterworth designs, wider bandwidths can be obtained with unequal-ripple hybrid ladder filters for the same maximum value of coupling capacitor. In addition, there is the added convenience of being able to ignore the issue of mesh frequencies and use the same value of capacitor for coupling throughout the filter for at least the first form of hybrid design. The second form, with half-lattice end sections, requires C_{12} and its mirror image to be reduced by $2C_n$, so although the design value is the same throughout the filter, the actual values used are not. The lack of a broad LF spurious response with half-lattice end sections means that this form is probably the better solution for low-order filters and the simplicity of the other form makes it more suitable for high-order designs where some of the extra ultimate attenuation can afford to be sacrificed for better symmetry.

Designing Unequal-Ripple Hybrid Ladder Filters

Designs for both the first and second types of hybrid crystal ladder filter can be based on QER ladder filter designs of the same bandwidth. Either the "Dishal" program by Horst Steder, DJ6EV, or the k and q values presented in the 2010 *ARRL Handbook* can be used to establish the termination resistance and coupling capacitor values required for the target bandwidth.²

The value of L_p for the first form of hybrid ladder filter needs to allow for both the self-capacitance of the coil and differences in the value of C_0 when the metal case of the crystal is grounded. Once the value of L_p has been determined, a preferred value of miniature RF choke can be selected that is close to $0.55 L_p$. Of course, toroidal inductors with a higher Q can be used, but tend to be bulkier and not so convenient.

The circuit of a 6 pole variant on the QER type of hybrid ladder filter is presented in Figure 14. This is based on the QER values predicted by Steder's "Dishal" program for crystals (X1 thru X6) with $C_m = 0.02131$ pF, $L_m = 31.503$ mH, and $C_0 = 3.8$ pF. The inductance used for the parallel inductor was the closest preferred value to the one calculated using $C_p = 5.6$ pF (an extra 1.8 pF was allowed for the self-capacitance of the miniature RF choke). The target bandwidth (-3 dB) used in the "Dishal" program was chosen as 6.050 kHz to round off the coupling capacitor value to a convenient figure (25 pF). The predicted value for the termination resistance was 899 Ω. Analysis showed that the passband response could be improved with $R_T = 800$ Ω. This gave a bandwidth of 6.059 kHz and an insertion loss of 0.22 dB for crystals with a Q of 200,000, as shown in Figure 15. It can be seen from this plot of the passband that there is only one ripple (dip) in the center, where it reaches a maximum of 0.6 dB. This sort of response is fairly typical of 6-pole unequal-ripple filters when the ratio of C_{m1} / C_{m2} is much greater than 2. An 8-pole QER variant would have 3 ripples in the central region of the passband. The depth of the ripple in the middle of the passband can be controlled to some extent by varying the value of the terminating resistance.

The bandwidth of this filter is equivalent to 0.35 PZ. The reduction in R_T is to be expected at this bandwidth since the effective value of motional inductance for the end crystals is lower than the "Dishal" program expects it to be for two uncompensated crystals in parallel. A correction could be calcu-

lated for R_T using the reciprocals of C_{mf} / C_m in Figures 8 and 9. It is much simpler just to model the filter on a computer to see what passband shapes can be produced by altering R_T . Then, the most acceptable one can be chosen. The close-in response of the filter, which covers ± 150 kHz around the center frequency, is shown in Figure 16. There are only two transmission zeroes on the low side of the response compared with four on the high side, so symmetry is not perfect. The 6/60 dB shape factor is less than 2.3, which is similar to the figure that would be achieved by a Dishal LSB design, but in this case the response is considerably more balanced.

The motional parameters used in this simulation were taken from measurements made on some miniature HC-18/U crystals marked as “6.144 MHz,” which had a resonant frequency of around 6.1426 MHz. A prototype 6-pole hybrid filter made with these crystals produced a measured -3 dB bandwidth of approximately 5.97 kHz. The actual coupling capacitors used in the prototype filter were 22 pF plate ceramic types with an additional 3 pF being allowed for the two times C_{case} of the grounded crystal cans on either side of each coupling capacitor. The measured passband response was extremely close to that shown in Figure 15 and the broad spurious response that normally occurs lower in frequency with this type of hybrid circuit was measured at 60 dB down on the filter passband level. As a matter of interest, increasing the order of the filter to 8 would suppress this spurious response by a further 36 dB and widen the bandwidth by another 2%.

The second type of hybrid ladder filter requires the selection of a suitable value for C_n . A standard value of fixed capacitor within the range 2.2 to 2.5 times C_0 usually gives adequate symmetry. The value of capacitor used for C_{12} and its mirror image then needs to be determined by subtracting $2C_n$ from the value used for the other coupling capacitors. If the reduced value of C_{12} is not convenient the next preferred value down will usually suffice. For example, 8.2 pF is a convenient preferred value for C_n in a half-lattice version of the 6.144 MHz filter circuit shown in Figure 14, and subtracting 16.4 pF from 25 pF leaves 8.6 pF. The actual value of the capacitor used for C_{12} can be reduced to 8.2 pF without noticeably affecting the passband response.

The termination resistance values predicted by Steder’s “Dishal” program should be within about 25% of the value required for most QER variants, despite the fact that the effective motional inductance of the end crystals is lower than half that of the inner crystals, because higher termination resistance values produce better passband responses when the motional parameter ratio

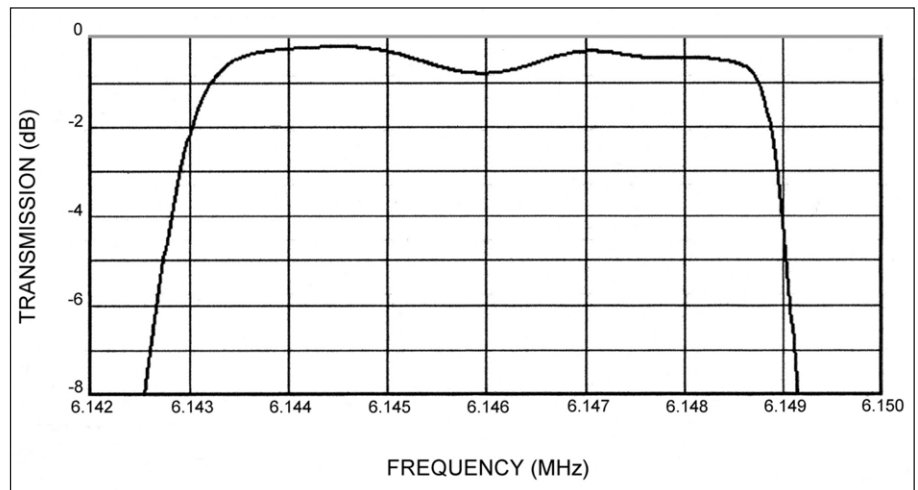


Figure 15 — Passband predicted for the 6.146 MHz, 6-pole hybrid AM crystal ladder filter. The response is a variant of the QER type ($BW_3 = 0.35$ PZ).

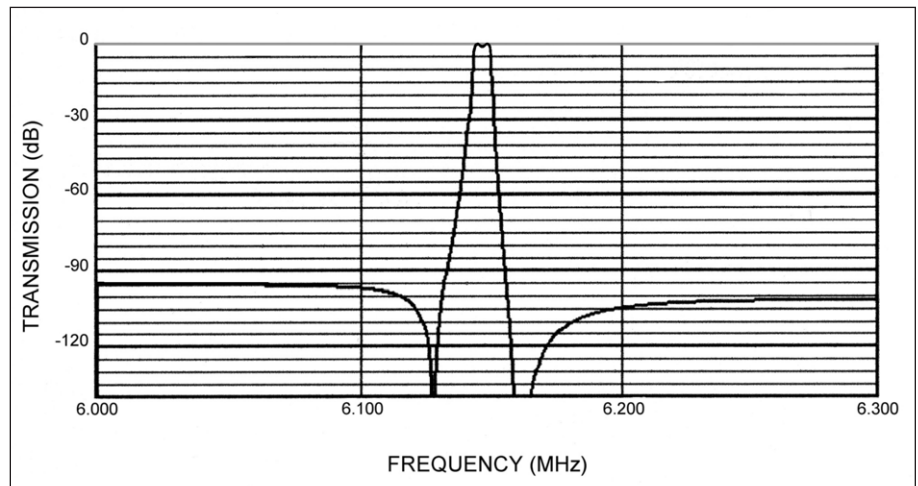


Figure 16 — Close-in response (within ± 150 kHz) for the 6.146 MHz, 6-pole hybrid AM crystal ladder filter of the first type, shown in Figure 14.

exceeds 2 by a reasonable margin. Hybrid ladder designs can also be used for bandwidths below 0.25 PZ, if better symmetry is required. The ratio of the motional parameters of the end and inner crystals is usually insufficient to produce a QER passband for narrower hybrid filters, and it’s often advisable to use a value 20% lower in capacitance for C_{12} and its mirror image, compared with the middle coupling capacitors, to achieve a good passband response.

Summary and Concluding Remarks

Much of the simplicity of the conventional Dishal LSB crystal ladder filter can be retained, and the asymmetry of extended bandwidth ladder filters much improved, if inductors of around $0.55 L_p$ are placed across just the end crystals of ladder filters with 6 or more poles. Ideally, high Q inductors should be used, but these can be bulky. Usually, miniature axial RF chokes of a suitable value

can be found that balance up the transition band reasonably well, even though they have quite low values of Q (around 80 to 100). Their self-capacitance is typically 1.5 to 2 pF, so this needs to be added to the effective value of C_0 (less half of C_{case} if the metal case is grounded) for calculating the value of L_p . The actual value of parallel inductance required to produce a more-or-less symmetrical response will usually be in the range 0.5 to $0.6 L_p$, and this causes the effective motional inductance of the end crystals to decrease with increasing bandwidth, and the motional capacitance to increase. Uncompensated crystals have an effective motional capacitance that is decreasing with frequency between the series and parallel resonances. Therefore, in hybrid ladder filters with bandwidths from about 0.25 PZ to 0.4 PZ the end and inner crystals can have ratios of effective motional capacitance anywhere between 1.8 and 3. Depending on the

exact ratio, this gives either QER or variations on the QER type of response with equal coupling capacitor values used throughout the design. The actual passband response varies somewhat towards the top end of this range, but usually the passband is reasonably symmetrical and the maximum ripple can be kept under 1 dB by the correct choice of termination resistance. Loss of ultimate attenuation inevitably occurs with this arrangement, but the main spurious response caused by these parallel inductors is sufficiently well away from the center frequency that a couple of tuned circuits are normally all that's required to reduce them to an acceptable level. Increasing the order of the filter can also reduce the spurious response level and could reduce the LC filtering requirement to one tuned circuit, or possibly none if the order is taken high enough.

The second type of hybrid ladder filter, which uses half-lattice end sections, can provide very acceptable performance up to bandwidths of 0.4 PZ, even in 4-pole designs. It can also be used in high-order filters to improve symmetry, of course, if the added circuitry is not considered too inconvenient. The 1:1 transformers used in this form of hybrid ladder design can be broadband or tuned. Tuned transformers have the advantage that they improve the ultimate attenuation, but are generally bulkier than broadband ones. I have used Toko KALS4520A 10.7 MHz IF transformers in 5 MHz, 6 MHz and 8 MHz hybrid ladder filters. It's quite easy to retune these transformers with an external capacitor, of course, and they have an offset tap (8 t:7 t) which can be reversed, if necessary, to better position the low-side nulls when using preferred-value fixed capacitors for C_n .

Differences between the effective motional parameters of the end and inner crystals preclude very precise equal-ripple Chebyshev responses from being produced in hybrid ladder filters. Despite this, quite acceptable equal-ripple passband responses can be achieved with simple 4-pole hybrid ladder filters using the standard k and q values as a rough guide, and then adjusting the mesh offset frequencies and refining the coupling and termination values using a computer modeling program. Unequal-ripple designs can produce such satisfactory pass-band responses with so little design effort that it is hardly worth considering Chebyshev responses for hybrid crystal ladder filters of any order.

The techniques described in this article should allow reasonably symmetrical crystal ladder filters to be produced with bandwidths of up to 0.4 PZ, or possibly more. The hybrid design with half-lattice end sections is to be preferred for low-order filters, whereas the other form with parallel inductors across the

end crystals is much more convenient for filters of higher order since only two additional inductors are required. The difference in the effective motional parameters of inner and end crystals in hybrid ladder designs makes them ideally suited to the QER response and its variants. The lack of a need for series tuning capacitors in the end sections and some of the inner meshes of high-order hybrid ladder filters could offset the increased number of components in the end sections to a large extent, making them quite an attractive proposition compared with a standard Chebyshev LSB ladder design. When wider filters are required, hybrid crystal ladder filters with QER responses also have the additional benefit that they provide an extra 4 to 5% of bandwidth for the same maximum value of coupling capacitor compared with Cohn or Chebyshev designs. In order to achieve bandwidths of up to 0.1% of the crystal frequency with QER hybrid ladder designs, however, the PZ spacing (with the effect of C_{case} removed) needs to be in the region of $F_R / 400$. This condition cannot be met by the low-profile HC-49/US or HC-49/S crystals, which tend to have a PZ spacing of around $F_R / 650$ at 4 MHz rising to $F_R / 500$ at 20 MHz. If 0.1% is much above 0.4 PZ, this can produce some deterioration of the passband shape — the central dip of a 6-pole hybrid filter moves higher in frequency and deepens, causing some asymmetry in the response and a narrow upper peak.

Many mass-produced crystals have relatively tightly controlled frequencies, so for wider bandwidth filters it can be tempting to build them without checking the crystals first. Building filters with untested crystals can be a risky business, however, because the ESR and Q values of modern miniature crystals vary enormously, and the poor ones really need to be weeded out prior to use. Adding an RF detector circuit to the G3UUR frequency-shift oscillator described in *Experimental Methods of RF Design* allows the ranking of individual crystals by the output they produce.³ The oscillator output level is inversely related to the crystal ESR value, which in turn is inversely related to its Q. So, the higher the RF output, the higher the crystal Q. A suitable circuit and a crude method of estimating crystal ESR and Q values have recently been described in *QRP Quarterly*.⁴ The oscillator output is non-linearly related to crystal Q, but measuring it using an RF detector provides a simple means of comparing the activity and Q of individual crystals. The better crystals can then be selected for use in filters and the poor ones discarded, or used in oscillators. The very best can be used in CW filters. Ranking individual crystals by their relative oscillator output is all that's required to make the best possible use of the

From **MILLIWATTS** to **KILOWATTS**
More Watts per Dollar



Taylor
TUBES

**Quality
Transmitting
& Audio Tubes**



- COMMUNICATIONS
- BROADCAST
- INDUSTRY
- AMATEUR



Immediate Shipment from Stock

3CPX800A7	3CX15000A7	4CX5000A	813
3CPX5000A7	3CX20000A7	4CX7500A	833A
3CW20000A7	4CX250B	4CX10000A	833C
3CX100A5	4CX250BC	4CX10000D	845
3CX400A7	4CX250BT	4CX15000A	866-SS
3CX400U7	4CX250FG	4X150A	872A-SS
3CX800A7	4CX250R	YC-130	5867A
3CX1200A7	4CX350A	YU-106	5868
3CX1200D7	4CX350F	YU-108	6146B
3CX1200Z7	4CX400A	YU-148	7092
3CX1500A7	4CX800A	YU-157	3-500ZG
3CX2500A3	4CX1000A	572B	4-400A
3CX2500F3	4CX1500A	807	M328/TH328
3CX3000A7	4CX1500B	810	M338/TH338
3CX6000A7	4CX3000A	811A	M347/TH347
3CX10000A7	4CX3500A	812A	M382

— TOO MANY TO LIST ALL —



ORDERS ONLY:

800-RF-PARTS • 800-737-2787

Se Habla Español • We Export

TECH HELP / ORDER / INFO: 760-744-0700

FAX: 760-744-1943 or 888-744-1943



An Address to Remember:

www.rfparts.com

E-mail:

rfp@rfparts.com



**RF PARTS
COMPANY**

crystals available, but should approximate ESR or Q values be required for modeling purposes, the method described in *QRP Quarterly* provides a quick and simple means of estimating either of these parameters.

The motional parameters and PZ spacing of crystals can vary quite considerably from manufacturer to manufacturer. The motional capacitance of a quartz crystal depends on its electrode area, and even at the same frequency different manufacturers use different electrode areas for reasons of economy, to suppress unwanted modes or to optimize the trimming range. The stray capacitance due to the leads and mounting structures will be pretty much the same for a particular sort of holder, so the PZ spacing and the maximum bandwidth attainable with any set of crystals will depend mainly on the manufacturer's choice of electrode area. Generally, the crystals with the largest values of C_m will produce the greatest bandwidth at any given frequency. HC-18/U and HC-49/U crystals being larger than the squat HC-49/US or HC-49/S crystals will tend to have a higher value of C_m and a better PZ spacing for wide filters, particularly below about 8 MHz. Some manufacturers may use small electrodes on crystals mounted in the larger holders, however, so it's impossible to tell beforehand which crystals will produce the widest bandwidth without characterizing them. It's a wise precaution, therefore, to get a sample to test first before buying a larger quantity of crystals. It would also be useful if constructors could post the details of any crystals they characterize on the Internet

somewhere, to establish a database of information on crystals from different sources. This would help others avoid the less suitable crystals for particularly exacting applications, such as wide bandwidth filters or VXOs. Anyone donating some space on their website for such a database would be providing a valuable service to all homebrewers around the world.

Notes

¹H. Ward Silver, NØAX, Ed., *The ARRL Handbook*, 2011 Edition, ARRL, 2010, "Crystal Filter Design," Chapter 11, Section 11.6.2. ARRL Publication Order No. 0953, \$49.95. ARRL publications are available from your local ARRL dealer or from the ARRL Bookstore. Telephone toll free in the US: 888-277-5289, or call 860-594-0355, fax 860-594-0303; www.arrrl.org/shop; pubsales@arrrl.org.

²The "Dishal" ladder filter design program by Horst Steder, DJ6EV, and Jack Hardcastle, G3JIR, is available as a free download from www.arrrl.org/qexfiles. Look for the file **11x09_Steder-Hardcastle.zip**. This program is described in "Crystal Ladder Filters for All," Nov/Dec 2009 QEX, pp 14-18.

³Wes Hayward, W7ZOI, Rick Campbell, KK7B, and Bob Larkin, W7PUA, *Experimental Methods in RF Design*, ARRL, 2003-2009. ARRL Order no. 9239, \$49.95. ARRL publications are available from your local ARRL dealer or from the ARRL Bookstore. Telephone toll free in the US: 888-277-5289, or call 860-594-0355, fax 860-594-0303; www.arrrl.org/shop; pubsales@arrrl.org.

⁴David Gordon-Smith, G3UUR, "Notes on the Measurement of Quartz Crystal Motional Parameters," *QRP Quarterly*, Fall 2010, Volume 51, Number 4, pp 30 - 33.

Dave Gordon-Smith, G3UUR, was first licensed in 1965 and concentrated mainly on home construction and 160-meter CW DX during his first few years on the air. Constructing his own equipment was a necessity in those days because he was an impoverished school-boy, but it later became a source of great fun and satisfaction. Filters, antennas and propagation have always fascinated him, and much of his Amateur Radio construction and experimentation has been driven by a desire to understand them. He tends to use theory to make up for a lack of test gear, and enjoys playing with novel and unusual circuits.

He served with VSO (British Peace Corps) on Grenada, where he taught math and chemistry, and operated as VP2GBR. He holds a PhD in material science and was a tenured member of the academic staff at the University of Warwick, specializing in the characterization and study of defects in crystalline solids. He has also spent quite a lot of time in the United States over the past 30 years, mainly doing research at Brookhaven National Laboratory and the State University of New York, Sony Brook (SUNY) on Long Island, NY. After working part time for several years, he decided to fully retire last year and devote more time to travel, volunteer work and Amateur Radio.



We Design And Manufacture To Meet Your Requirements

***Prototype or Production Quantities**

800-522-2253

This Number May Not Save Your Life...

But it could make it a lot easier! Especially when it comes to ordering non-standard connectors.

RF/MICROWAVE CONNECTORS, CABLES AND ASSEMBLIES

- Specials our specialty. Virtually any SMA, N, TNC, HN, LC, RP, BNC, SMB, or SMC delivered in 2-4 weeks.
- Cross reference library to all major manufacturers.
- Experts in supplying "hard to get" RF connectors.
- Our adapters can satisfy virtually any combination of requirements between series.
- Extensive inventory of passive RF/Microwave components including attenuators, terminations and dividers.
- No minimum order.

NEMAL
Cable & Connectors
for the Electronics Industry

NEMAL ELECTRONICS INTERNATIONAL, INC.

12240 N.E. 14TH AVENUE

NORTH MIAMI, FL 33161

TEL: 305-899-0900 • FAX: 305-895-8178

E-MAIL: INFO@NEMAL.COM

BRASIL: (011) 5535-2368

URL: WWW.NEMAL.COM



We are one of the world's leading suppliers of laser and photonics-based solutions to a broad range of commercial and scientific research customers. We design, manufacture and market lasers, laser-based systems, precision optics and related accessories for a diverse group of customers. Since our beginnings in 1966, we have expanded our business through a combination of internal growth and the strategic acquisition of companies with related technologies.

We have an immediate opening for an **RF Development Engineer** to join the technical staff of the CO2 laser business unit located in Bloomfield, CT. In this position, the successful candidate will participate in the design and development of pulsed and CW VHF band RF power sources operating at average powers from 300 W to 15 KW. In addition, this individual will participate in the design and development of diagnostics, controls, and other critical analog and digital circuitry which is embedded in the RF power supply.

BS required (advanced degree preferred) in Electrical Engineering or related field and significant laboratory experience. Proficiency with both general purpose test equipment (oscilloscopes, waveform generators, etc.) and RF test equipment (network analyzers, spectrum analyzers, etc.) is required. Familiarity with OrCAD Capture and Microsoft Office products is also required. While professional experience would be a plus, Coherent will consider candidates with recent degrees.

Please apply to: <http://www.coherent.com> Job# 1974

Upcoming Conferences

45th Annual Central States VHF Society Conference

July 29-30, 2011

The Westin, Dallas-Fort Worth Airport
4545 W John Carpenter Freeway
Irving, TX 75063

The Central States VHF Society, Inc is soliciting papers, presentations and poster displays for the 45th Annual CSVHFS Conference on 29-30 July, 2011. Papers, presentations, and posters on all aspects of weak-signal VHF and above Amateur Radio are requested. You do not need to attend the conference, nor present your paper, to have it published in the Proceedings. Posters will be displayed during the two days of the Conference.

Presentations at Central States aren't necessarily technical — they cover the breadth of the VHF/UHF ham radio hobby. Highlights in past years have been demonstrations of Software Defined Radio and LASER Communication beyond line-of-sight. Presentations generally vary from 15 to 45 minutes and step you through the highlights of the topic at hand, with complete texts published as articles in the *Proceedings*.

Topics of interest include:

- Antennas including Modeling/Design, Arrays, and Control
- Test Equipment including Homebrew, Using, and making measurements
- Construction of equipment, such as Transmitters, Receivers, and Transverters
- Operating including Contesting, Roving, and DXpeditions
- RF power amps including Single and Multi-band Vacuum Tube and solid-state
- Propagation including Ducting, Sporadic E, Tropospheric and Meteor Scatter, and so on
- Pre-amplifiers (low noise)
- Digital Modes, such as WSJT, JT65, and others
- Regulatory topics
- EME
- Software-defined Radio (SDR)
- Digital Signal Processing (DSP)

Non-weak signal topics, such as FM, Repeaters, packet radio, and similar topics are generally not considered acceptable. There are always exceptions, however. Please contact the folks below if you have any questions about the suitability of a topic.

Strong editorial preference will be given to those papers that are written and formatted specifically for publication, rather than as visual presentation aids.

Deadline for submissions:

- For the Proceedings: Monday, May 1, 2011

- For Presentations delivered at the conference: Monday, 28 June 2011
- For notifying the Conference organizers that you will have a Poster to be displayed at the conference: Monday, 27 June 2011. Bring your poster with you on July 29.

Electronic formats (preferred)

Via e-mail

Upload to a web site for subsequent downloading

On media (CD/DVD, USB stick/thumb drive)

Contact: Kent Britain, WA5VJB; wa5vjb@flash.net, 1626 Vineyard, Grand Prairie, TX 75052.

There is more information about this year's conference available on the Central States VHF Society website at www.csvhfs.org/2011conference/index.html.

Microwave Update 2011 and 37th Eastern VHF/UHF Conference

Joint Conference Announcement
Microwave Update 2011 and the
37th Eastern VHF/UHF
Conference, both Sponsored by
the North East Weak Signal Group.
October 13-15, 2011
Holiday Inn, Enfield, CT, USA

This year the premier microwave Amateur Radio conference and the Eastern VHF/UHF conference will include tours, hospitality, swap session, equipment for measuring and tweaking, banquet and of course technical presentations.

Please visit www.microwaveupdate.org for the latest updates and registration. Contact Paul Wade W1GHZ, w1ghz@arri.org by July 15, 2011 for paper and talk arrangements. Papers must be submitted by August 30, 2011.

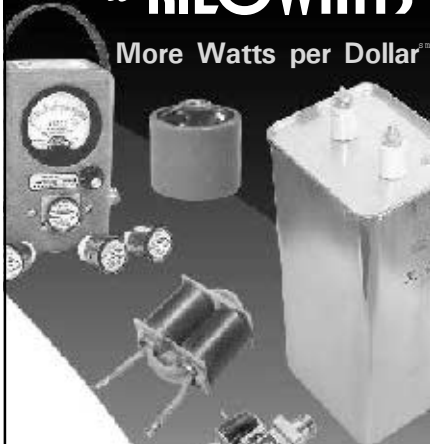
The 30th Annual ARRL and TAPR Digital Communications Conference

September 16-18, 2011
Four Points by Sheraton BWI
Airport
7032 Elm Road
Baltimore, Maryland 21240

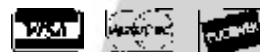
Mark your calendar now and start making plans to attend the premier technical conference of the year, the 30th Annual ARRL and

from
MILLIWATTS
to **KILOWATTS**SM

More Watts per DollarSM



- **Wattmeters**
- **Transformers**
- **TMOS & GASFETS**
- **RF Power Transistors**
- **Doorknob Capacitors**
- **Electrolytic Capacitors**
- **Variable Capacitors**
- **RF Power Modules**
- **Tubes & Sockets**
- **HV Rectifiers**



ORDERS ONLY:

800-RF-PARTS • 800-737-2787

Se Habla Español • We Export

TECH HELP / ORDER / INFO: 760-744-0700

FAX: 760-744-1943 or 888-744-1943



**An Address to Remember:
www.rfparts.com**

E-mail:

rfp@rfparts.com



2011 ARRL/TAPR Digital Communications Conference

September 16-18
in Baltimore, Maryland

Make your reservations now for three days of learning and enjoyment at the Four Points Sheraton Hotel at BWI airport. The Digital Communication Conference schedule includes forums, demonstrations, a Saturday evening banquet and an in-depth Sunday seminar. This conference is for everyone with an interest in digital communications—beginner to expert.

Call Tucson Amateur
Packet Radio at:
972-671-8277,
or go online to:
www.tapr.org/dcc



TAPR Digital Communications Conference to be held September 16-18, 2011, in Baltimore, MD. The conference location is the Four Points by Sheraton BWI Airport, Baltimore, MD.

We recommend that you book your room prior to arriving. TAPR has reserved a block of rooms at the special DCC room rate of \$90.00 single/double. This special rate is good until August 15, 2011. After that you will pay the regular room rate. To book your room, use the link on the TAPR website under Conferences (tapr.org/dcc.htm) or call the hotel directly (Reservations: 1-800-368-7764 Phone: 410-859-3300) and mention the group code **DCC** (Digital Communications Conference) when making reservations. *Be sure to book your rooms early!*

The ARRL and TAPR Digital Communications Conference is an international forum for radio amateurs to meet, publish their work, and present new ideas and techniques. Presenters and attendees will have the opportunity to exchange ideas and learn about recent hardware and software advances, theories, experimental results, and practical applications.

Topics include, but are not limited to: Software defined radio (SDR), digital voice (D-Star, P25, WinDRM, FDMDV, G4GUO), digital satellite communications, Global Position System (GPS), precision timing, Automatic Packet Reporting System®

Down East Microwave Inc.

We are your #1 source for 50MHz to 10GHz components, kits and assemblies for all your amateur radio and Satellite projects.

Transverters & Down Converters, Linear power amplifiers, Low Noise preamps, coaxial components, hybrid power modules, relays, GaAsFET, PHEMT's, & FET's, MMIC's, mixers, chip components, and other hard to find items for small signal and low noise applications.

We can interface our transverters with most radios.

Please call, write or see our web site
www.downeastmicrowave.com
for our Catalog, detailed Product descriptions and interfacing details.

Down East Microwave Inc.
19519 78th Terrace
Live Oak, FL 32060 USA
Tel. (386) 364-5529

(APRS), short messaging (a mode of APRS), Digital Signal Processing (DSP), HF digital modes, Internet interoperability with Amateur Radio networks, spread spectrum, IEEE 802.11 and other Part 15 license-exempt systems adaptable for Amateur Radio, using TCP/IP networking over Amateur Radio, mesh and peer to peer wireless networking, emergency and Homeland Defense backup digital communications, using *Linux* in Amateur Radio, updates on AX.25 and other wireless networking protocols and any topics that advance the Amateur Radio art.

This is a three-Day Conference (Friday, Saturday, Sunday). Technical and introductory sessions will be presented all day Friday and Saturday.

Join others at the conference for a Friday evening social get together. A Saturday evening banquet features an invited speaker and concludes with award presentations and prize drawings.

The ever-popular Sunday Seminar focuses on a topic and provides an in-depth four-hour presentation by an expert in the field. Check the TAPR website for more information: tapr.org.

Call for Papers

Technical papers are solicited for presentation and publication in the *Digital Communications Conference Proceedings*. Annual conference proceedings are published by the ARRL. Presentation at the conference is not required for publication. Submission of papers are due by 31 July 2011 and should be submitted to: Maty Weinberg, ARRL, 225 Main Street, Newington, CT 06111, or via the Internet to maty@arrl.org.

AMSAT 2011 Space Symposium and Annual Meeting

November 4-6, 2011
Wyndham Hotel
San Jose, CA

There are no details available yet, but mark your calendars now to attend this year's AMSAT Space Symposium. Check the AMSAT website for the latest information: www.amsat.org.

QEX

Next Issue in *QEX*

Arch Doty, W7ACD, follows up on his March/April 2011 *QEX* article about "The Effects of Ground Conductivity on Antenna Radials" with an expanded study. Soil composition, moisture content and temperature all affect soil resistivity (and ground conductivity). In this portion of the study, W7ACD investigates the extent of changes resulting from variations in moisture content of the soil.

License Study Materials

Technician Class

- Exam:** 35-question Technician test (Element 2)
The ARRL Ham Radio License Manual—Revised 2nd Edition. Ham radio's most popular license manual! Organized in easy-to-understand "bite-sized" sections, this is all you need to become an Amateur Radio operator. **Now including practice exam software on CD-ROM.**
 Order No. 0977 \$29.95
ARRL's Tech Q & A—5th Edition. Order No. 0847 \$17.95
The ARRL Instructor's Manual for Technician License Courses.
 Order No. 8737 \$19.95
Ham Radio for Dummies. Order No. 9392 \$21.99
Technician Class Flash Card Set. Order No. 1345 \$24.95



General Class (upgrade from Technician)

- Exam:** 35-question General test (Element 3)
NEW! The ARRL General Class License Manual—7th Edition. All the exam questions with answer key, for use July 1, 2011 to June 30, 2015. **Now including practice exam software.**
 Order No. 8119 \$29.95
NEW! ARRL's General Q & A—4th Edition.
 Order No. 8089 \$17.95
General Class Flash Card Set. Order No. 1357 \$39.95



Extra Class (upgrade from General)

- Exam:** 50-question Extra test (Element 4)
The ARRL Extra Class License Manual—Revised 9th Edition. Achieve the highest level of Amateur Radio licensing! **Now including practice exam software.**
 Order No. 8874 \$29.95
ARRL's Extra Q & A—2nd Edition. Order No. 1379 \$17.95
Extra Class Flash Card Set. Order No. 1366 \$39.95



Operating and Reference

- The ARRL Operating Manual—9th Edition.** The MOST COMPLETE book about Amateur Radio Operating. It contains everything you need to explore new activities, learn new skills, find new references, and more.
 Order No. 1093 \$29.95
NEW! ARRL Repeater Directory®—2011/2012 Edition.
Pocket-sized (3.75" x 5.25"), Order No. 1769 \$10.95
Desktop Edition (6" x 9"), Order No. 1936 \$15.95
NEW! TravelPlus for Repeaters™—2011-2012 Edition.
 CD-ROM, version 15.0. Order No. 7921 \$39.95
NEW! ARRL's Hamspeak—A Dictionary for Radio Amateurs.
 Order No. 8423 ARRL Member Price \$15.95 \$17.95
NEW! The ARRL DXCC List. March 2011 Edition. Order No. 7617 \$5.95
The ARRL DXCC Handbook. Order No. 9884 \$19.95
DXing on the Edge. Order No. 6354 \$19.95 \$29.95
RF Exposure and You. Order No. 6621 \$22.95
50 Years of Amateur Radio Innovation. Order No. 0228 \$39.95
50 Years of Amateur Radio CD-ROM. Order No. 3558 \$19.95
Hints & Kinks. 17th Edition. Order No. 9361 \$17.95
Low Profile Amateur Radio. 2nd Edition. Order No. 9744 \$19.95
The ARRL Field Day Handbook. Order No. 0885 \$19.95
FCC Rules and Regulations. 2nd Edition. Order No. 1173 \$5.95
Getting Started with Ham Radio. Order No. 9728 \$19.95
The ARRL Software Library for Hams. CD-ROM, version 3.0
 Order No. 1424 \$19.95
Amateur Radio on the Move. Order No. 9450 \$19.95
Storm Spotting and Amateur Radio. Order No. 0908 \$22.95
ARRL's Vintage Radio. Order No. 9183 \$19.95
Your Introduction to Morse Code. Order No. 8314 \$12.95
Two-Way Radios & Scanners for Dummies. Order No. 9696 \$21.99
2011 Super Frequency List on CD-ROM. Order No. 0137 \$44.95
2011 Shortwave Frequency Guide. Order No. 0113 \$59.95
Remote Operating for Amateur Radio. Order No. 0992 \$22.95
Pocket Ref (by Glover). Order No. 1148 \$12.95
Marine Amateur Radio. Order No. 9723 \$12.95
Shortwave DX Handbook. Order No. 9953 \$34.95
A Year of DX. Order No. 0040 \$20
The Complete DX'er. Order No. 9073 \$19.95

MAPS

- ARRL Map of North America.** 27 x 39 inches. Includes grids!
 Order No. 8977 \$15
ARRL Map of the World (Azimuthal). 27 x 39 inches.
 Order No. 7717 \$15
ARRL Map of the World (Robinson). 26 x 34.5 inches.
 Order No. 8804 \$15
ARRL Worked All States (WAS) Map. 11 x 17 inches.
 ARRL Frequency Chart on reverse side. Order No. 1126 \$3
The Radio Amateur's World Atlas. Order No. 5226 \$12.95

- NEW! RSGB Amateur Radio Operating Manual.** Order No. 2300 \$29.95
RSGB IOTA Directory. Order No. 0112 \$19.95
RSGB 6 Metre Handbook. Order No. 0340 \$24.95
RSGB LF Today. 2nd Edition. Order No. 0220 \$24.95
RSGB Radio Orienteering. Order No. 0131 \$19.95
NEW! RSGB Prefix Guide. 9th Edition. Order No. 0180 \$19.95
RSGB Morse Code for Radio Amateurs. Order No. 0221 \$15.95

Antennas and Transmission Lines

- The ARRL Antenna Book—21st Edition.** The ultimate reference for Amateur Radio antennas, transmission lines and propagation. **CD-ROM included.**
Softcover. Order No. 9876 \$44.95
Basic Antennas. Order No. 9994 \$29.95
International Antenna Collection.
Volume 1. Order No. 9156 \$19.95
Volume 2. Order No. 9465 \$21.95
The ARRL Antenna Designer's Notebook.
 Order No. 1479 \$34.95
ON4UN's Low-Band DXing. 5th Edition. Order No. 8560 \$44.95
NEW! ARRL's Small Antennas for Small Spaces.
 Order No. 8393 ARRL Member Price \$22.95 \$25.95
Antenna Towers for Radio Amateurs. Order No. 0946 \$34.95
The ARRL Guide to Antenna Tuners. Order No. 0984 \$22.95
ARRL's Yagi Antenna classics. Order No. 8187 \$17.95
Simple and Fun Antennas for Hams. Order No. 8624 \$22.95
ARRL's Wire Antenna Classics. Order No. 7075 \$14
More Wire Antenna Classics—Volume 2. Order No. 7709 \$17.95
More Vertical Antenna Classics. Order No. 9795 \$17.95
Vertical Antenna Classics. Order No. 5218 \$12
ARRL's VHF/UHF Antenna Classics. Order No. 9078 \$14.95
ARRL Antenna Compendium. Vol. 1. Order No. 0194 \$20
ARRL Antenna Compendium. Vol. 2. Order No. 2545 \$14
ARRL Antenna Compendium. Vol. 3. Order No. 4017 \$14
ARRL Antenna Compendium. Vol. 4. Order No. 4912 \$20
ARRL Antenna Compendium. Vol. 5. Order No. 5625 \$20
ARRL Antenna Compendium. Vol. 6. Order No. 7431 \$22.95
ARRL Antenna Compendium. Vol. 7. Order No. 8608 \$24.95
ARRL Antenna Compendium. Vol. 8. Order No. 0991 \$24.95
RSGB Practical Wire Antennas. Order No. R878 \$17
RSGB Practical Wire Antennas 2. Order No. 9563 \$24.95
RSGB HF Antennas for Everyone. Order No. 0145 \$24.95
RSGB HF Antennas for All Locations. Order No. 4300 \$34.95
RSGB Antennas for VHF and Above. Order No. 0501 \$29.95
RSGB Building Successful HF Antennas.
 Order No. 0800 \$34.95
RSGB The Antenna Experimenter's Guide.
 Order No. 6087 \$34.95
RSGB HF Antenna Collection. Order No. 3770 \$34.95
RSGB Stealth Antennas. Order No. 3208 \$24.95
RSGB Backyard Antennas. Order No. RBYA \$34.95
RSGB Radio Propagation - Principles and Practice.
 Order No. 9328 \$29.95
NEW! Antenna Zoning for the Radio Amateur. 2nd Edition.
 Order No. 1192 \$49.95
Antennas: Fundamentals, Design, Measurement. Standard Edition.
 Order No. 0320 \$99
Antennas: Fundamentals, Design Measurement. Deluxe Edition.
 Order No. 0175 \$149
Tower Climbing Safety & Rescue. Order No. 1108 \$29.95
Electronic Applications of the Smith Chart. Order No. 7261 \$75
Radio-Electronic Transmission Fundamentals.
 Order No. RETF \$89
Transmission Line Transformers. Order No. TLT4 \$59
Transmission Line Transformers. CD-ROM. Order No. 9088 \$129

CD-ROM Collections

- QST on CD-ROM!**
 2010 Periodicals on CD-ROM. Order No. 2001 \$24.95
 2009 Periodicals on CD-ROM. Order No. 1486 \$24.95
 2008 Periodicals on CD-ROM. Order No. 9406 \$24.95
 2007 Periodicals on CD-ROM. Order No. 1204 \$19.95
 2006 Periodicals on CD-ROM. Order No. 9841 \$19.95
 2005 Periodicals on CD-ROM. Order No. 9574 \$19.95
 2004 Periodicals on CD-ROM. Order No. 9396 \$19.95
 2003 Periodicals on CD-ROM. Order No. 9124 \$19.95
 2002 Periodicals on CD-ROM. Order No. 8802 \$19.95
 2001 Periodicals on CD-ROM. Order No. 8632 \$19.95
 2000 Periodicals on CD-ROM. Order No. 8209 \$19.95
 1999 Periodicals on CD-ROM. Order No. 7881 \$19.95
 1997 Periodicals on CD-ROM. Order No. 6729 \$19.95
 1996 Periodicals on CD-ROM. Order No. 6109 \$19.95
 1995 Periodicals on CD-ROM. Order No. 5579 \$19.95
NEW! Callbook CD-ROM. Summer 2011 Edition. Order No. 0210 \$49.95
HamCall™ CD-ROM. Order No. 8991 \$49.95

Continued on next page

Practical Circuits and Design



The ARRL Handbook—2011 Edition.
The most comprehensive guide to radio electronics and experimentation. Part reference and part applied theory, it is filled with electronic fundamentals, RF design, digital and software radio technology, and antenna construction. **Always Revised!** This 88th edition includes new topics, project material, and expanded content.
Fully searchable CD-ROM Included! (version 15.0)
Softcover. Book and CD-ROM.
Order No. 0953.....\$49.95

- Understanding Basic Electronics.** 2nd Edition.
Order No. 0823.....ARRL Member Price \$29.95.....**\$32.95**
- Basic Radio—Understanding the Key Building Blocks.**
Order No. 9558.....\$29.95
- Digital Signal Processing Technology.**
Order No. 8195.....\$34.95.....**\$44.95**
- ARRL's Hands-On Radio Experiments.** Order No. 1255.....\$19.95
- Hands-On Radio Parts Kit.** Order No. 1255K.....\$79.95
- The ARRL RFI Book.** 3rd Edition. Order No. 0915.....\$29.95
- Experimental Methods in RF Design.** Revised 1st Edition.
Order No. 9239.....\$49.95
- ARRL's Pic Programming for Beginners.** Revised 1st Edition.
Order No. 0892.....ARRL Member Price \$39.95.....**\$44.95**
- ARRL PIC Programming Kit.** Order No. 0030.....\$149.95
- ARRL Morse Code Oscillator Kit.** Order No. 0022.....\$24.95
- Morse Code Key.** Order No. 0242.....\$15.95
- Keyer Touch Paddle Kit.** Order No. 0670.....\$49.95
- MFJ 20-meter CW Cub Transceiver Kit.** Order No. 0018.....\$89.95
- L/C/F and Single-Layer Coil Winding Calculator.** Order No. 9123.....\$12.95
- Introduction to Radio Frequency Design.** Order No. 4920.....\$39.95
- ARRL's RF Amplifier Classics.** Order No. 9310.....\$19.95
- More QRP Power.** Order No. 9655.....\$19.95
- QRP Romps.** Order No. 0160.....\$18
- ARRL's Low Power Communication.** 3rd Edition. Order No. 1042.....\$19.95
- ARRL's Low Power Communication with Cub CW Transceiver Kit.**
Order No. 1042K.....\$99.95
- Do-It-Yourself Circuitbuilding for Dummies.** Order No. 0015.....\$24.99
- Electronics for Dummies.** 2nd Edition. Order No. 0196.....\$24.99
- Electronics Projects for Dummies.** Order No. 9944.....\$24.99
- Practical Digital Signal Processing.** Order No. 9331.....\$46.95
- Power Supply Handbook.** Order No. 9977.....\$29.95
- Electromagnetic Compatibility Engineering.** Order No. 0192.....\$120
- Discrete-Signal Analysis and Design.** Order No. 0140.....\$125
- RF Components and Circuits.** Order No. 8759.....\$50.95
- Practical Radio Frequency Test & Measurement.** Order No. 7954.....\$66.95
- Communications Receivers.** Order No. CR3E.....\$94.95
- Radio Receiver Design.** Order No. RRCD.....\$95
- HF Radio Systems & Circuits.** Order No. 7253.....\$89
- Build Your Own Low-Power Transmitters.** Order No. 9458.....\$54.95
- AC Power Interference Handbook.** Order No. 1103.....\$34.95
- Power Supply Cookbook.** Order No. 8599.....\$54.95
- Instruments of Amplification.** Order No. 9163.....\$19.95
- RSGB Homebrew Cookbook.** Order No. 0232.....\$24.95
- NEW! RSGB Elimination of Electrical Noise.** Order No. 1082.....\$12.95
- RSGB International QRP Collection.** Order No. 0020.....\$24.95
- RSGB Weekend Projects for the Radio Amateur.** Order No. 0123.....\$24.95

Digital and Image Communications

- VHF Digital Handbook—1st Edition.**
Everything you need to get started in digital radio applications. Includes Packet Radio, APRS, D-Star, digital applications in public service and emergency communications, and more!
Order No. 1220.....\$19.95
- ARRL's HF Digital Handbook.** 4th Edition.
Order No. 1034.....\$19.95
- VoIP: Internet Linking for Radio Amateurs.** 2nd Edition.
Order No. 1431.....\$24.95
- GPS and Amateur Radio.** Order No. 9922.....\$18.95
- The ARRL Image Communications Handbook.**
Order No. 8616.....\$19.95.....**\$25.95**
- Your Guide to HF Fun.** Order No. 0153.....\$16
- RSGB RTTY/PSK31 for Radio Amateurs.** Order No. 0329.....\$15.95
- Nifty E-Z Guide to PSK31 Operation.** Order No. 0370.....\$12.95
- Nifty E-Z Guide to D-STAR Operation.** Order No. 0125.....\$13.95
- NEW! Nifty E-Z Guide to EchoLink Operation.** Order No. 1094.....\$13.95
- Digital Communication Systems Using SystemVue.** Order No. 1084.....\$49.99

Public Service and Emergency Communications

- The ARRL Digital Technology for Emergency Communications Course.**
CD-ROM, version 1.0 Order No. 1247.....\$49.95
- The ARRL Emergency Communications Handbook.** Order No. 9388.....\$19.95
- The ARRL Emergency Communication Library.** CD-ROM, version 1.0
Order No. 9868.....\$19.95
- ARES Field Resource Manual.** Order No. 5439.....\$12.95
- Emergency Power for Radio Communications.** Order No. 9531.....\$19.95
- PR-101 Course on CD-ROM.** Order No. 0133.....\$19.95
- ARES Hat.** Order No. 0099.....\$14.95
- ARES Mesh Vest. (M-3XL)** Order No. 0128.....\$15.95
- ARES Solid Vest with Pockets. (M-3XL)** Order No. 0136.....\$24.95

Space and VHF/UHF/Microwave Communications

- The ARRL Satellite Handbook.** Order No. 9857.....\$24.95
- NOVA for Windows.** CD-ROM. Order No. 8724.....\$59.95
- RSGB Radio Nature.** Order No. 0240.....\$24.95
- NEW! RSGB Amateur Radio Astronomy.** 2nd Edition. Order No. 0388.....\$32.95
- The ARRL UHF/Microwave Projects CD.** Order No. 8853.....\$24.95
- International Microwave Handbook.** 2nd Edition. Order No. 0330.....\$29.95
- RSGB VHF/UHF Handbook.** 2nd Edition. Order No. 1229.....\$29.95
- RSGB Microwave Projects.** Order No. 9022.....\$29.95
- RSGB Microwave Know How.** Order No. 0303.....\$21.95

History and Adventure

- The Secret Wireless War—Softcover Edition.**
The Story of M16 Communications—1939-1945 (World War II). This is an extraordinary story that includes hams among those patriots that undoubtedly helped the allied war effort.
Order No. 0262.....\$39.95
- Edgar Harrison.** Order No. 0270.....\$29.95
- YASME—The Danny Weil and Colvin Radio Expeditions.**
Order No. 8934.....\$24.95
- Hiram Percy Maxim.** Order No. 7016.....\$19.95
- 200 Meters and Down.** Order No. 0011.....\$12
- The Gil Cartoon Book.** Order No. 0364.....\$15.95
- The Story of W6RO and the Queen Mary.** DVD Order No. 1344.....\$15.95
- Crystal Clear.** Order No. 0353.....\$58.50
- Don C. Wallace: W6AM, Amateur Radio's Pioneer.** Order No. 0016.....\$29.95
- World War II Radio Heroes: Letters of Compassion.**
Order No. 1268.....\$15.95
- Perera's Telegraph Collector's Guide.** Order No. 1277.....\$19.95
- Perera's Telegraph Collectors Reference CD-ROM.** Order No. 1282.....\$15
- The Story of the Enigma CD-ROM.** Order No. 1296.....\$15
- NEW! Inside Enigma.** Order No. 0611.....\$19.95
- Keys II: The Emporium.** Order No. 1372.....\$16
- Keys III: The World of Keys.** Order No. 1381.....\$18
- Oscar's Amateur Radio Adventure.** Order No. 0341.....\$19.95
- Full Circle: A Dream Denied, A Vision Fulfilled.** Order No. 0152.....\$13.95
- Frozen in Time.** Order No. 0098.....\$14.95

Ordering Information

For a complete publications listing or to place an order, please contact us:

- To order or obtain the address of an ARRL Dealer near you, call toll-free (US): **1-888-277-5289** (non-US call **860-594-0355**) 8 AM-5 PM Eastern time, Monday-Friday.
- Fax **1-860-594-0303** 24 hours a day, 7 days a week.
- By mail to: ARRL, 225 Main St, Newington CT 06111-1494
- Visit our World Wide Web site: <http://www.arrl.org/shop>

Shipping and Handling Rates:

Add the following amounts to your order to cover shipping and handling (S/H). US orders will be shipped via a ground delivery method. Orders outside of the US will be shipped via an international delivery service. Express delivery options and other specialty forwarding services are available. Please call, write or email for more information.

Order Value	US	International Economy 2-4 weeks delivery
Up to \$20.00	\$7.50	\$15.00
\$20.01 to \$50.00	\$10.50	\$25.00
\$50.01 to \$250.00	\$12.50	\$35.00
Single CD-ROM	First Class Mail \$2.75	n/a
Over \$250	Contact ARRL for shipping options and rates: orders@arrl.org	



Sales Tax:
CT add 6% state sales tax (including S/H). VA add 5% sales tax (excluding S/H). Canadian Provinces NS, NB and NL add 13% HST (excluding S/H), all other Provinces add 5% GST (excluding S/H).

ARRL License Manuals

Now Including Practice Exam Software!



Level
1



Level
2



Level
3

ARRL's popular license manuals just got even better! Each book now includes the ARRL Exam Review CD-ROM. Use the software with your book to review the study material. Take randomly-generated practice exams using questions from the actual examination question pool. Additional features allow you to print sample exams...as many as you like. ARRL Exam Review tracks your progress, giving you the feedback you need to fine-tune your studies. **You won't have any surprises on exam day!**

Get your **FIRST** ham radio license!

The ARRL Ham Radio License Manual—**Second Edition**

Let ARRL guide you as you get started in Amateur Radio—as you select your equipment, set-up your first station and make your first radio contact.

- **Easy-to-understand “bite-sized” sections.** Pass the 35-question Technician Class exam.
- **Includes the latest question pool with answer key,** for use through June 30, 2014.
- **Software** included featuring the **ARRL Exam Review** CD-ROM.
- **Designed for self-study and classroom use.** Intended for all newcomers, instructors and schoolteachers.

ARRL Order No. 0977

Also Available—
The ARRL Instructor's Manual
ARRL Order No. 8737
\$19.95*

Upgrade and enjoy more frequency privileges!

NEW Edition!

The ARRL General Class License Manual—**Seventh Edition**

Upgrade to General and experience the thrill of worldwide communications!

- Pass the 35-question General Class exam.
- **All the Exam Questions with Answer Key,** for use July 1, 2011 to June 30, 2015.
- **Software** included featuring the **ARRL Exam Review** CD-ROM.
- Detailed explanations for all questions, including **FCC rules.**

ARRL Order No. 8119

Achieve the highest level of Amateur Radio licensing!

The ARRL Extra Class License Manual—**Ninth Edition**

Complete the journey to the top and enjoy all the operating privileges that come with earning your Amateur Extra Class license.

- Pass the 50-question Extra Class exam.
- **All the Exam Questions with Answer Key,** for use through June 30, 2012.
- **Software** included featuring the **ARRL Exam Review** CD-ROM.
- Detailed explanations for all questions, including **FCC rules.**

ARRL Order No. 8874

Book and CD-ROM
Only \$29.95*/ea.
Order Today!

*Shipping and Handling charges apply. Sales Tax is required for orders shipped to CT, VA, and Canada. Prices and product availability are subject to change without notice.



ARRL The national association for
AMATEUR RADIO®

225 Main Street, Newington, CT 06111-1494 USA

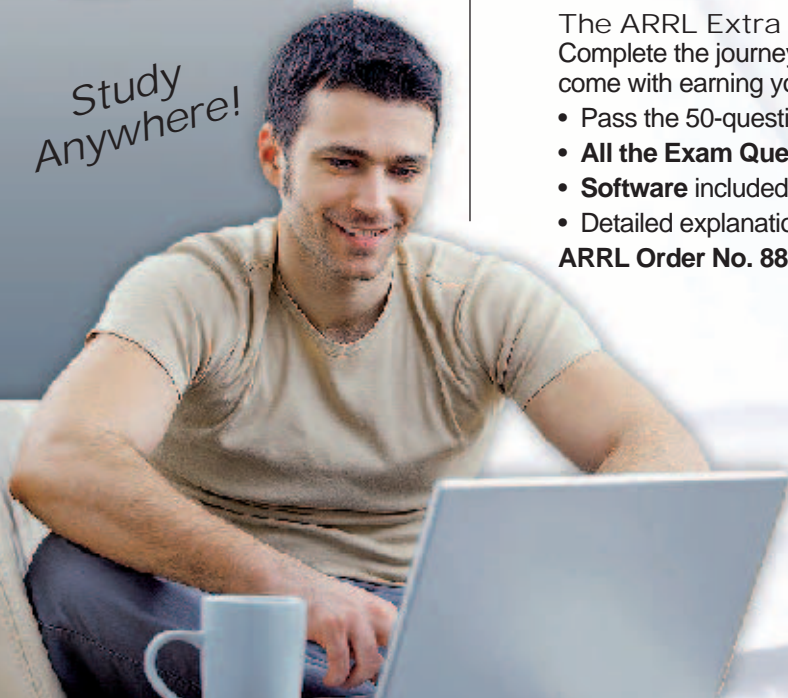
SHOP DIRECT or call for a dealer near you.

ONLINE WWW.ARRL.ORG/SHOP

ORDER TOLL-FREE 888/277-5289 (US)

QEX 7/2011

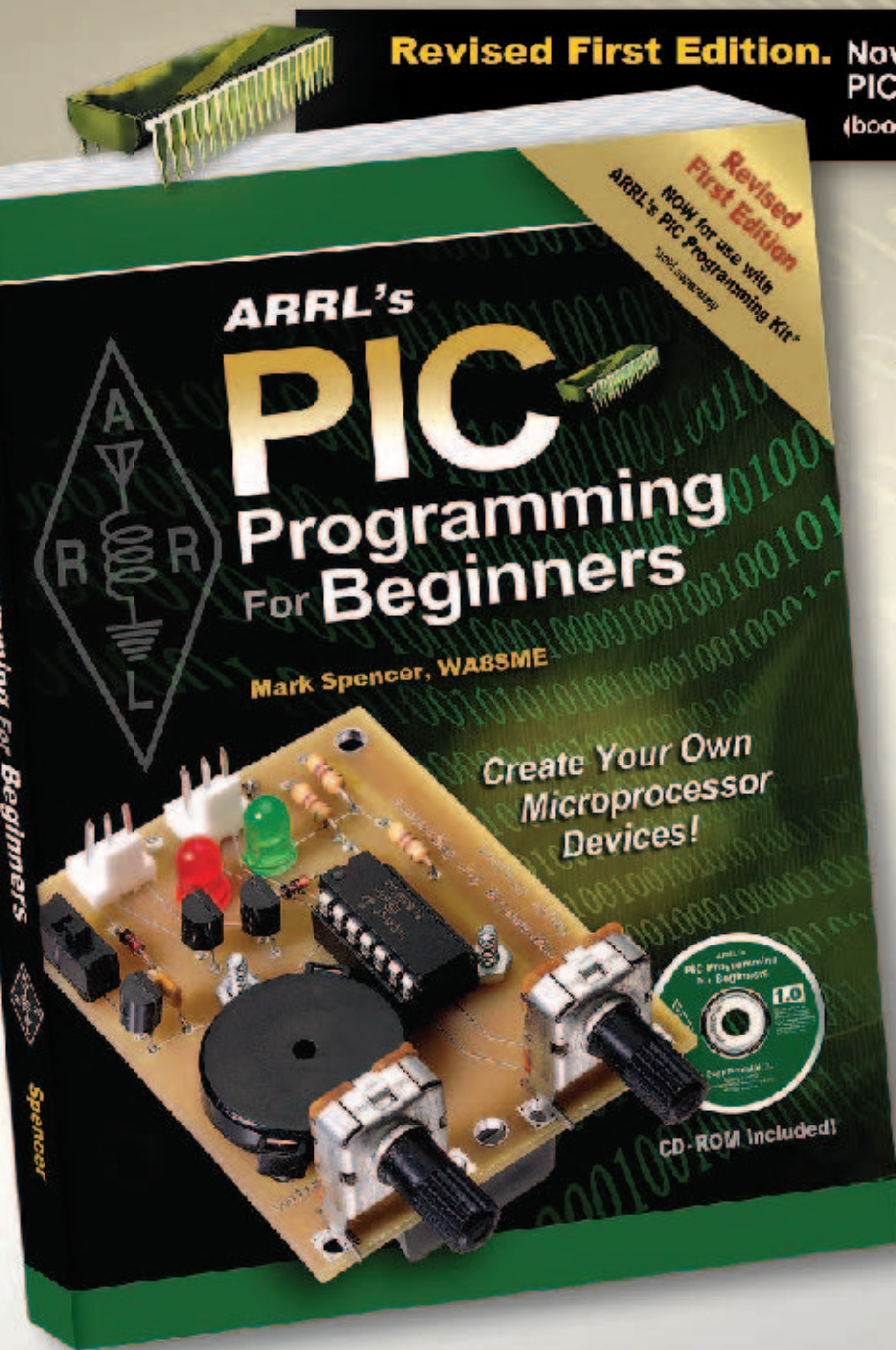
Study
Anywhere!



Create Your Own Microprocessor Devices!

ARRL's PIC Programming For Beginners

Revised First Edition. Now for use with ARRL's PIC Programming Kit. (book and kit sold separately)



Mark Spencer, WA8SME

ARRL's PIC Programming for Beginners is an introductory guide to understanding PIC[®] design and development. Written in a building block approach, this book provides readers with a strong foundation on the subject. As you explore the potential of these powerful devices, you'll find that working with PICs is easy, educational and most importantly fun.

CD-ROM included with programming resources, supplementary reading, short video clips and other helpful data.

Contents:

- Inside the PIC16F676
- Software and Hardware Setup
- Program Architecture
- Program Development
- Working With Registers —The Most Important Chapter
- Instruction Set Overview
- Device Setup
- Delay Subroutines
- Basic Input/Output
- Analog to Digital Converters
- Comparators
- Interrupts
- Timer 0 and Timer 1 Resources
- Asynchronous Serial Communications
- Serial Peripheral Interface Communications
- Working With Data
- Putting It All Together
- ...and more!



ARRL The national association for **AMATEUR RADIO**[®]

225 Main Street, Newington, CT 06111-1494 USA

SHOP DIRECT or call for a dealer near you.
ONLINE WWW.ARRL.ORG/SHOP
ORDER TOLL-FREE 888/277-5289 (US)

ARRL's PIC Programming Book

ARRL Order No. 0892

Special ARRL Member Price!
Only \$39.95* (regular \$44.95)

ARRL's PIC Programming Kit

ARRL Order No. 0030

Build the Kit Yourself!
Only \$149.95*

*Plus shipping and handling. Book and Kit sold separately.

